Research and Development Technical Report

ECOM–7034

DOD ADVANCED IMAGE-EVALUATION PROGRAM

(ARPA ORDER 1938 – PHASE I REPORT)

June 1974

Approved for public release, distribution unlimited.

ECOM

UNITED STATES ARMY ELECTRONICS COMMAND . FORT MONMOUTH, N. J.

DISCLAIMER NOTICE

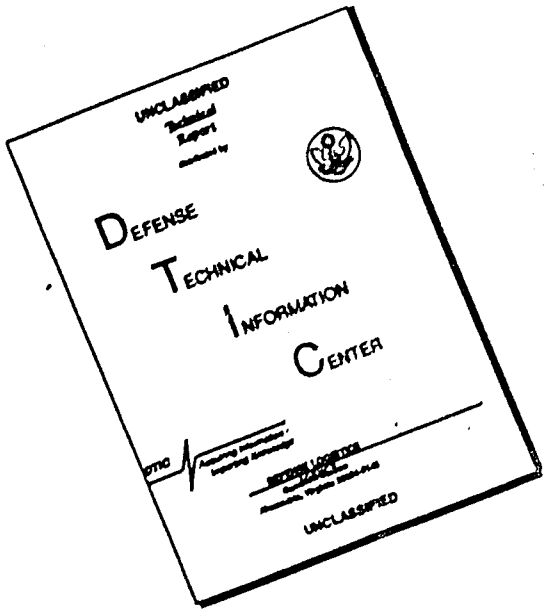

THIS DOCUMENT IS BEST QUALITY AVAILABLE. THE COPY FURNISHED TO DTIC CONTAINED A SIGNIFICANT NUMBER OF PAGES WHICH DO NOT REPRODUCE LEGIBLY.

Destroy this report when no longer needed.
Do not return it to the originator.

The citation in this report of trade names of commercially available products does not constitute official endorsement or approval of the use of such products.

UNCLASSIFIED

SECURITY CLASSIFICATION OF THIS PAGE (When Data Entered)

REPORT DOCUMENTATION PAGE		READ INSTRUCTIONS BEFORE COMPLETING FORM
1. REPORT NUMBER ECOM-7034	2. GOVT ACCESSION NO.	3. RECIPIENT'S CATALOG NUMBER
4. TITLE (and Subtitle) DOD ADVANCED IMAGE-EVALUATION PROGRAM ARPA ORDER 1938 – PHASE I REPORT		5. TYPE OF REPORT & PERIOD COVERED Interim September 1971-July 1972 6. PERFORMING ORG. REPORT NUMBER
7. AUTHOR(s) Night Vision Laboratory Joseph R. Moulton James T. Wood Clifford E. Lowe R. L. Migliorini J. R. Adamson and others (continued)		8. CONTRACT OR GRANT NUMBER(s)
9. PERFORMING ORGANIZATION NAME AND ADDRESS Night Vision Laboratory Fort Belvoir, Virginia 22060		10. PROGRAM ELEMENT, PROJECT, TASK AREA & WORK UNIT NUMBERS ARPA Order 1938 001 CJ
11. CONTROLLING OFFICE NAME AND ADDRESS Advanced Research Projects Agency (ARPA) Arlington, Virginia		12. REPORT DATE June 1974 13. NUMBER OF PAGES 150
14. MONITORING AGENCY NAME & ADDRESS(if different from Controlling Office)		15. SECURITY CLASS. (of this report) Unclassified 15a. DECLASSIFICATION/DOWNGRADING SCHEDULE

16. DISTRIBUTION STATEMENT (of this Report)

Approved for public release: distribution unlimited.

17. DISTRIBUTION STATEMENT (of the abstract entered in Block 20, if different from Report)

18. SUPPLEMENTARY NOTES

19. KEY WORDS (Continue on reverse side if necessary and identify by block number)

Photon imaging system evaluation
Procurement specifications for thermal imaging systems
Procurement specifications for image intensifier systems
Procurement specifications for low light level TV systems
Laboratory performance of night vision systems

20. ABSTRACT (Continue on reverse side if necessary and identify by block number)

The objective of this program, sponsored under ARPA Order 1938, is the development of uniform image quality measurement techniques and standard procedures that can be used throughout DOD laboratories for determining performance levels of photon-imaging systems. In addition to developing uniform techniques and procedures, the program calls for the development of an advanced, image-evaluation facility for use in Image Evaluation Centers of Excellence to be established at selected laboratories throughout DOD. Phase I of this program was completed March 1972. This phase was the formulating phase of the program and consisted of: (1) surveying selected laboratories in DOD and

(continued)

DD FORM 1 JAN 73 1473 EDITION OF 1 NOV 65 IS OBSOLETE

UNCLASSIFIED

SECURITY CLASSIFICATION OF THIS PAGE (When Data Entered)

(Block 7 Cont'd)

Naval Air Development Center
S. Campana
T. Pohle
M. Hess
T. Shopple

University of Rhode Island
S. Nudelman
H. Roehrig
J. Hall
R. Zirkind

Naval Electronics Laboratory Center
C. Zeisse
D. Fisher
R. Potter

Wright Patterson Air Force Base
S. Richard
S. Parker
A. Berg

(Block 20 Cont'd)

related industry to determine existing image-evaluation capabilities and requirements: (2) selecting program participants and allocating individual work tasks to insure a comprehensive approach to the problem with a minimum of overlap: (3) designing and initiating procurement of a prototype of the DOD Advanced, Image-Evaluation Facility; and (4) selecting candidate advanced, image-evaluation procedures for consideration for use throughout DOD. This report describes the results of the survey, the candidate procedures, and the design of the prototype facility.

PREFACE

This report describes a DOD program on advanced, image-evaluation techniques being conducted under Colonel William Kirlin of the Advanced Sensors Office of the Advanced Research Projects Agency. Particular credit should be given to Richard Bailey of Systems Technology Associates (STA) for his efforts in editing this document.

The following organizations and individuals provided technical information under the survey on DOD image evaluation:

General Electric Company
Utica, New York
- Dr. Herb Levin
- Mr. Louis Lego
- Mr. John Walker
- Mr. Jim Juliano

Electro Optical Systems
Los Angeles, California
- Mr. Robert Sendall
- Mr. Louis Reynolds
- Mr. L. Green

Texas Instruments, Inc.
Dallas, Texas
- Dr. George Hopper
- Mr. Ronald Dunn
- Mr. Don Miller

Westinghouse Corporation
Baltimore, Maryland
- Dr. Fred Rosell

Hughes Aircraft Company
Culver City, California
- Mr. Don Holscher
- Mr. Peter Laakmann

Boeing Company
Wichita, Kansas
- Mr. Ernest Ashenfelter

University of Rhode Island
Kingston, Rhode Island
- Dr. Ralph Zirkind
- Dr. Sol Nudelman
- Dr. Jim Hall
- Mr. Lucien Biberman

Aerospace Guidance and Metrology Center
Newark, Ohio
- Mr. Arron Sanders
- Mr. Robert Hinebaugh
- Mr. Dick Hackett

Sacramento Army Depot
Sacramento, California
- Mr. Al Turner
- Mr. William Bowman

Naval Weapons Center
China Lake, California
- Mr. Phil Arnold
- Mr. Doug Cowan

Naval Air Development Center
Warminster, Pennsylvania
- Mr. Steward Lee
- Mr. Tom Shopple
- Mr. Steve Campana
- Mr. Tom Pohle
- Mr. George Shanlian

Air Force Avionics Laboratory
WPAFB, Dayton, Ohio
Mr. Dave Power
Capt. Mike Kiya
Mr. Norm Griswold
Mr. Bill Martin
Mr. Dan Groening
Mr. Frank McCann

Air Force Armament Laboratory
Eglin AFB, Florida
Col. William Geiser

Night Vision Laboratory
Fort Belvoir. Virginia
Mr. Mike Lloyd
Mr. Fred Petito
Dr. Herbert Pollehn
Dr. Richard Franseen
Mr. Bill Dateno
Mr. Al Effkeman
Mr. Jack Hilldreth
Mr. John Johnson
Dr. Walter Lawson
Mr. Jim Wood
Mr. Russ Moulton

CONTENTS

ILLUSTRATIONS

TABLES

DOD ADVANCED, IMAGE-EVALUATION PROGRAM

(ARPA ORDER 1938 – PHASE I REPORT)

I. INTRODUCTION

1. **Background.** Photon-imaging-systems development is being addressed extensively throughout DOD by numerous individual agencies of the Army, Navy, and Air Force. In addition, related industries are sponsoring in-house efforts toward the development of similar electro-optical imaging devices in an attempt to exploit proprietary imaging concepts. A clear, almost urgent requirement exists in DOD for a program that defines image-quality measurements which can be applied uniformly to a broad class of these photon-imaging systems. No such program presently exists although recent programs, such as those sponsored by DDR&E, IDA, and others, have provided an impressive compilation of image-quality technology. The objective of this program, sponsored under ARPA Order 1938, is to fill this gap by implementing uniform evaluation techniques and procedures throughout DOD and related industry that are based upon the most advanced technology that exists today.

2. **Overview of DOD Advanced, Image-Evaluation Program: (ARPA Order 1938).** In general, the objective of this program calls for the development of uniform, image-quality-measurement techniques and standard procedures that can be used throughout DOD laboratories for determining performance levels of photon-imaging systems. In addition to developing uniform techniques and procedures, the program calls for the development of an advanced, image-evaluation facility for use in Image Evaluation Centers of Excellence to be established at selected laboratories in DOD. This program is being conducted in four phases (Fig. 1):

- Phase I was the formulating phase of the program and consisted of: (1) surveying selected laboratories in DOD and related industry to determine existing, image-evaluation capabilities and requirements: (2) selecting program participants and allocating individual work tasks to insure a comprehensive approach to the problem with a minimum of overlap: (3) designing and initiating procurement of a prototype of the DOD Advanced, Image-Evaluation Facility; and (4) selecting candidate, advanced, image-evaluation procedures for consideration for use throughout DOD (June 1971 – March 1972).

- Phase II involves the fabrication and final design of a prototype DOD Advanced, Image-Evaluation Facility for use as a testbed for final development and selection of DOD image-evaluation procedures (March

1972 – September 1973).

- Phase III addresses the problem of developing and adopting the advanced, image-evaluation procedures for photon-imaging systems for uniform use throughout DOD and related industry (March 1972 – September 1973).

- Phase IV concerns the establishment of DOD Centers of Excellence at selected laboratories. The level of support by ARPA in establishing these centers is somewhat undefined at this time. Assistance to the selected DOD and private laboratories, in the form of training and administrative support for facility procurement, is the minimum effort envisioned. It is not known if funding to establish these DOD Centers of Excellence will be obtained through A. O. 1938 or internal funding channels (September 1973 – September 1974).

Additional phases for addressing the problem of establishing evaluation techniques for major components of photon-imaging systems have been defined. There is also a need for a follow-on investigation of the sensitivity of adopted laboratory, image-evaluation procedures to the system field performance.

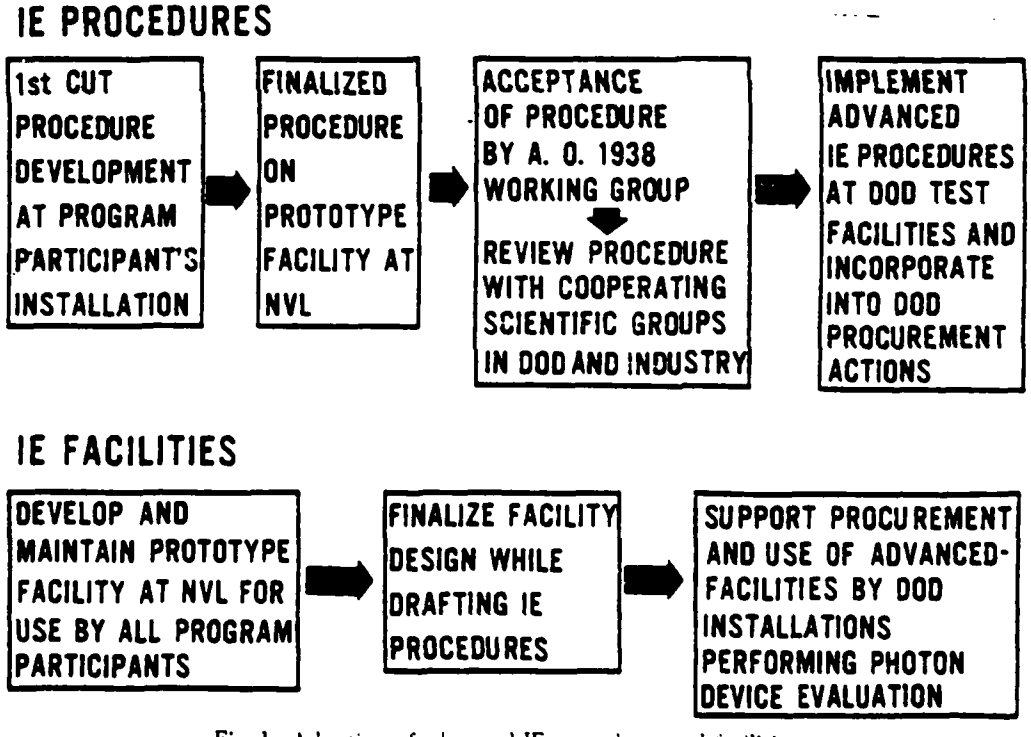

Fig. 1. Adoption of advanced IE procedures and facilities.

a. **Program Participants.** This report describes the DOD Advanced, Image-Evaluation Program as it has been formulated and the efforts expended through Phase I. The participants in this program represent the three services, each of which is committing some 2 to 3 man years of effort. The participants are:

- U. S. Army, Night Vision Laboratory, Fort Belvoir, Virginia.
- U. S. Navy, Naval Air Development Center, Warminster, Pennsylvania.
- U. S. Navy, Naval Electronics Laboratory Center, San Diego, California
- U. S. Air Force, Air Force Avionics Laboratory, WPAFB, Dayton, Ohio
- University of Rhode Island, Kingston, Rhode Island

Table 1 provides a general delineation of responsibilities of each program participant. All participants meet on a bi-monthly basis to exchange technical information and to ensure maximum program coordination.

Table 1. Program Participants and Responsibilities

Participant	Responsibility
U. S. Army NVL, Fort Belvoir, Va.	Lead Laboratory for program
	Survey existing IE facilities in DOD and industry
	Develop and maintain the DOD Advanced, IE Facility
	Develop IE procedures for System Responsivity, System Spatial Response, and System Resoltivity
U. S. Navy NADC, Warminster, Penna.	Develop IE procedures for System High-Signal Response, System Temporal Response, and System Geometric Response
U. S. Air Force Avionics Laboratory, WPAFB, Dayton, Ohio	Develop IE procedures for Photographic Readout Systems
University of Rhode Island (URI), Kingston, R. I.	Develop IE procedures for display measurements for System S/N and Uniformity
Naval Electronics Laboratory Center (NELC), San Diego, Calif.	Develop IE procedures for Electrical-Out (video line) Measurements

b. **Phase I Report.** Section II summarizes the information contained in Sections III through V.

Section III contains the results of the survey conducted by NVL of selected laboratories in DOD and industry. The status of current system procurement is discussed as well as general image-evaluation capabilities and requirements.

Section IV contains a detailed description of the prototype of the DOD Advanced, Image-Evaluation Facility under development. Included in this section are the physical performance specifications of the Facility.

Section V provides information on present candidate, image-evaluation procedures and techniques selected for possible use throughout DOD. Procedure development assignments of each program participant are delineated in this section.

The Appendix contains a report by NELC on the joint efforts of NELC and URI during the reporting period of Phase I.

II. SUMMARY

3. **DOD Advanced, Image-Evaluation Facility.** A recent survey of image-evaluation facilities and capabilities at selected laboratories in DOD and related industry has indicated that implementation of uniform, image-quality techniques is not possible with existing facilities. The purpose of the DOD Advanced, Image-Evaluation Facility is to provide the *common equipment base* upon which uniform, image-evaluation procedures can be applied to a broad class of photon-imaging systems. The need for uniformity in facility capability at cognizant DOD laboratories is clear if uniform measurement techniques are to be implemented.

The prototype of the DOD Advanced, Image-Evaluation Facility has been designed for use in the evaluation of a wide variety of photon-imaging systems, e.g., Low Light Level Television (LLLTV), Infrared (IR), and Image Intensifier (I^2) Systems. The implementation of this facility throughout DOD will provide the *common equipment base* required for performing standard, image-quality measurements in the laboratory.

It is envisioned that a limited number of facilities based on this prototype would be established at major laboratories in DOD. These laboratories would be the "Centers of Excellence." It should not be inferred that every DOD photon-imaging-device contract would require such a comprehensive facility for use at the DOD originating laboratory and in the related industrial laboratories. Rather, less expensive and specialized equipments would be derived from the Evaluation Facilities at the DOD "Centers of Excellence."

The Advanced. Image-Evaluation Facility Prototype which has been designed is based on a modular concept and lends itself well to changes that may be required due to future advances in image-evaluation procedures. The Facility (Fig. 2) is divided into five major modules (Fig. 3). Each module may be modified or replaced without altering the basic structure or capability of the Facility.

A Real Time Data Processor Module is incorporated into the facility design to provide complete electro-mechanical control of the Facility and to process the data required to characterize the performance of the system under test. The high-level, conversive, basic language that controls this processor is such that engineers and scientists can easily program and operate the Facility without the support of specialized computer personnel. In addition, a manual override capability for the electro-mechanical controls is provided for most functions.

The Facility is primarily housed on a 120-inch reflective collimator which presents a target image at infinite conjugate to the system under test. The patterns used to present these target images are mounted on a rotating wheel located inside a Hybrid Target Generator Module.

The Hybrid Target Generator utilizes the same patterns to cover all the spectral regions from the visible to the far infrared. It incorporates several energy sources that emit controlled amounts of radiant energy over a wide dynamic range of contrast.

The target energy is transmitted by the Collimator Module and is focused by the photon-imaging system which is mounted directly on the Output Monitor Module.

The Output Monitor Module rotates the photon-imaging system about its nodal point in both azimuth and elevation. This rotation allows the target to be dynamically slewed and positioned throughout the field of view.

On the same platform, behind the photon-imaging system, is a scanning optical probe which is coupled to a photomultiplier tube via fiber optic rope. The output of the tube is sent to the Real Time Data Processor Module for analysis.

The Processor provides for three major types of photo-imaging-system output: analog optical scanner, direct electrical, and subjective performance via keyboard entry.

In addition to processing data and generating parametric evaluation curves, the Processor continuously monitors and controls the condition of all the variables of each module. Monitoring these variables ensures the validity of test parameters such as differential temperature, target contrast, target type, and scanner position. If a

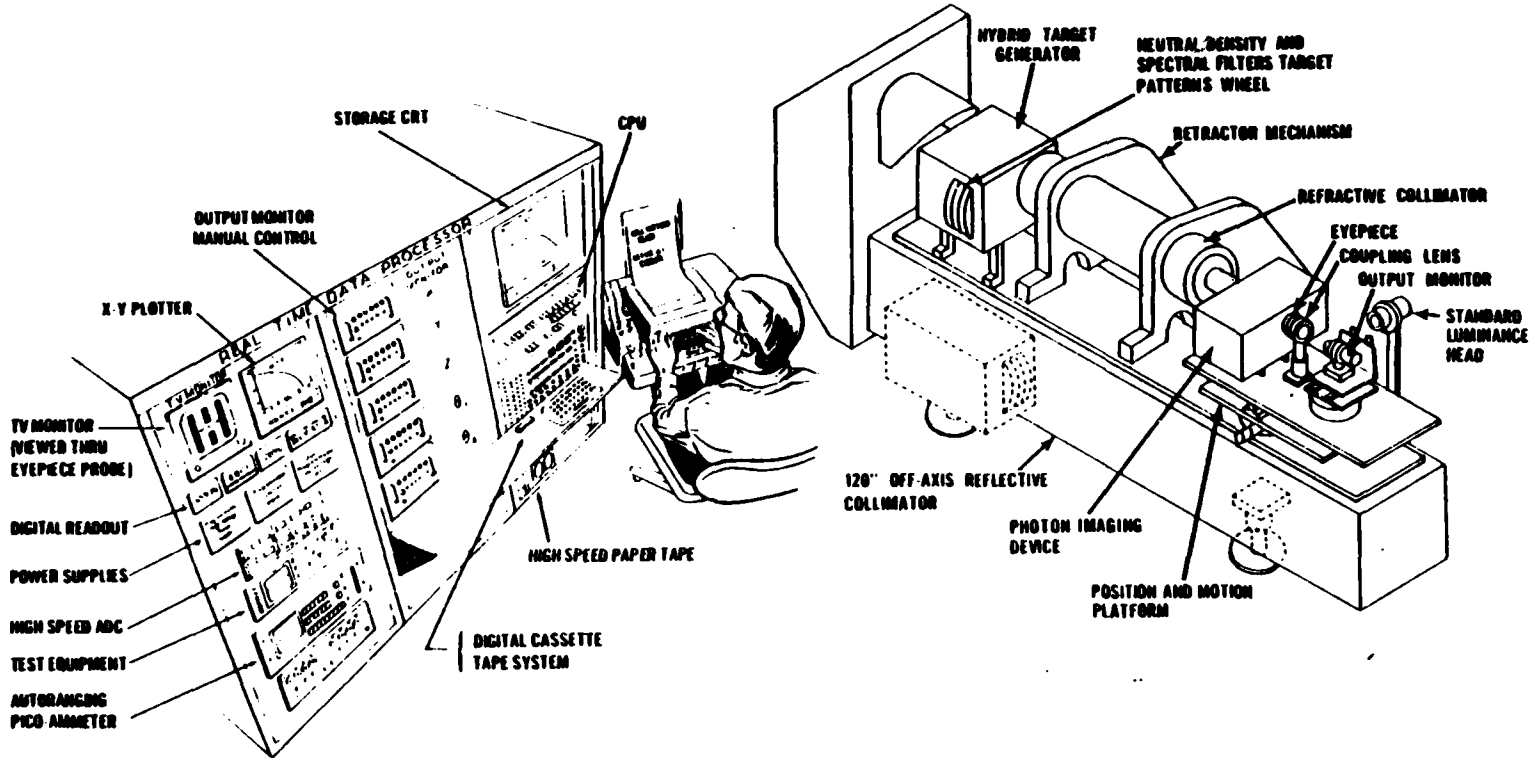

Fig. 2. Prototype of DOD advanced image evaluation facility.

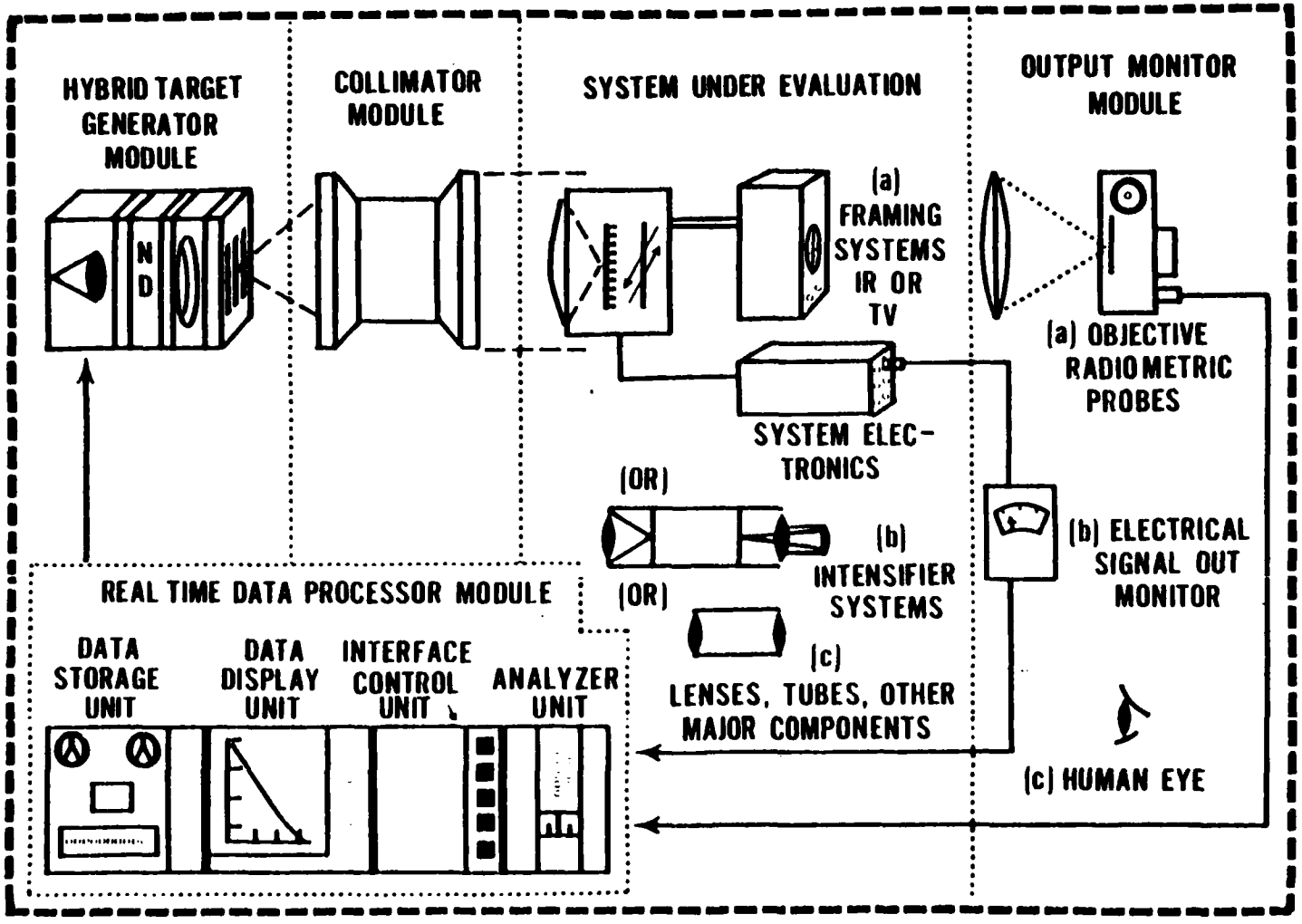

Fig. 3. Major modules of the DOD advanced image evaluation facility.

specified parameter, e.g., differential temperature, is not maintained within preset tolerances. the priority-interrupt feature of the Processor will stop the test and notify the user. In a severe case, the Processor will cycle into an automatic shutdown mode to prevent damage to the Facility or photon-imaging system under test.

Each module consists of sets of elements whose use depends upon the specific photon-imaging system under test and the image-evaluation procedure being applied. For example, the Collimation Module consists of a set of infrared and visible refractive collimating lenses as well as a large-aperture, reflective, parabolic collimator. The reflective collimator is used with all imaging systems whereas the refractive lenses are used only with systems possessing matching spectral responses. The prototype facility as presently configured is described in detail in Section IV.

4. **Advanced, Image-Evaluation Procedures Development.** Laboratory image-evaluation procedures that are based upon modern communication theory concepts will be developed for uniform use throughout DOD. These procedures will yield the laboratory performance parameters that are required by current predictive performance models. In addition, procedures that yield nonlinear performance parameters that are not now required by linear predictive models but are obviously related to field utility will be devised. In general, the procedures will follow the *two-port, image-evaluation concept* shown in Fig. 4. That is, excitation energy will be applied to the system through its normal input port (collecting aperture) via the source pattern and collimating optics modules. The response to this excitation by the system under test will be measured through the normal output port (viewing eyepiece or display) using elements of the image-monitoring, sensor module. The output of this module will be received by the data analyzer module for automatic processing and plotting. The four primary areas under which system-evaluation procedures will be developed are:

- System Responsivity – the objective measures of amplitude transfer, spectral transfer, and contrast transfer response functions of the system under test.
- System Spatial Resolution – the objective measures of system spatial response such as the optical transfer function, modulation transfer function, resolving power, field of view, magnification, etc.
- System Signal-to-Noise – the measurement of the mean and RMS fluctuation of signals at the display of photon-imaging systems. Includes measurements of noise frequency associated with cosmetic effects such as fixed pattern noise, periodic noise, and nonuniformity.
- System Resoltivity Response – Resoltivity refers to observer performance tests that combine the system spatial resolution and sensitivity

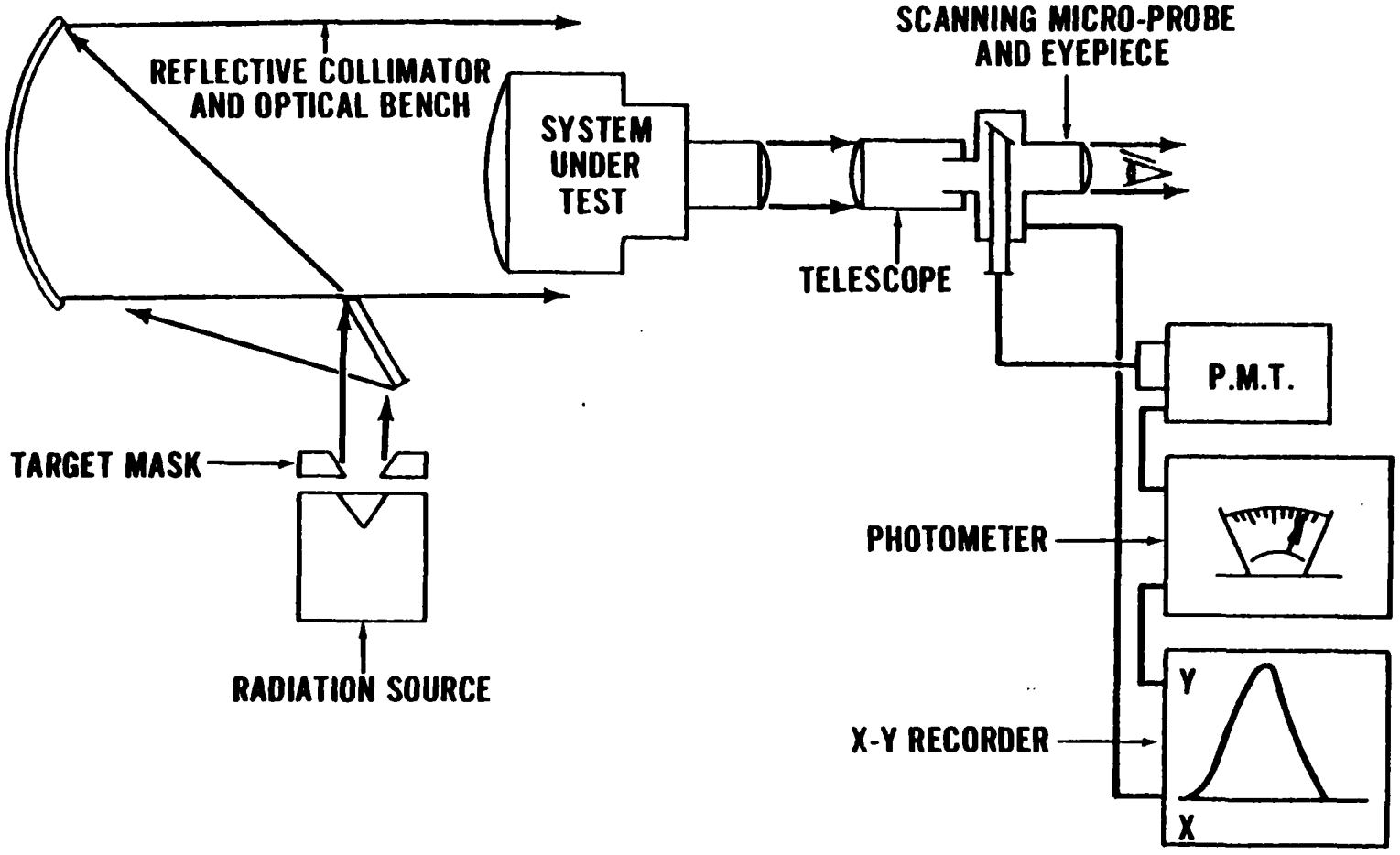

Fig. 4. Two-port image evaluation concept.

(responsivity and S/N) to yield the combined observer-system laboratory performance. Examples of candidate procedures to be investigated under this category are Minimum Resolvable Temperature (MRT), Noise Limited Resolution (NLR), and Resolving Power.

The development of the procedures is being undertaken by participants from the Army, Navy, Air Force, and the University of Rhode Island. The approach is to first review both the procedures currently being used and those proposed as more advanced techniques. These procedures are labelled "candidate procedures." A summary listing of the candidate procedures selected to date is given in Table 2.

In the process of researching the candidates, the procedures will be judged against three major criteria. First, because the primary objective of any photon-imaging device is to satisfy some real-world tactical need, the parameters being measured must be relatable to field performance. Second, since ultimately the parameters and the measurement techniques themselves will be integrated into procurement performance specifications, the techniques must be compatible with this specification effort. For example:

a. Any procedure must be developed with careful consideration for the cost of the equipment necessary to implement it.

b. The procedures must lend themselves to well-defined calibration.

c. The data from any measurement should be quickly obtainable in a form which is immediately usable.

d. The facility and procedures should be compatible with the talents of an average technician.

Third, because of the potential of modeling in the analysis of future concepts and performance studies for different applications, the procedures must provide data which is consistent with existing model needs. Composite laboratory performance criteria such as Signal-to-Noise Ratio Display (SNR_D), Modulation Transfer Function Area (MTFA), and Detective Quantum Efficiency (DQE) will be investigated for possible use in specifying system performance directly. In any case, image-evaluation procedures recommended for DOD adoption will yield the input parameters required by these and other performance models.

III. IMAGE EVALUATION SURVEY

5. Survey Methodology. A survey of a limited number of laboratories involved in the development and/or evaluation of photon-imaging systems was conducted during

Table 2. Candidate Procedures

Category	Procedure
System Responsivity[a]	Objective Signal Transfer Function Subjective Signal Transfer Function Spectral Transfer Function
System Spatial Resolution[a]	Optical Transfer Function Resolving Power
System Resoltivity Response[a]	Visual Resoltivity (Full Dynamic Range) Resolving Power (Limiting Resolution)
System High-Signal Response[b]	Image Spreading Saturation Effects
System Temporal Response[b]	Image Motion Effects System Time Constant System Jitter
System Geometric Response[b]	Magnification and Field of View Off-Axis Distortion
System Display Uniformity[c]	Fixed Pattern Noise Raster and Scan Line Effects
System Sensitivity Response[c]	Temporal Noise Signal-to-Noise Detective Quantum Efficiency
Front-End Sensitivity Response[d]	Signal Level and Noise Level SNR_D
Front-End Spatial Response[d]	Optical Transfer Function Resolving Power
Front-End Temporal Response[d]	Image Motion and Lag Jitter Response
System Responsivity (film readout only)[e]	–
System Spatial Resolution (film readout only)[e]	–
System Resoltivity Response (film readout only)[e]	–

(a) Procedures contributed by Night Vision Laboratory.

(b) Procedures contributed by Naval Air Development Center.

(c) Procedures contributed by University of Rhode Island.

(d) Procedures contributed by Naval Electronics Laboratory Center.

(e) Procedures contributed by Air Force Avionics Laboratory.

Phase I of this program. The prime objective of this survey was to determine the laboratory, image-evaluation capability and requirement throughout DOD so that this program could be formulated to address first-priority requirements. The laboratories selected for this survey represented a cross section of the technical areas in both government and private industry that are involved with photon-imaging systems. The specific laboratories that participated in the survey are listed below:

- Night Vision Laboratory, Fort Belvoir, Virginia
- Naval Air Development Center, Warminster, Pennsylvania
- Air Force Avionics Laboratory, WPAFB, Dayton, Ohio
- Aerospace Guidance and Meteorology Center, Newark AFB, Newark, Ohio
- Sacramento Army Depot, Sacramento, California
- Naval Weapons Center, China Lake, California
- General Electric Company, Utica, New York
- Westinghouse Corporation, Baltimore, Maryland
- Electro Optical Systems (Xerox Corporation), Los Angeles, California
- Texas Instruments Incorporated, Dallas, Texas
- Hughes Aircraft Corporation, Culver City, California

The survey was conducted by forwarding a questionnaire to each of the selected laboratories. The questionnaire explained the purpose of the survey and provided questions that encompassed the general evaluation of photon-imaging systems. One purpose of the questionnaire was to enable uniform responses to be obtained from the various technical areas surveyed. The questionnaire was followed up with an on-site visit by several NVL personnel for a firsthand discussion of the image-evaluation capabilities and requirements and an inspection of the physical facilities. The questionnaire used in the survey follows.

6. Questions Pertinent to Electro-Optical (E-O) Image-Evaluation Survey Being Conducted Under ARPA Order 1938.

Q-A. What is your facility's general, image-evaluation capability in determining the laboratory performance of the following classes of electro-optical devices?

1. Image Intensifier Devices
   a. Special components
   b. Major assembly
   c. System
2. LLL Television Systems
   a. Special components
   b. Major assembly
   c. System
3. Thermal Imaging Systems
   a. Special components
   b. Major assembly
   c. System

Q-B. What specific IE techniques and procedures do you presently utilize in evaluating the electro-optical devices listed in Q-A? Group your techniques into the following E-O parameter categories:

1. Sensitivity Response
2. Spatial Response
3. Cosmetic Response
4. Temporal Response
5. Other

Q-C. What laboratory image evaluation is required to characterize the E-O systems specified in Q-A at least for typical field applications?

Q-D. Is the image evaluation required under Q-C the same that your facility performs to insure the E-O equipments meet design goal and procurement specification requirements?

Q-E. Are the performance levels obtained by the evaluation under Q-D knowingly relatable to field performance or field utility?

Q-F. Who are the users of the test data and image-evaluation information your Facility generates?

Q-G. How is the data obtained for each E-O parameter category under Q-B utilized?

Q-H. Does your Facility perform tests that correlate field performance to laboratory image-evaluation performance?

Q-I. What critical gaps are recognized by your Facility as existing in the E-O laboratory image-evaluation area in which you are involved? How are they being addressed?

7. **Typical Survey Responses.** The results of this survey provided information that was quite useful in formulating this A. O. 1938 Program to insure that DOD's image-evaluation needs would be addressed. The following reflect several of the typical responses that were obtained from some of the questions in the survey questionnaire.

a. **Newark Air Force Station, Aerospace Guidance and Metrology Center Survey Response.** The Newark Air Force Station is a prime metrology laboratory for the Air Force. They have experience in performing optical-transfer-function measurements on lenses and are presently engaged in a program to establish the capability to evaluate FLIR systems.

Response to Q-A. 1: We calibrate only the optical components for systems using image-intensifier devices. We additionally calibrate the sources used for testing the image intensifiers.

Response to Q-A. 2: We have not yet done any testing on LLL Television Systems. We do, however, have a special source made for the purpose of evaluating the system.

Response to Q-A.3: We have at this time tested only the optical components of such thermal-imaging devices.

Response to Q-B: The only image-evaluation testing presently being conducted at our facility is the optical-transfer-function measurement of optical components.

Response to Q-C: The tests discussed by R. Moulton, L. Biberman, M. Lloyd, and others seem to be very good in that respect. Parameters such as optical-transfer function, signal-transfer function, spectral-transfer function, and minimum resolvable temperature (MRT) should be good indicators of the system performance in field applications, particularly if the human factor is included in the evaluation as in the MRT measurement.

Response to Q-D: We are not presently using these techniques. We do plan, however, to incorporate those tests known to insure that the FLIR's meet design goal and procurement specification requirements.

Response to Q-E: Since this facility has not used or tested entire

imaging systems at this point, we cannot knowingly say from experience that the tests mentioned in Q-D are relatable to field performance. However, judging from the literature discussing these evaluations, it certainly seems that they should be indicative of field performance.

Response to Q-F: In general, we have provided image evaluation test data to the Army, Navy, Air Force, and private industry working under government contract.

Response to Q-G: The data is usually used by the requesting agency as part of the acceptance test for a particular optical component that is being purchased under government contract. In some cases, it is just used to better define the imaging characteristics of a component.

Response to Q-H: No tests of this type are presently being conducted.

Response to Q-I: The most pressing problem we see is to make available for the Air Force a dynamic and versatile program for the laboratory testing of FLIR's. We have now made available two people and the facilities and equipment to attack this problem. The second problem we see is that perhaps not enough testing is performed. Many of the optical items, especially in the infrared, fail to meet procurement specifications when they are carefully tested. However, we suspect that only a small percentage of such procured items is actually sent to a laboratory such as ours for testing.

b. **Westinghouse Electric Corporation, Defense and Space Center Survey Response.** One of the prime businesses at Westinghouse is the design, fabrication, and testing of electro-optical equipment. Some of the programs for which special evaluation equipment has been built include the B57G Weapon Delivery System, the B52 EVS, the Pave Spike, and the Skylab space color camera. Also parallel analytical and experimental efforts are being made under Air Force Program 698DF to correlate theoretical, laboratory, rooftop, and flight test performance.

Response to Q-A, 1: We are not now fabricating or testing image intensifier devices except as noted in Q-A, 2.

Response to Q-A, 2: We test and evaluate components such as image intensifiers, TV camera tubes, and lenses to assure compliance with specification. We test and evaluate major assemblies such as image intensifier television cameras. We test overall systems, including the lens, to assure that overall performance requirements are met. Tests include dynamic range, resolution, tracking capability, etc. Both active and passive equipments undergo tests.

Response to Q-A. 3: We do not maintain test facilities in this area.

Response to Q-B. 1: We use test pattern projectors with constant 2854°K color temperature and variable light-level range of approximately 5×10^{-8} to 10^{-1} ft-c. The variable light-level range is controlled by selectable apertures.

Test areas with constant 2854°K color temperature sources provide scene radiance range of 1×10^{-6} ft-lamberts to 10^{-2} ft-lamberts over a 10- by 15-foot test target format. Sun guns cover the range of 10^{-2} to 10^{3} ft-lamberts.

We also use outside test facilities for day-night test capabilities.

A Perkin Elmer Model 112 Spectrometer modified for single-pass operation provides the capability to measure spectral sensitivity of image tubes over the range of 350 nanometers to 30 micrometers.

Response to Q-B. 2: An Optics Technology, Inc. Modulation Transfer Function Analyzer K-la is used for measuring the MTF of lenses and first-generation image intensifiers.

Response to Q-B. 3: We use observers and photographs only.

Response to Q-B. 4: We utilize an image motion head for use with test-pattern projectors. The head is continuously variable from DC to less than 5 seconds to cover the field of view.

Response to Q-C: The ability of a camera to produce an image of sufficient signal-to-noise ratio is the most sensitive indicator of field capability.

Response to Q-D: Not directly although image signal-to-noise ratio capability is inferred from indirect measurements and used, in conjunction with the results of parallel psychophysical experimentation, to predict field performance.

Response to Q-E: A considerable effort has been and is underway to relate field performance to lab performance. Use is made of lab tests, tower tests, and flight tests using common scene test objects.

Response to Q-F: Customers of our equipment and the various services.

Response to Q-G: Primarily to reject substandard devices or components and for overall equipment acceptance testing.

Response to Q-H: Yes.

Response to Q-I: The most critical gap is in the area of image degradation to be expected due to image motion and sensor lag effects. An analytical and experimental program is being conducted in conjunction with our Electron Tube Department but is in an early phase.

c. **General Electric Company, Aircraft Equipment Division Survey Response.** General Electric is involved in the development and evaluation of Low Light Level Television Systems and related intensifier devices. They have an extensive evaluation facility for conducting component and system tests on the television systems. They also have the capability to make limited measurements on real-time, thermal-imaging systems. This thermal capability is derived primarily out of their SCIRT program. The response from General Electric reflected a capability superior to that generally found in DOD or related industry. Their response included an in-depth answer to every question with a detailed description of the purpose, equipment, setup, procedure, and problem areas associated with every test they perform. Due to its length, the complete response is not included here. However, a few sample question responses are presented below:

Response to Q-C: It is felt that all of the tests conducted in our laboratory on Low Light Level Television Systems are important in determining the field performance of the system. Though the tests performed are necessary, this is not to say they are sufficient. In a number of cases, the tests performed are incomplete. We are continually improving our facilities and techniques to fill in these gaps.

Another equally important concern however is that if we were able to measure performance factors such as optical-transfer function or camera noise spectral power density more accurately we should still be faced with the problem of ranking the importance of these parameters in determining how a system will perform on a specific mission requirement. It is not clear, for example, what the relative importance of modulation transfer function and signal-to-noise is. By high frequency peaking, or aperture correction, we can improve the modulation transfer, but the peaking also tends to peak the noise and produce an irregular noise spectral power density function. The point is that, if both these parameters could be measured accurately, additional data would be necessary to determine how the measurements could be used to design a camera or predict field performance.

In spite of these uncertainties, it is generally felt that some measured parameters are better performance indicators than others. Tests conducted at Boeing[1] indicate that MTFA, i.e., the area bounded by the sensor modulation transfer function

[1] *Quantitative Determination of Image Quality*, Boeing Co., Report No. D2-114058-1, May 1967.

curve, the observer's size/modulation requirement curve called the demand modulation curve, and the high and low frequency cutoff curves is a strong predictor of the image quality and more importantly the data which can be extracted from an image. Tests conducted at Martin Marietta[2] indicated that, other factors being equal, contrast at the display was a strong indicator of probability of detection of a target. The "other factors being equal" does impose a severe limitation on the applicability of this data. In summary, although we can measure a number of parameters which are necessary to characterize a television system for field evaluation, we have very limited information on the sufficiency of this data and on the relative significance of the measured parameters in determining field performance.

Response to Q-D: Because the parameters which most affect television system field performance have not been identified with any certainty, it is very difficult for the specification writer to select the proper parameters. Those parameters which are believed to most nearly relate to field performance are usually not specified due to the lack of universally accepted measurement standards or procedures.

Response to Q-E & Q-H: Some attempts have been made to predict the limiting resolution of a camera system in a real-world environment using data measured on the camera system in the laboratory. A mathematical model was generated to calculate the spectral irradiance and contrast on the sensor photocathode as a function of parameters such as nocturnal irradiance, atmospheric visibility, field of view, target and background spectral reflectance, and others.[3] Limiting resolution at various contrast and irradiance levels was measured on the laboratory standard camera. In addition, signal-to-noise ratio and square wave amplitude response were measured at various irradiance levels.

This laboratory data was used with the mathematical model, and curves of expected performance were generated. The camera system was then tested at our Cazenovia test facility, and the limiting resolution was measured at ranges to several miles. For those ranges and conditions tested, agreement was within about 15% to 20%. The weakest link in the test was the estimation of visibility which had to be made by viewing large, high-contrast objects at ranges near the contrast threshold for the eye (same method as used by local weather bureau). Using the data from the previously referenced Martin Marietta report, probability of detection and recognition of a number of objects was predicted. In a series of field tests conducted with different observers from General Electric and Rome Air Development Center, ranges for detection and

---

[2] Ozkaptan, Ohmart, Bergert, & McGee: *Target Acquisition Studies for Fixed Television Field of View.* Martin Marietta, Contract No. N0014-67-C-0340.

[3] D. Cleverly: *An Active Television Mathematical Model.* General Electric Co., Technical Information Series R70EML3.

recognition of these objects were measured, and the probability of detection and recognition was calculated. Analysis of this data has not been completed at this date.

This type of field/laboratory correlation is at best a meager beginning. A great deal more testing of the correlation of field performance to laboratory data on television systems is necessary before system designers and specification authors will know what parameters should be specified and optimized in a camera system.

d. **Sacramento Army Depot Survey Response.** The Sacramento Army Depot has an extensive facility for supporting the Army's intensifier systems. The facility includes equipment for conducting the component and system tests necessary to repair a system and to then confirm that the system meets the original procurement specifications. Facilities were recently completed for evaluating the ARMY INFANT system, a system which incorporates a Low Light Level Television. There are also plans to modify some of their equipment to allow evaluation of FLIR systems.

Response to Q-A. 1: We have complete capability to determine the laboratory performance of all components, assemblies, and systems. The Depot has a long and extensive history of complete repair and testing of Starlight Scopes, NOD's etc., in all sizes.

Response to Q-A.2: The installation of a facility for complete evaluation of LLLTV systems and components was completed this past summer. A modular laboratory addition that increased Electro-Optical Division area by 50% permitted installation of the entire Hughes Aircraft Company INFANT test and evaluation equipment.

Response to Q-A. 3: The above-mentioned INFANT test facility is being adapted for complete repair and evaluation of several Army thermal-imaging systems. This Depot will assume 100% mission responsibility 1 January 1972 for one of these – the FLIR. Extensive training programs of Depot personnel (professional and skilled technical) to handle these systems has been in progress for 6 months. Special calibration equipment for these far-infrared-type systems was procured over a year ago.

Response to Q-C: The evaluation tests performed are intended to analyze system performance very adequately in regard to field applications.

Response to Q-D: Design and procurement requirements for fielded items are covered by DMWR's and MIL Specifications. The test and evaluation program at this Depot conforms with these documents.

Response to Q-E: *See Q-H.*

Response to Q-F: The test data is recorded and consolidated for use in studies by the PMO and Night Vision Lab.

Response to Q-G: The data is used primarily for accept-reject criteria in production testing but also used as stated in Q-F.

Response to Q-H: Engineering, calibration, and product-improvement personnel at this Depot are currently engaged in a joint study and experiment with the Night Vision Lab relating various combinations of image tube and night vision scope measurement parameters to field performance.

Response to Q-I: The evaluation problems presently of concern to Sacramento Army Depot mainly relate to conversion of existing LLLTV test equipment to the evaluation of thermal-imaging devices. The Maintenance Division Engineering staff and Product Improvement group in the Electro-Optical Division are attacking this program.

8. Survey Analysis. As a result of information obtained from the written survey responses and/or the on-site surveys, the following observations appear to best reflect the general status of image evaluation in DOD and related industry:

- There is no unified image-quality methodology for determining the laboratory performance of photon-imaging systems in terms relatable to field performance or utility existing in DOD today.
- The image-quality technology that has been advanced and consolidated by DDR&E, IDA, and others has not been implemented in most DOD image-evaluation areas.
- Expertise in performing image-evaluation measurements and the physical facilities required are generally lacking in government laboratories.
- Many governmental equipment procurement areas are completely dependent upon industry in determining what image-quality performance tests are required for procurement of photon-imaging systems. The lack of in-house expertise on the part of many government laboratories allows only crude cross checks between tested laboratory performance and system field utility.
- In general, laboratory facilities that do exist in DOD and related industry are rigid in design and can be used to perform only the archaic image-quality measurements for which they were originally designed.

- The Army's Night Vision Laboratory at Fort Belvoir and the Naval Air Development Center appear to be exceptions to the above observations. These laboratories are leading industry toward accepting advanced laboratory image-quality specifications that have potential to reflect field performance or utility.

- There appears to be an awareness on the part of all technical areas surveyed of a general lacking in DOD of meaningful laboratory image-evaluation techniques. This awareness seemed to be somewhat recent on the part of the government laboratories visited.

- The technology of specifying photon-imaging systems is lagging that of specifying system components.

- The use of MRT as advanced by Sendall and Lloyd appears to be the only image-quality system performance specification in use today. Unfortunately, as presently measured in DOD, there is little uniformity in the measurement procedure and the type of pattern used.

- Several major industrial firms, such as Texas Instruments and General Electric, are embarking on an image-evaluation facility modernizing program using in-house funds.

IV. PROTOTYPE OF DOD ADVANCED, IMAGE-EVALUATION FACILITY

9. **Introduction.** The prototype of the DOD Advanced, Image-Evaluation Facility has been designed to evaluate a wide variety of photon-imaging systems, e.g., Low Light Level Television (LLLTV), Infrared (IR), and Image Intensifier (I^2) Systems. The implementation of this facility throughout DOD will provide a *common equipment base* for performing standard, image-quality measurements in the laboratory.

It is envisioned that a limited number of facilities based on this prototype would be established at major laboratories in DOD. These laboratories would be the "Centers of Excellence." It should not be inferred that every DOD photon-imaging-device contract would require such a comprehensive facility for use at the DOD originating laboratory and in the related industrial laboratories. Rather, less expensive and specialized equipments would be derived from the Evaluation Facilities at the DOD "Centers of Excellence."

The Advanced, Image-Evaluation Facility Prototype which has been designed is based on a modular concept and lends itself well to changes that may be required due to future advances in image-evaluation procedures. The Facility (Fig. 5) is divided into

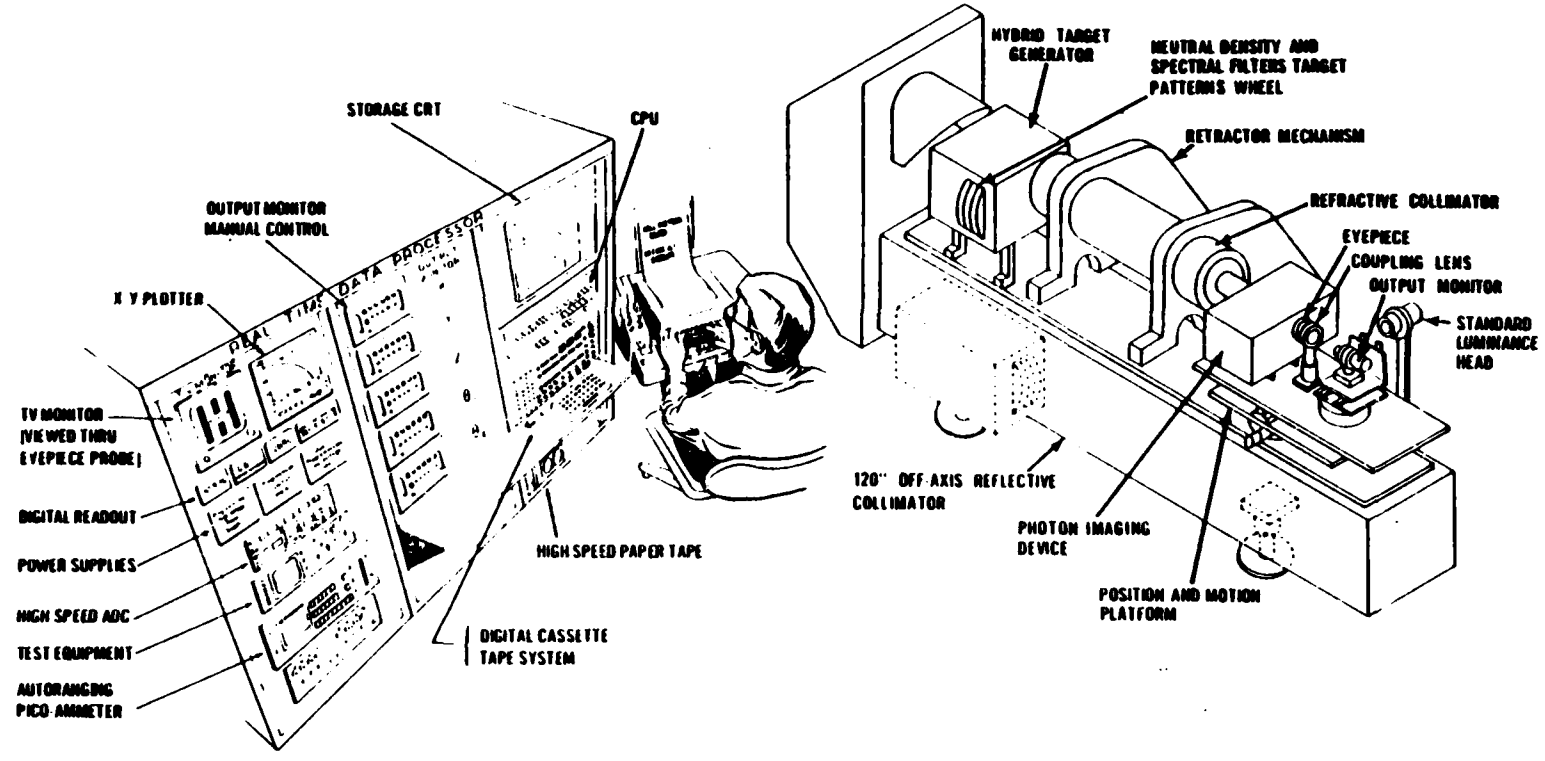

Fig. 5. Prototype of DOD advanced image evaluation facility.

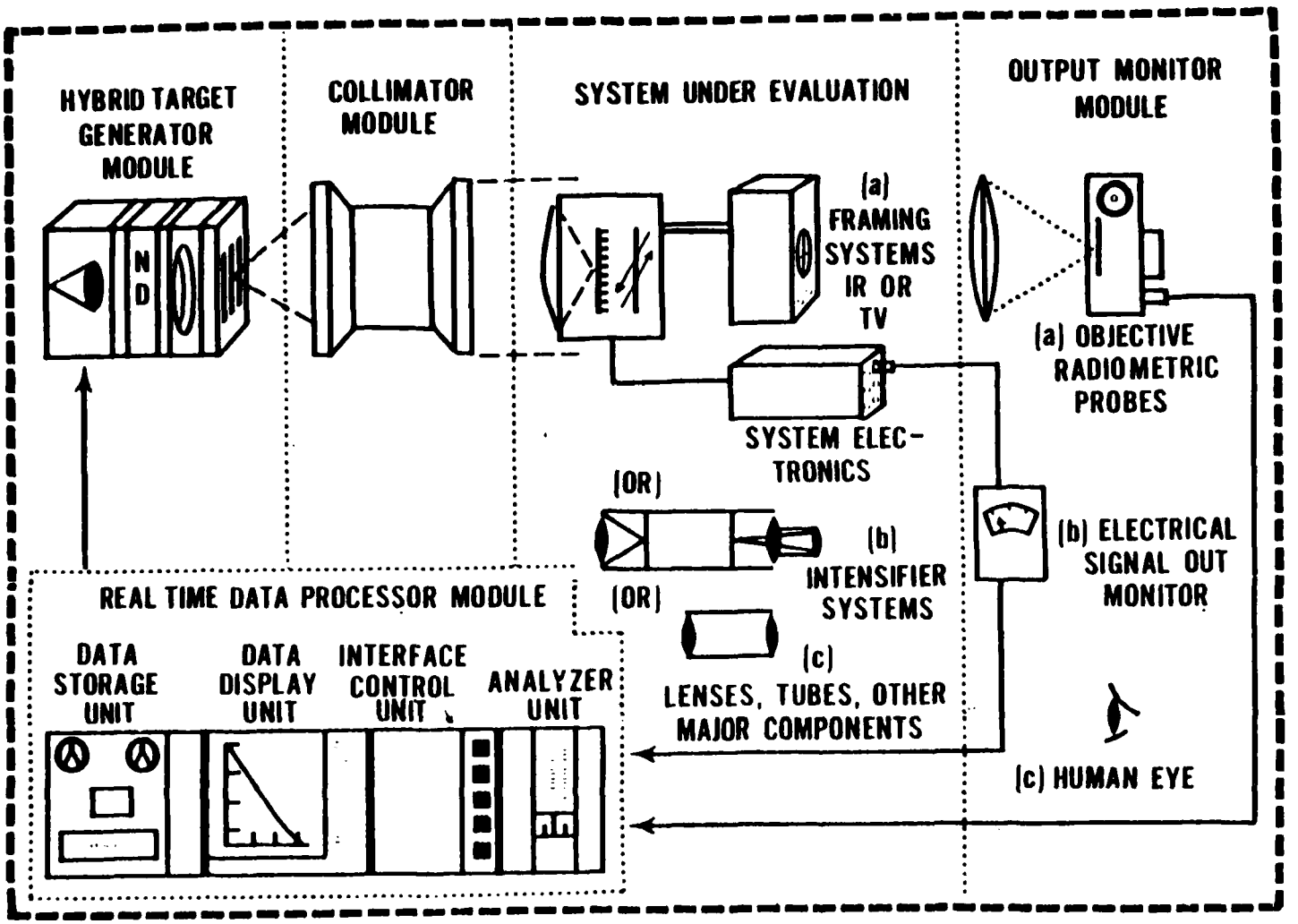

Fig. 6. Major modules of the DOD advanced image evaluation facility.

five major modules (Fig. 6). Each module may be modified or replaced without altering the basic structure or capability of the Facility.

A Real Time Data Processor Module is incorporated into the facility design to provide complete electro-mechanical control of the Facility and to process the data required to characterize the performance of the system under test. The high-level, conversive, basic language that controls this processor is such that engineers and scientists can easily program and operate the Facility without the support of specialized computer personnel. In addition, a manual override capability for the electro-mechanical controls is provided for most functions.

The Facility is primarily housed on a 120-inch reflective collimator which presents a target image at infinite conjugate to the system under test. The patterns used to present these target images are mounted on a rotating wheel located inside a Hybrid Target Generator Module.

The Hybrid Target Generator utilizes the same patterns to cover all the spectral regions from the visible to the far infrared. It incorporates several energy sources that emit controlled amounts of radiant energy over a wide dynamic range of contrast.

The target energy is transmitted by the Collimator Module and is focused by the photon-imaging system which is mounted directly on the Output Monitor Module.

The Output Monitor Module rotates the photon-imaging system about its nodal point in both azimuth and elevation. This rotation allows the target to be dynamically slewed and positioned throughout the field of view.

On the same platform, behind the photon-imaging system, is a scanning optical probe which is coupled to a photomultiplier tube via fiber optic rope. The output of the tube is sent to the Real Time Data Processor Module for analysis.

The Processor provides for three major types of photon-imaging-system output:

- Analog optical scanner
- Direct electrical
- Subjective performance via keyboard entry.

In addition to processing data and generating parametric evaluation curves, the Processor continuously monitors and controls the condition of all the variables of each module. Monitoring these variables ensures the validity of test parameters such as differential temperature, target contrast, target type, and scanner position. If a specified parameter, e.g., differential temperature, is not maintained within preset tolerances, the priority-

interrupt feature of the Processor will stop the test and notify the user. In a severe case, the Processor will cycle into an automatic shutdown mode to prevent damage to the Facility or photon-imaging system under test.

Each of the major modules is described in detail in the ensuing paragraphs.

10. Hybrid Target Generator Module. The Hybrid Target Generator Module generates the targets which are projected into the input port of the photon-imaging system under test. It is a hybrid generator in that it provides calibrated target radiation in both the visible (.4μ to 1.2μ) and infrared (3.0μ to 14μ) spectral regions by using one of two possible energy sources behind a common target wheel. The actual targets, which mount in a target wheel, consist of a wide range of geometric patterns that are presented to systems over a wide field of view.

This module is designed so that it is compatible with both the long focal length reflective and short focal length refractive collimators. The following paragraphs describe the three basic components of the Hybrid Target Generator Module: the infrared source, the visible source, and the target pattern wheel.

a. Infrared Source. The infrared source provides a 5- by 5-inch, uniform-temperature, controllable blackbody source that ranges in temperature from 10° to 100°C. This source is slewable from 100°C to 10°C in 10 minutes. A 40-inch target wheel which has 50 interchangeable target patterns near its circumference, is located in front of the blackbody plate. As illustrated in Fig. 7, the source is centered on these target patterns. The targets are etched in metal and have front surfaces with emissivities identical to the source itself. The temperature of the etched-out area is that of the blackbody source, while the temperature of the remaining pattern background assumes that of the wheel. Both the temperature of the wheel and the temperature difference ($\triangle$T) between the wheel and the source are monitored and controlled. In front of the wheel is a baffle plate whose temperature is also controllable. The function of this plate is to provide a uniform background for systems having a wide field of view. As an example, if the plate is 24 inches square and a 48-inch focal length collimator is being utilized to project the target information at infinite conjugate, the field of view of the photon-imaging system could be as large as 28° and still be viewing a uniform-background target area. For the same collimator, the target area itself subtends 5° for the 4-inch format target. The front surface emissivity of the baffle plate matches that of both the source and target pattern background. The baffle plate has aperture inserts that are matched to the size of the target in the wheel. Detail specifications for this source are shown in Table 3. Note that all significant temperature levels are monitored and controlled by the computer and that a manual override is provided.

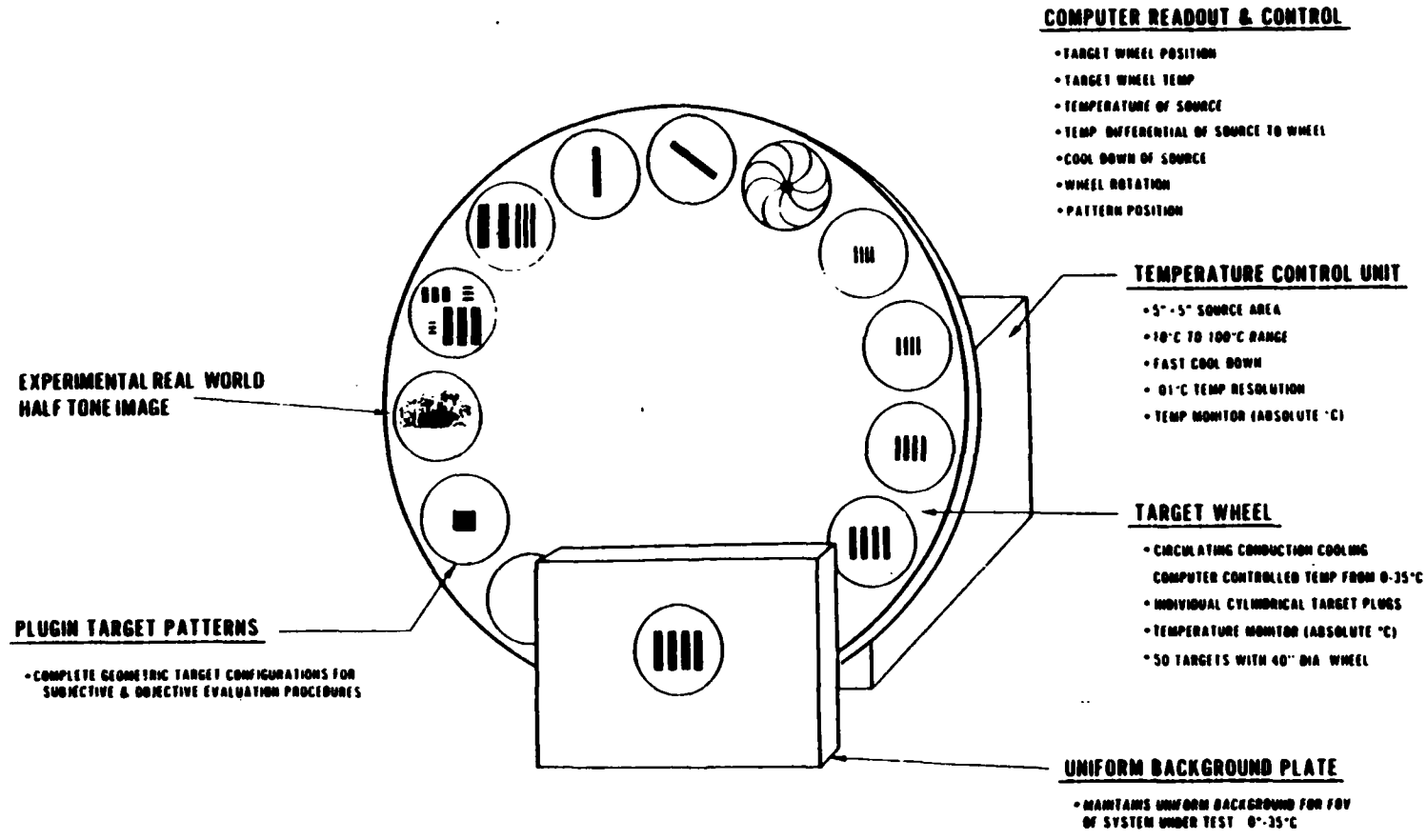

Fig. 7. Hybrid target generator module (thermal mode).

Table 3. Hybrid Target Generator Component Specifications (Thermal)

Component	Specifications					
	Temperature Range	Temperature Stability	Temperature Differential		Size	Aperture
1. IR Source	10°-100°C ± 1°C[a][b][c]	± 0.1°C	1-2 1-3	0.01°C[a][b] 0.02°C[a][b]	5" x 5" Format	Full Open
2. Target Wheel	0°-35°C ± 1°C[a][b]	±0.1°C	2-1 2-3	0.01°C[a][b] 0.02°C [a][b]	40" Diameter	4.0" Circular 1.0" Circular 0.75" Circular 0.5" Circular
3. Baffle Plate	0°-35°C ± 1°C[a][b]	± 0.1°C	3-1 3-2	0.02°C[a][b] 0.02°C [a][b]	24" x 24"	4.0"Circular 1.0 " Circular 0.75" Circular 0.5" Circular

(a) Monitored with platinum resistance thermometer with computer readout.

(b) Computer controlled with manual override.

(c) Computer controlled slew rate of 10 minutes from 100°C to 10°C with manual override.

b. **Visible Source.** The visible source provides a uniform, lambertian, 4- by 4-inch, luminance format at 2854°K which is continuously variable from 10^{-6} fL to 100 fL. In addition, when the target wheel is placed in near proximity to the lambertian format, the apparent contrast of the target pattern may be varied from 0 to 95% (modulation definition) by using a second source and a pellicle. A general schematic of this configuration is shown in Fig. 8 where L_1 and L_2 are the two visible sources. Visible source L_2 acts to superimpose light on the target image that is seen when viewing through the collimator. These two sources are well matched in spectral radiance and, in fact, are identical except that L_1 allows spectral filters to be inserted in the light path to make L_1 a spectrally narrow-band source for spectral-response measurements. A more detailed schematic of the mechanical configuration that constitutes the visible source of the Hybrid Target Generator is shown in Fig. 9. Note that tungsten bulbs (calibrated by Eppley Laboratories and traceable to NBS) are the heart of these sources. These bulbs are movable giving square-law changes in the energy impinging on the large sphere entrance aperture. In addition to the square-law change, the bulbs can be moved into the smaller, 3-inch, integrating sphere where a greater solid angle of bulb irradiance can be utilized. A light-attenuation wheel, which is positionable at a variety of filter and aperture combination settings, serves to provide additional light attenuation.

Table 4 contains a detailed review of the visible-source specifications. Note that all major light contrast and luminance levels are monitored and controlled by the computer and that a manual override is provided.

c. **Target Wheel.** The last major component of the Hybrid Target Generator Module is the target wheel (Fig. 7). It is designed to allow its energy source to be either visible or thermal. This design feature means that, regardless of the spectral energy to which any photon-imaging system is sensitive, the patterns are the same. The wheel is designed to allow cooling from 0° to 35°C when used with the thermal source. When used with the visible source, the coolant and wheel are allowed to obtain ambient temperature and no control is necessary. In addition to the flexibility of use in either the thermal or visible mode, the wheel has a variety of target patterns. They are etched to a tolerance of ±0.0002 inch and are interchangeable in the various slots in the wheel. There are four target sizes in the wheel: 4.0, 1.0, 0.75, and 0.5 inch. Fifty target patterns are available on one target wheel. Some initial patterns to be used as targets for image evaluation procedure development are listed in Table 5. As procedure development advances, a second wheel will be added to accommodate additional target patterns that may be required.

11. **Collimator Module.** Many photon-imaging systems are unable to focus on a target closer than 25 meters. From a facility standpoint, such distant targets would require working distances unobtainable in the laboratory. In addition, the targets are

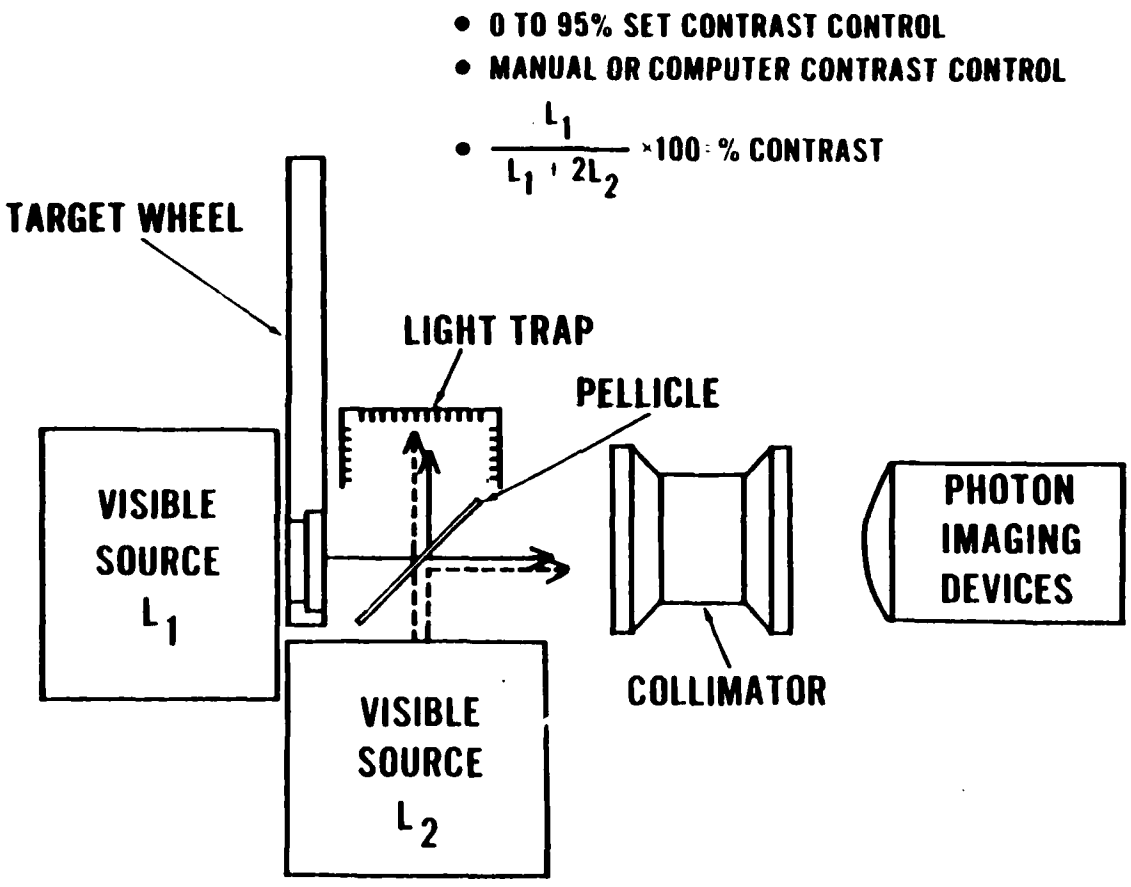

Fig. 8. Hybrid target generator module (visible mode).

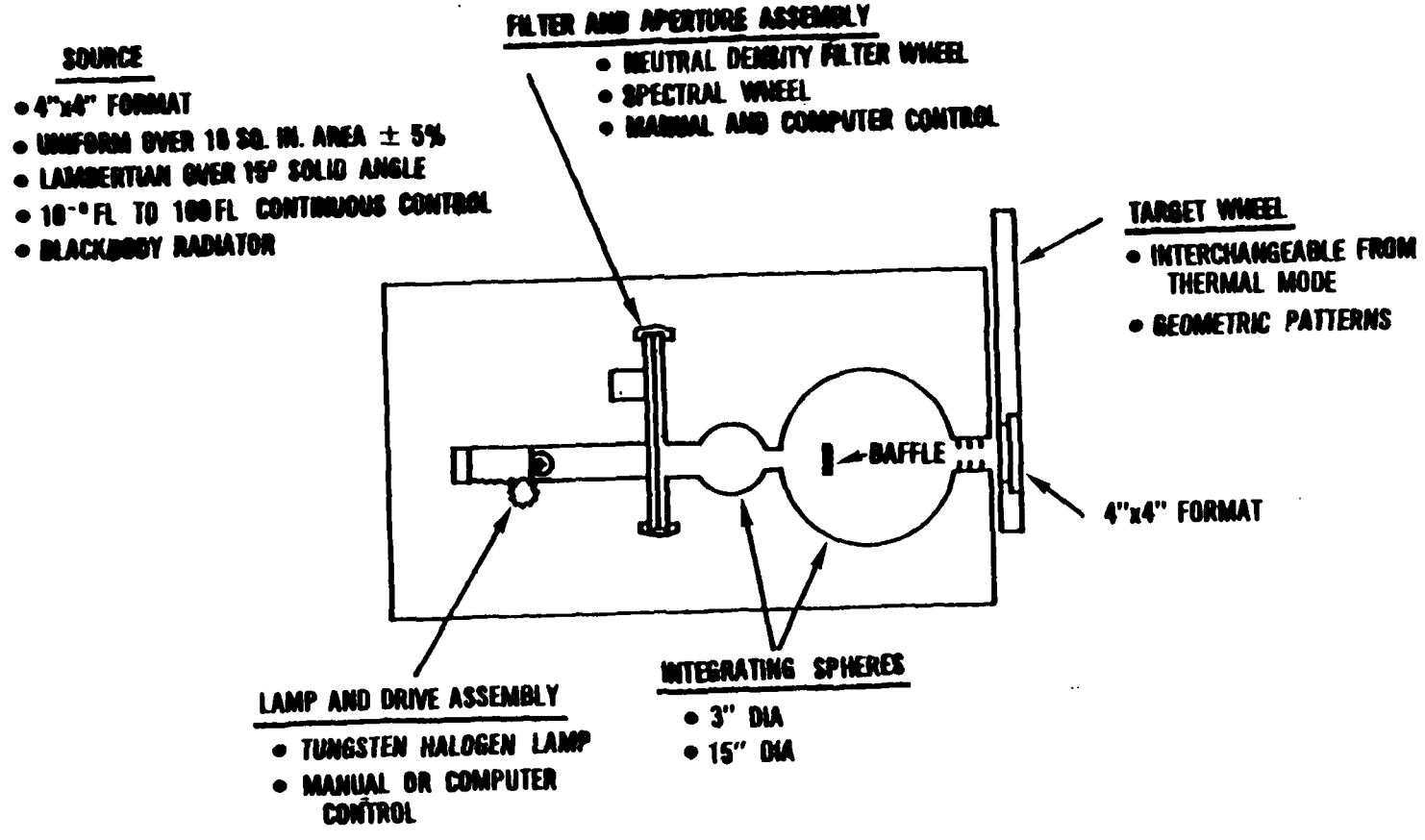

Fig. 9. Hybrid target generator module (visible mode).

Table 4. Hybrid Target Generator Component Specifications (Visible)[a]

Component	Specifications			
	Spectral Distribution	Luminance	Contrast $(L_1/L_1 + 2L_2)$	Sizes
1. Visible Source (L_1)	2854°K[b] or any of 24 spectral narrow-band filters[c] [d] from 0.4μ to 1.2μ meters	~ 10^{-6} fL to 100 fL ± 2% 10^{-4} -100 ± 5% 10^{-6} -10^{-4}	0-95%[d] ± 5% of set control contrast value simulated using 50/50 pellicle	4" x 4" format[e] uniform to ± 2%
2. Visible Source (L_2)	2854°K[b]	~ 10^{-6} fL to 100 fL[d] ± 2% 10^{-4} -100 ± 5% 10^{-6} -10^{-4}		4" x 4" format[e] uniform to ± 2%
3. Target Wheel	NA	Rm background black 10^{-6}	Apparent contrast determined by L_1 and L_2	40" dia. with 4.0" 1.0", 0.75", and 0.5" circular apertures

(a) Power supply for source is regulated to 0.02% with line voltage variation of ± 10% with 0.1 hour resolution elapsed time meter.

(b) Bulbs used in the source are run at a current which allows their spectral irradiance curve to most closely match that of a 2854°K blackbody curve. This current and a full calibration curve of spectral irradiance from .4 to 1.2μ are supplied for each lamp by Eppley Laboratories. The relative spectral response for any light level at the sphere output through the beam splitter does not vary from that of the bulb itself (when normalized to 600 nm) by more than 5% from .4μ to .75μ and not more than 10% from .75 to 1.2μ.

(c) To be ordered.

(d) Computer controlled with manual override.

(e) Lambertian over 15° solid angle verified by making luminance measurements from 0-15° off-axis. Variation in luminance measured from any off-axis angle over the 15° range is less than 5% of the luminance measured on axis.

Table 5. Target Pattern Specifications

Pattern	Quantity	Specifications[a]
Single Slit	1	0.001″ width, 0.75″ height, 1″ format, vertical
Single Slit	1	0.001″ width, 0.75″ height, 1″ format, horizontal
Single Slit	1	0.003″ width, 0.75″ height, 1″ format, vertical
Single Slit	1	0.003″ width, 0.75″ height, 1″ format, horizontal
4-Bar[b] (Variable Aspect Ratio)	19	0.75″ constant height, variable width, 1″ format 0.197 to 1.64 c/mm frequency range
4-Bar[b] (7:1 Aspect Ratio)	20	0.75″ format for 0.2 c/mm to 0.3 c/mm, 0.50″ format for 0.4 c/mm to 1.75 c/mm
Distortion	1	4″ format, cross-hair reticle
Blank	1	4″ format
Blank	5	1″ format

(a) All patterns etched to ±.0002 inch.

(b) Both sets of 4-bar patterns will be extended in range to 3.50 c/mm on a second target wheel.

not available in small sizes for high-resolution tests and must be optically minified. A single, reflective collimator located between the target and the photon-imaging system satisfies these two requirements but not a third, and equally important, requirement of providing a wide field of view with low, off-axis distortion.

To satisfy the third requirement, two types of collimators are utilized. A 120-inch focal length, off-axis, reflective collimator with extremely high resolution and narrow field of view provides high resolution. Three refractive collimators, each with 48-inch focal length and 12-inch clear aperture, provide an on-axis resolution of 10 cycles per milliradian at reasonable modulation. The amount of modulation decreases somewhat at 5 degrees off-axis but is still usable.

The spectral range of each of the three refractive collimators is as follows:

- 0.4 micrometer to 1.6 micrometers (visible and near infrared),
- 3 micrometers to 6 micrometers (mid infrared),
- 8 micrometers to 15 micrometers (far infrared).

12. **Output Monitor Module.** The Output Monitor Module is the optical interface that acquires optical-output information from the photon-imaging systems. The module is divided into two, optical-scanning systems. The first scanning system is shown in Fig. 10. The photon-imaging-system display is focused through its eyepiece and a coupling lens onto a fiber-optic probe or slit. The total amount of light transmitted to the probe, as restricted by an entrance pupil in the Output Monitor Module, emulates the light that would be transmitted to the retina of the human eye. The probe is mounted on a translation unit that provides scanning in the x and y directions, focusing in the z direction, and rotation (ω). This translation unit is mounted on a position and motion platform that accommodates the coupling lens and the photon-imaging system.

The function of the position and motion platform (Fig. 10) is twofold: (1) it rotates (ϕ, θ) the photon-imaging system around its nodal point in two planes allowing an image to be positioned accurately in a system having a field of view as large as 60 degrees; (2) it moves an image across a system's field of view at a given rate which allows characterizing time lag and persistence performance of the system. The maximum speed of rotation is 30 degrees per second. The speed at which the system rotates (ϕ, θ) is continuously variable.

The second scanning system (Fig. 11) is for analyzing those photon-imaging systems whose outputs are remote view and do not include an eyepiece. This scanning system is mounted on a platform that provides four freedoms of motion: x, y, z, and θ. However, only motion in the x-y plane is used for photon-imaging-system characterization. This platform travels a maximum of 14 inches in the x or y directions in 40 seconds and maintains position accuracy within 3 micrometers. The z direction is used for focus; rotation (ω) is used for self calibration of its probe with a standard-luminance light source.

The complete motion and rate functions of both scanning systems are monitored and controlled by the computer. A manual override for these functions is provided.

13. **Real Time Data Processor Module.** The Real Time Data Processor Module controls and monitors the electro-mechanical functions of all modules in the Facility in addition to processing the system performance data from the Output Monitor Module. Ease of operating and manually overriding this module were important design considerations. The high-level, conversive language that controls this module is such that scientists and engineers can program and operate the Facility without the support of highly trained computer programmers and operators. Figure 12 depicts the major features of this module.

Unlike some computer-based systems, this module is not in a closed-loop control-cycle with the other modules in the Facility. It transmits instructions to each

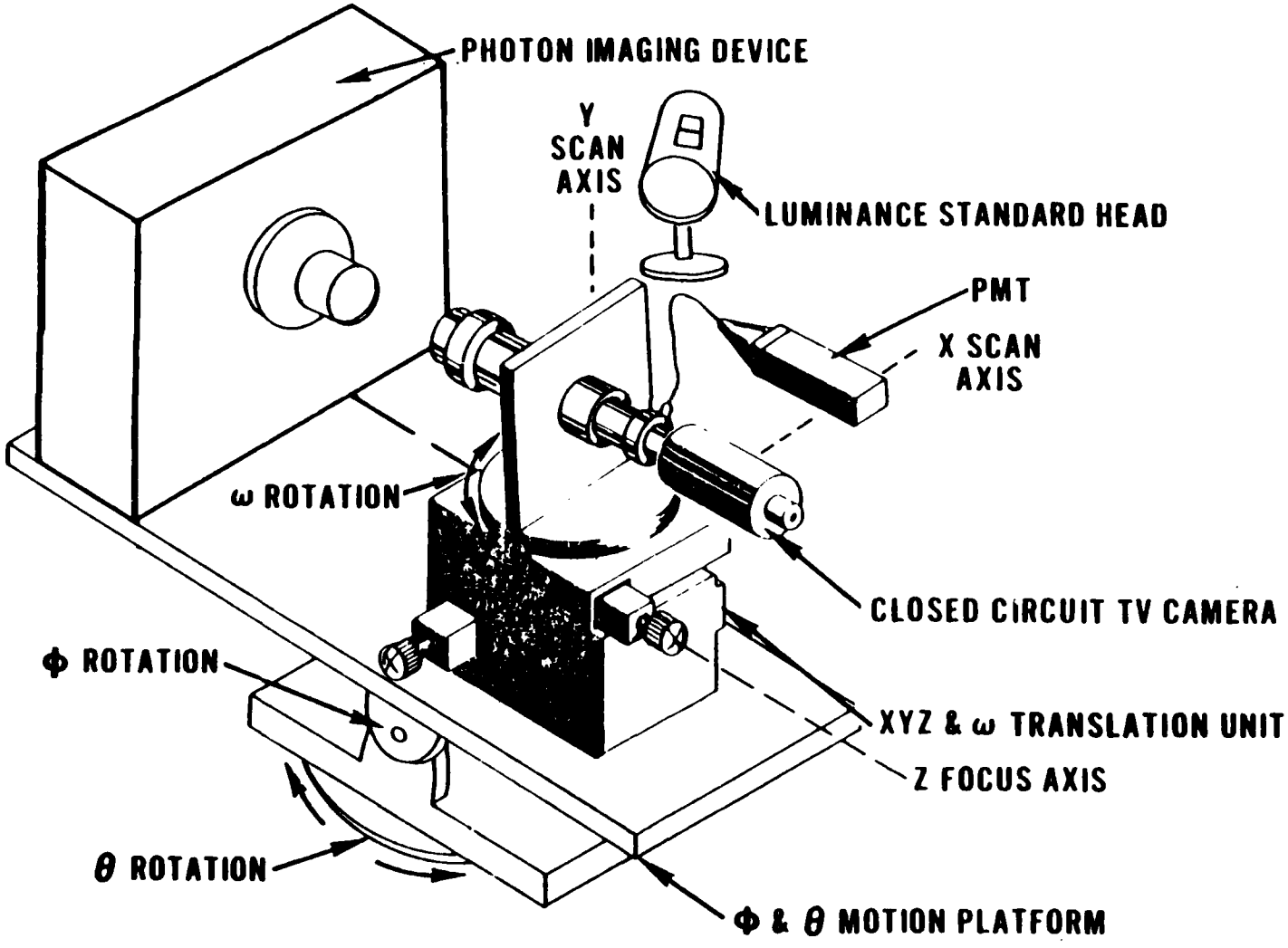

Fig. 10. Output monitor module.

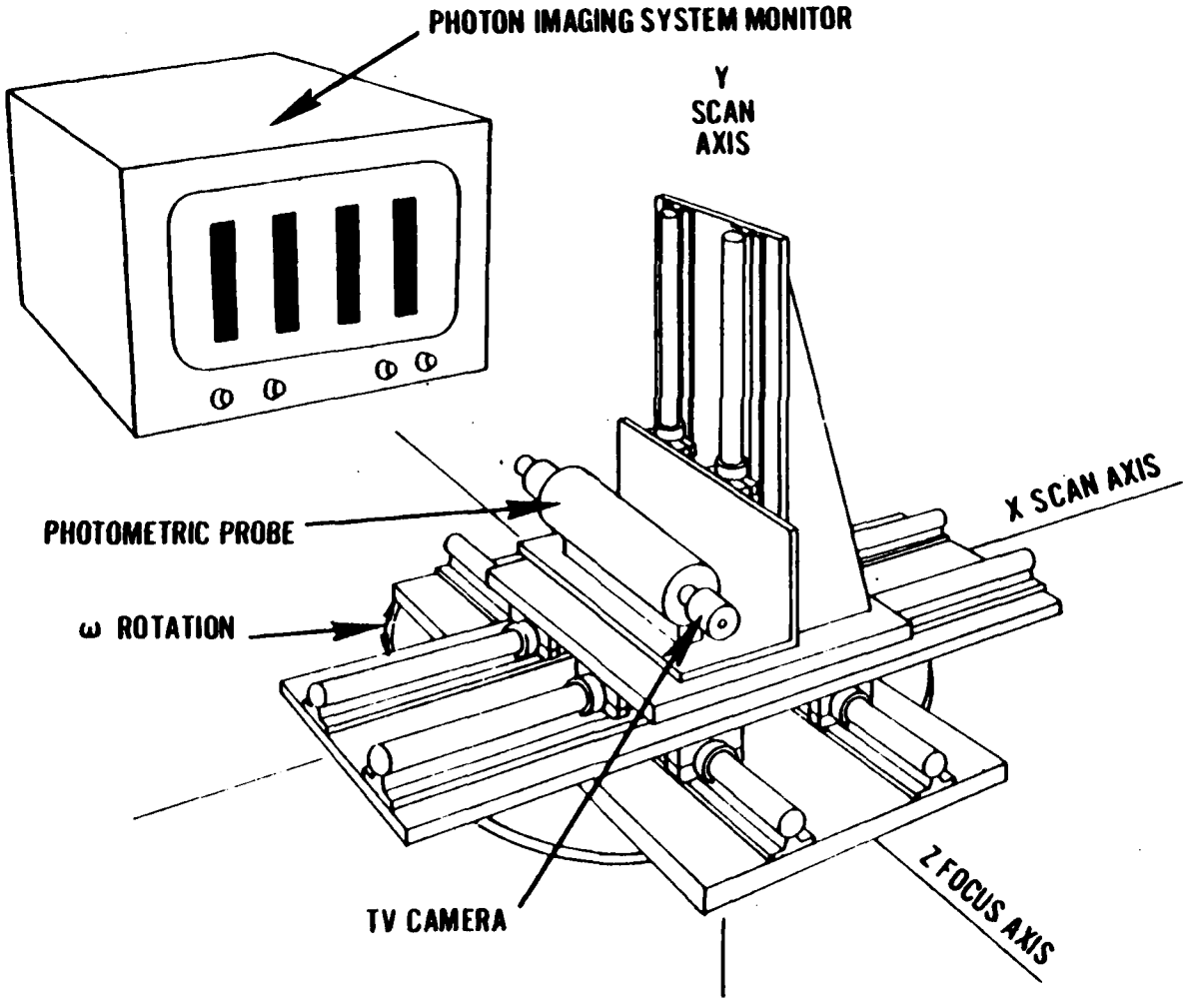

Fig. 11. Remote display scanning unit.

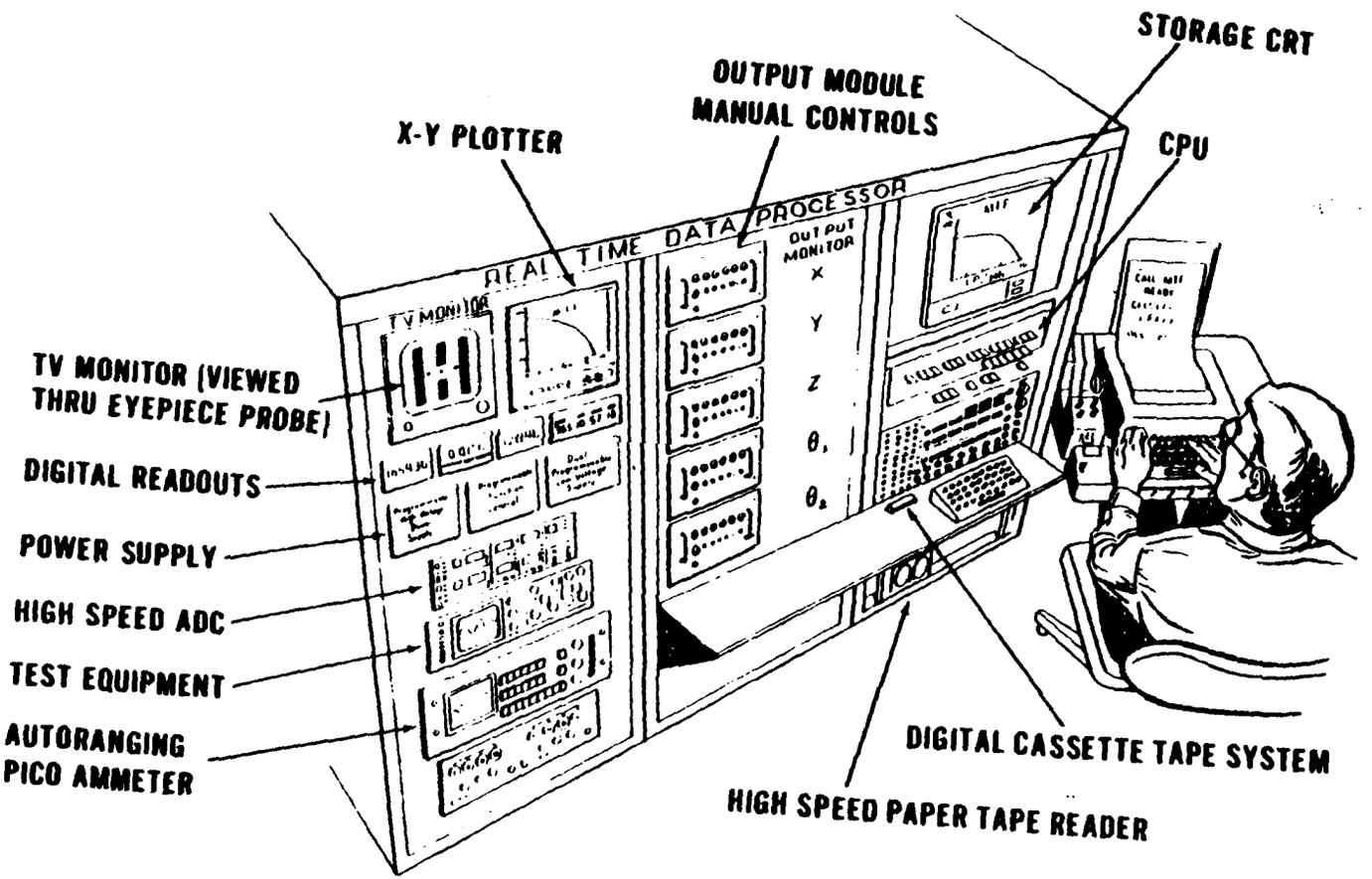

Fig. 12. Real time data processor module.

module according to the test configuration specified by the user (e.g., light level, contrast, ΔT, scanning speed, travel distances, etc). After all modules have been initialized, it cycles through an integrity check for each module to ensure that all test criteria have been satisfied. The Processor, then, either indicates that the test may be executed or identifies any particular problems. In the event that a severe problem is encountered, the Processor automatically cycles into a complete shutdown mode, thus, avoiding any possible damage to the Facility or photon-imaging system under test. The user may then attempt to rectify the problem. Should a failure occur in the central processing unit (CPU), the Facility's manual mode may be employed to initialize the modules and to execute the test. The manual mode is slower and data cannot be processed until the CPU is operable. However, the output data can be tabulated and stored for future processing, and a real-time plot of the data can be generated.

The Real Time Data Processor Module utilizes a high-level, conversive language called Extended Basic. For all practical purposes, this computer language enables the user to communicate with the Processor in English. A list of commands is compiled in Table 6. The user may enter commands to the Processor via a teletypewriter or an interactive keyboard. The output from the Processor appears in the form of (1) teletype copy, (2) storage CRT, and (3) hard copy (X-Y plotter) in tabular or graphic form for a real-time data review.

The quick storage and retrieval feature of the Processor allows vital programs and large amounts of data to be saved and retrieved by entering commands like: "SAVE PROG 1" or "LOAD TABLE 2." The disk memory holds key system programs and data for fast retrieval. A cassette tape device complements the disk storage and is useful for exchanging software and large data files with other similar facilities.

A sample list of the application programs currently available is compiled in Table 7. The application programs are in the form of a library stored within the system. The user can select individual programs by name and combine them to work with other programs.

Data acquisition and control from the Real Time Data Processor Module combine convenient front-access interfacing for special experiments with the hardwired facility interface. A wide variety of analog and digital I/O modules, including an interrupt capability, a real-time clock, and operating-system software, enables the user to fully control the operation of the Facility. It is important to remember that the user retains ease of programming with Extended Basic to control input/output functions but that all I/O functions are actually performed in machine language to maximize throughput. Complete system architecture is shown in Fig. 13.

Table 6. Extended Basic Commands

General commands	
LET [variable] = [formula]	assigns to the variable the value of the formula
READ [variable list]	assigns to the variable list values obtained from the DATA list
DATA [number list]	lists the numbers which will be assigned to the variables named in a READ statement
PRINT [variable, literal, formula]	prints formatted alphanumeric information on the teleprinter or CRT
FOR [variable] = [formula] TO [formula] STEP [formula]	causes a program to loop through a sequence from an initial value to a final value according to a step size
NEXT [variable]	terminates a FOR loop when the final value is reached
IF [formula] [relation] [formula] THEN [line number]	branches to the specified line number if the relationship of two formulas is true
GOTO [line number]	branches to the specified line number unconditionally
GOTO [formula] OF [line number list]	branches to one of several line numbers depending on the value of the formula
DIM [array list]	reserves array storage for arrays larger than 10 by 10
END	terminates a program
DEF FN [letter] [variable] = [formula]	defines a function used later in the program
INPUT [variable list]	allows data to be entered via the teleprinter and stored as the specified variables
STOP	causes the computer to halt
REM [remark]	supplies remarks for program descriptions
RESTORE	reinstates a DATA list to allow it to be reread by another READ statement
GOSUB [line number]	branches to a subprogram that begins at the specified line number
GOSUB [formula] OF [line number list]	branches to one of several subprograms depending on the value of the formula
GOSUB [line number] [parameter list]	branches to a subprogram and passes the specified parameters to it
SUB [variable list]	defines the variables in a subprogram to be passed by a GOSUB parameter list statement
RETURN	returns control to the main program after a GOSUB subprogram has been executed
WAIT [formula]	causes the program to pause for the number of milliseconds specified by the value of the formula
CALL [name] [parameter list]	branches to an assembly language program appended to BASIC for high speed processing
File Commands	
FLIST [null A B]	lists the names of all program and data files stored on disc, tape or cassette
DELETE [name –null –A –B]	deletes the named program or data file from one of 3 file units
SAVE [name –null –A –B]	copies the named program file in core onto one of 3 file units
COPY [name –null –A –B TO [name –null –A –B]	copies the named program or data file in one file unit onto another unit
CLEAR [A B]	deletes all files from tape or cassette
ASSIGN [name –null –A –B] [file no 1 2 3]	relates logical data file numbers to actual file names
LOAD [name –null –A –B]	copies the named program file from one of 3 file units into core
OPEN [file no] [write read] [variable]	initializes access to a data file, specifies whether it is write-only or read-only, and sets a variable to the number of values in the file
CLOSE [file no] [variable list]	terminates access to a data file and sets a variable to the number of values in the file
GET [file no] [variable list]	copies the specified data file from one of 3 file units into core as the named variables
PUT [file no] [variable list]	copies the data file having the named variables from core onto one of 3 file units
Control Commands	
RESTART	initializes ADAPTS by specifying the hardware configuration and loading a new copy of Extended BASIC and its various modules into core from the system disc, accomplished by teleprinter dialogue
SCRATCH	deletes the current in-core BASIC program
LIST [line number]	lists the current in-core BASIC program on the teleprinter or CRT from the specified line number to the end of the program
PLIST [line number]	punches the current in-core BASIC program on the teleprinter or high-speed punch from the specified line number to the end of the program
PTAPE	reads a BASIC program into core from the teleprinter or high-speed punched tape reader
RUN [line number]	starts execution of the current in-core BASIC program from the specified line number
REMOVE [line number] TO [line number]	deletes selected lines from the current in-core BASIC program
CALL RENUMB [line number] [increment]	renumbers the entire current in-core BASIC program
ESC key	interrupts program execution and returns to the "READY" state
CTRL FORM keys	initializes the CRT to the beginning of a new page

Table 6 (cont'd)

CRT Commands	
CALL CRT	switches the output of alphanumeric information from teleprinter to CRT
CALL TTY	switches the output of alphanumeric information from CRT to teleprinter
CALL SIZE [character size]	defines the size of alphanumeric characters to be displayed on the CRT from 1 to 60
CALL ERASE	clears the CRT
CALL POS [X] [Y] [mode]	positions the X and Y coordinates of the CRT absolutely or relative to the last position does not write
CALL POINT [X] [Y] [mode]	same as CALL POS but writes a dot at the selected coordinates
CALL VECT [X] [Y] [mode]	writes one straight line on the CRT from current coordinates to specified coordinates relative or absolute

Input-Output Commands	
CALL DATAI [channels] [array variable] [values] [frame] [delay]	inputs the number of [values] of analog or digital data via the selected [channels] of the general purpose multiplexer according to the [frame] and [delay] times and stores these as floating point numbers in [array variable]
CALL DATAIF [channels] [file no.] [values] [frame] [delay]	same as CALL DATAI but stores as integers into [file no.]
CALL DATAO [channels] [array variable] [values] [frame] [delay]	outputs the number of [values] of analog or digital data from the [array variable] to the selected [channels] according to the [frame] and [delay] times
CALL STATUS [status no.] [variable]	stores the true-false condition of the selected status line number as the indicated variable
CALL PULSE [pulse no.]	outputs a control pulse to the selected pulse line number

Matrix Commands	
MAT READ [array variable list]	assigns to the array variable list a matrix of values obtained from the DATA list
MAT PRINT [array variable list]	prints the values of the array variable list as a matrix on the teleprinter or CRT
MAT [array] = [array]	equates matrices
MAT [array] = [array] + [array]	adds matrices
MAT [array] = [array] − [array]	subtracts matrices
MAT [array] = [array] * [array]	multiplies matrices
MAT [array] = [formula] * [array]	multiplies a matrix by the value of the formula
MAT [array] = ZER [array]	sets all elements of a matrix to zero
MAT [array] = CON [array]	sets all elements of a matrix to one
MAT [array] = IDN [array]	forms an identity matrix
MAT [array] = TRN [array]	forms the transpose of a matrix
MAT [array] = INV [array]	inverts a square matrix

Functions	Definition	Operators	Definition
SIN (X)	Sine of X	+	Addition
COS (X)	Cosine of X	−	Subtraction
TAN (X)	Tangent of X	*	Multiplication
ATN (X)	Arctangent of X	/	Division
EXP (X)	Constant e to the X power	↑	Exponentiation
LOG (X)	Natural logarithm of X	<	Less than
SQR (X)	Square root of X	<=	Less than or equal to
ABS (X)	Absolute value of X	=	Equal to
INT (X)	Largest integer = X	>	Greater than
RND (X)	Random number between 0 and 1	>=	Greater than or equal to
SGN (X)	1 if X > 0; 0 if X = 0; −1 if X < 0	<>	Unequal to
TAB (X)	Space to column # where X > 0 (through 71)	AND	A AND B = 0 if A = 0 or B = 0 A AND B = 1 if A = B = 1
FN (X)	User defined function of X where FN = FNA, FNB, ... FNZ	OR	A OR B = 0 if A = B = 0 A OR B = 1 if A = 1 or B = 1
		NOT	X = 0 if X = 1 X = 1 if X = 0

Variable Types	
1)	A, B, ... Y, Z
2)	A0, A1, ... B0, B1, ... Z8, Z9
3)	A(1), A(2), ... B(1), B(2), ... Z(255)
4)	A(1,1), A(1,2), ... B(1,1), B(1,2), ... Z(255,255)

Types (3) and (4) are subscripted variables of one or two dimensions. Subscripts can be integers, variables or formulas.

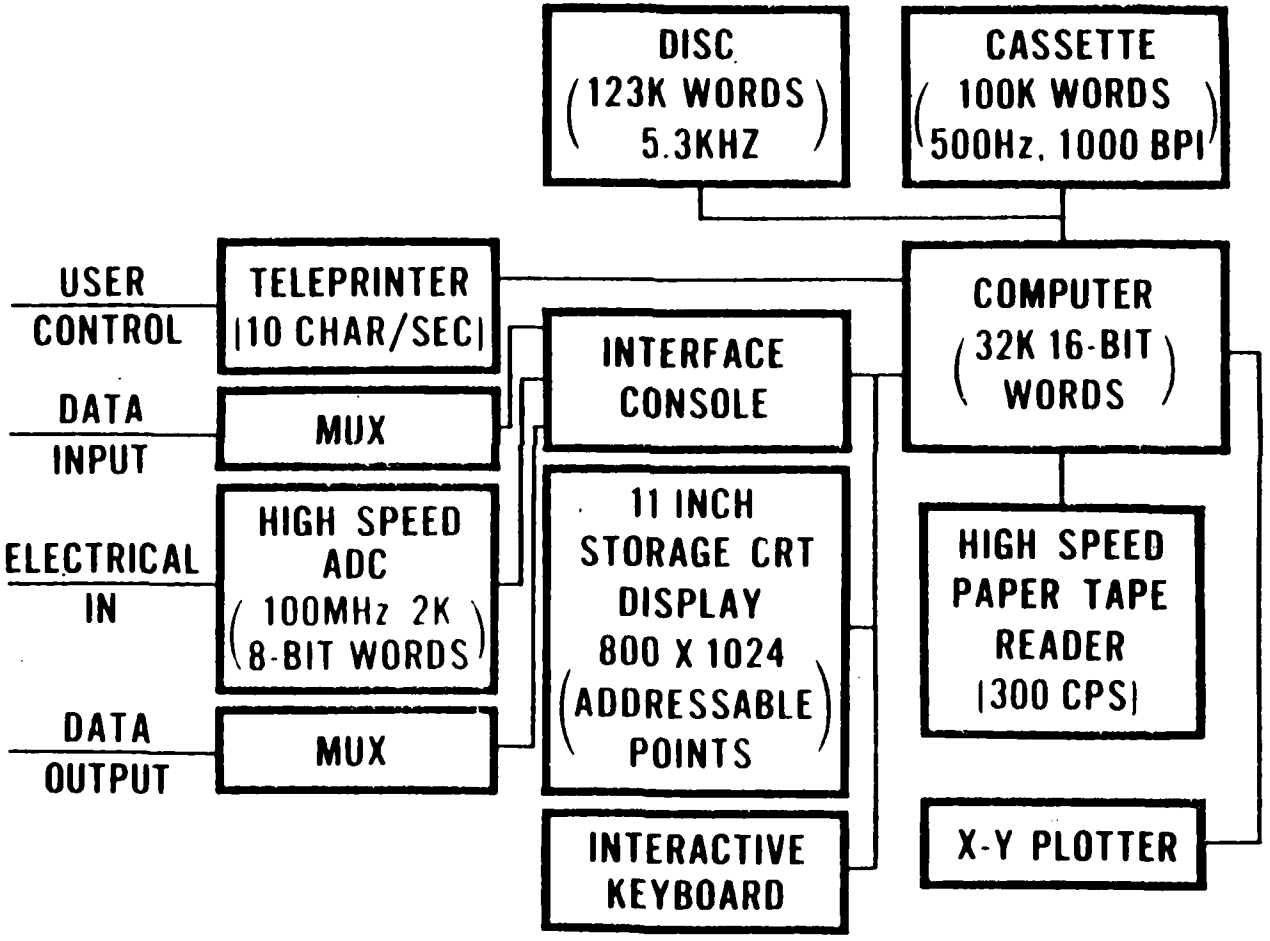

Fig. 13. Architecture of the real time data processor module.

Table 7. Typical Software Supported in Extended Basic

Name	Description
FFT	Fast Fourier Transform (1 millisecond per data point, exceeds 4096 data points)
IFFT	Inverse Fast Fourier Transform
BESSEL	Bessel function of first kind of any real argument
DERIV	Calculates the derivative of the function FNF = F(X)
FOURER	Calculates and saves in a file the fourier coefficients of any given function F(X)
INTGRT	Integration using Simpson's rule
LIN FIT	Computes best linear fit for a set of independent variables to a dependent variable
LSCF	Least squares polynomial curve fit
BINOMD	Predicts probabilities using binomial distribution
F TEST	Gives approximate probability that an F random variable exceeds F, based on N and D degrees of freedom
GEOMEN	Computes the geometric mean and the geometric standard deviation for a geometrically normal set of data
STATO	Computes the mean, variance, standard deviation, and the standard error of the mean for one or more sets of data

V. LABORATORY MEASURED PERFORMANCE PARAMETERS

14. Introduction. As stated in Section I, the primary objective of the ARPA Order 1938 Program is to address the problem of (1) developing uniform, image-evaluation procedures for photon-imaging systems, and (2) having these procedures accepted by the scientific community of DOD and major private industry so that specifications can be accurately and uniformly written in a manner which will reflect the field performance or utility of any given system. Of course, "image evaluation procedures for photon-imaging systems" in the greater sense includes procedures for evaluation of minor and major components in the system as well as the completed system itself. Since the funding required to establish procedures in all categories from smallest component to entire systems would be prohibitively high, this ARPA program is concentrating its efforts where the need and potential payoff are the greatest.

The analysis of the survey described in Section III and experience with critical problems in DOD procurement cycles dictated that the program philosophy

should be a "systems approach" philosophy. It is essential that DOD be able to ensure that the fielded system will satisfy specific performance criteria which have been translated into laboratory-measured performance specifications. Although the clear emphasis is on the total system, the importance of major component testing from a diagnostic and theoretical model point of view requires that at least a limited effort be expended as part of this program. To that end, electrical-out measurements at the video line are being investigated by one of the program participants.

The image-evaluation procedures and techniques under development are based around the two-port, image-evaluation concept shown in Fig. 14. That is, radiation of a target pattern is projected into the input port or collecting aperture of the photon-imaging system under evaluation. The output port, either eyepiece or display, is then monitored by a photometric device or the human eye.

The development of the procedures is being investigated by participants from the Army, Navy, Air Force, and the University of Rhode Island. The approach is to first review both the procedures currently being used and those proposed as more advanced techniques. These procedures are labelled "candidate procedures." A summary of those procedures considered as candidates to be investigated before proposing a single procedure for any particular measurement is provided in Paragraph 16.

In the process of researching the candidates, the procedures will be judged against three major criteria. First, because the primary objective of any photon-imaging device is to satisfy some real-world tactical need, the parameters being measured must be relatable to field performance. Second, since ultimately the parameters and the measurement techniques themselves will be integrated into procurement performance specifications, the techniques must be compatible with this specification effort. For example:

a. Any procedure must be developed with careful consideration for the cost of the equipment necessary to implement it.

b. The procedures must lend themselves to well-defined calibration.

c. The data from any measurement should be quickly obtainable in a form which is immediately usable.

d. The facility and procedures should be compatible with the talents of an average technician.

Third, because of the potential of modeling in the analysis of future concepts and performance studies for different applications, the procedures must provide data which

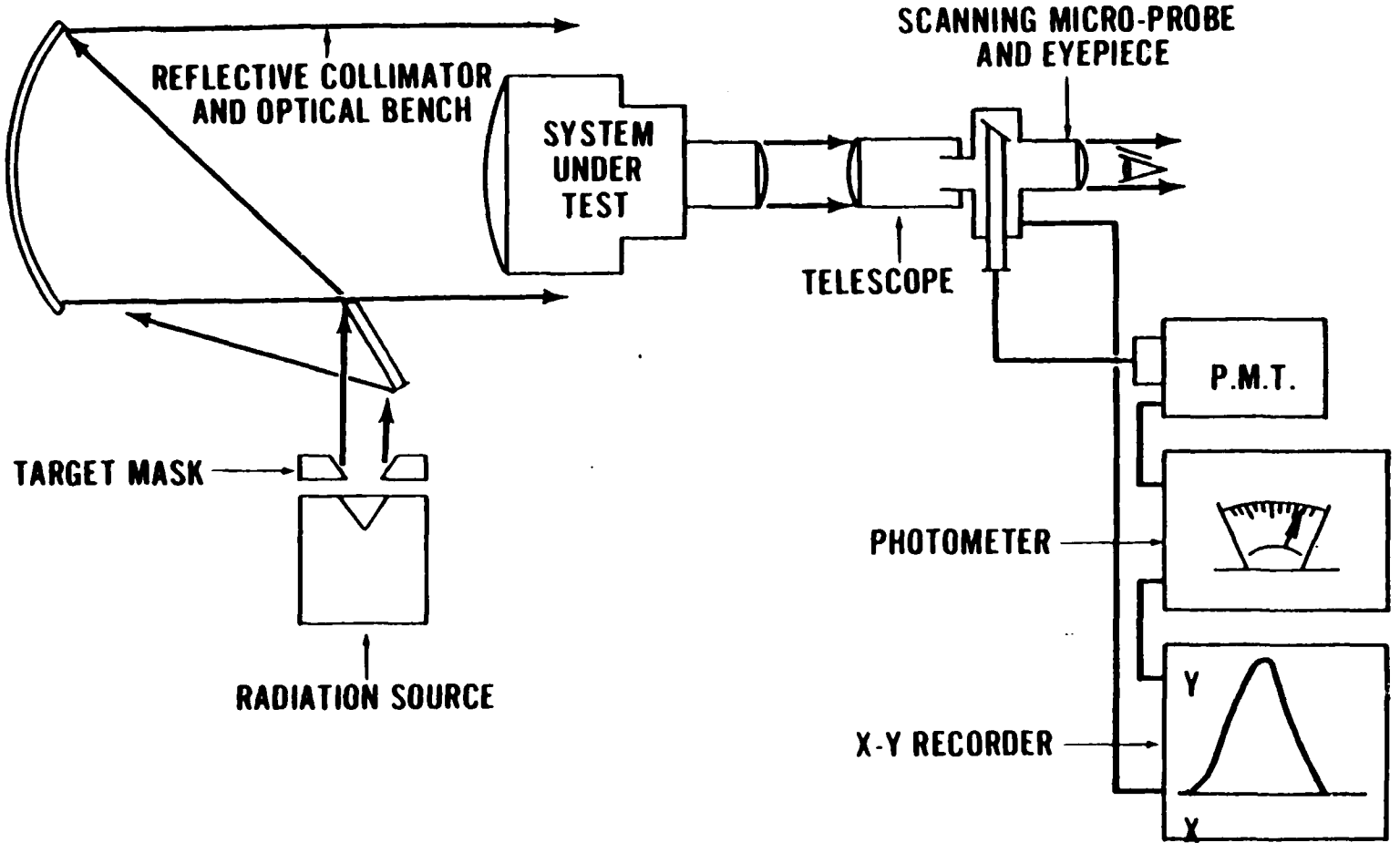

Fig. 14. Two-port image evaluation concept.

is consistent with existing and future model needs. The following paragraph reviews contemporary modeling from the standpoint of its utilization of system laboratory-evaluation parameters.

15. **Laboratory Data Requirements for Performance Models.** Models are being developed in ever increasing numbers to predict the performance of photon-imaging systems when viewing various types of imagery. As their sophistication improves, they are destined to reduce the need for field testing to a minimum and may eventually lead to total system simulation.

Since the models ultimately attempt to predict performance of systems under operational conditions, they must be sensitive to real-world targets and backgrounds and must utilize parameters measured in the laboratory which reflect total system performance. In addition, proper account must be given to the man-machine interface in systems where an observer is required. Thus, there are two areas where initial scene information can be degraded – in the eye or in the photon-imaging device itself. These models generally associate a generalized signal-to-noise ratio to an image appearing at the display of a photon-imaging system. Then, use is made of experimentally determined data describing the observer's detection probability versus known signal-to-noise ratios at the display. By matching the photon-imaging-device capability with the observer's requirements, overall photon-imaging-system performance is then predicted.

The procedures being developed under this ARPA program will provide basic objective data to describe the image-degrading effects of the photon-imaging system. To demonstrate the requirements that models have for this data and to understand where image-evaluation development should direct its efforts, consider the following three sample models.

a. The performance model typically used by Dr. Walter Lawson of NVL is based in most cases on the following expression for signal-to-noise:

$$(S/N) = \frac{t_i C^2 B^2}{\eta} \int I_n^2 H^2 d^2 w \quad \text{(assuming noise is white and targets are rectangular)}$$

where

C	=	the contrast of the target on the display
B	=	background brightness in the display
η	=	the frequency independent power spectrum of the noise
I_n	=	the Fourier transform of the target normalized to unity amplitude
t_i	=	the integration time of the eye
H	=	the eye-system transfer function

At present, the system-performance parameters which are directly utilized in the model are System MTF, System Spectral Response, and System Magnification. Other parameters needed for calculations are based on theoretical assumptions or theoretical modeling of the parameter itself utilizing component measurements.

b. Recent performance models utilized by Dr. Fred Rosell of Westinghouse are based on the following expression for signal-to-noise:

$$SNR_{D/A} = \left[\frac{t/\alpha}{N_v \cdot N_h}\right]^{1/2} \frac{C \mid R_o(N_h) \mid i_{s_{max}}}{\left[(2\text{-}C) \mid R_o(N_h) \mid ei_{s_{max}}\right]^{1/2}} \quad \text{(for square-wave input targets)}$$

where

t	=	integration time of the eye
α	=	aspect ratio of the CRT
N_v	=	TV line height of the target
N_h	=	TV line width of the target
C	=	target contrast
$\mid R_o(N_h) \mid$	=	sine wave response or modulation transfer function in the horizontal dimension
$i_{s_{max}}$	=	the maximum current emitted by the sensor layer for peak target radiance
e	=	electron charge

The model generating this equation assumes that the system is linear and that the noise generated is due to the photon-photoelectron conversion process. At present, for actual detection or recognition calculations, component evaluation data is used as opposed to complete system evaluation data.

c. The performance model developed by Dr. George Hopper of Texas Instruments for FLIR systems is as follows:

$$SNR_D = (K)\left(\frac{t_E}{t_F}\right)^{1/2} \left(\frac{WL}{\Delta\theta^2}\right)^{1/2} Q^{-1/2} \left(\frac{\Delta T_o}{NET}\right) TF$$

where

t_E	=	integration time of the eye
t_F	=	system frame time
$\left(\frac{WL}{\Delta\theta^2}\right)^{1/2}$	=	term dependent on the image size at the display

$Q^{-1/4}$ = term dependent on the frequency spectrum of the noise throughout the system
ΔT_o = input target temperature difference
NET = system noise equivalent temperature
TF = system amplitude response
K = a constant

System performance laboratory data is not generally utilized directly in the SNR_D expression for performance calculations. Rather, basic component data is utilized for the input parameters to Hopper's derived expressions for NET and MTF. Dr. Hopper also derives an expression for MRT off the display using a recognition threshold value for SNR_D.

In the above three model samples, the assumptions concerning the system and the observer for the expressions illustrated are numerous. In general, the systems are assumed to be linear. Dynamic measurements of system performance are not considered, displays are assumed to be uniform and free from fixed pattern noises and other cosmetic problems, and assumptions must be made to account for the temporal and spatial noise power spectra at the display.

Clearly, photon-imaging-system prediction models are in a developmental phase. Future work will strive toward greater precision and will extend the model complexity to account for more realistic imaging situations. This future development can be strongly impacted by laboratory-system, image-evaluation measurements. Procedures like those being investigated in this ARPA program can support modeling efforts in the following ways:

- The system, laboratory-measured parameters should be utilized in the present model expressions where possible. Such system parameters as MTF can be directly substituted into all the above models.

- Modeled parameters can be correlated to laboratory-measured parameters for validation and for isolating image-degrading factors not accounted for in the modeled parameters.

- More general expressions exist for the signal-to-noise ratio than those presented above. In these expressions, system measurements of spatial and temporal noise power spectra could be substituted directly eliminating assumptions now necessary concerning their functional form. Also, full utilization of measured families of signal-transfer functions and more complete information describing the noise characteristics measured at the display should allow

development and validation of nonlinear modeling. Finally, direct use of temporal effects measured in the laboratory should aid models in their inclusion of target motion.

16. **Candidate Laboratory System Evaluation Procedures.** This paragraph describes the system evaluation procedures considered as candidates for adoption by DOD and major private industry for the laboratory evaluation of photon-imaging systems. The basic concept in these procedures is system testing where the photon-imaging system is treated as a black box having an input port and an output port. The basic laboratory setup for an evaluation is shown in Fig. 14. Energy from some target pattern is projected into the input port of the system under evaluation. Then some monitor, either a photometer or the human eye, collects the output port information and feeds it to some analytical or hard-copy equipment. This concept is illustrated in Figs. 15, 16, and 17 which summarize the parameters and candidates of three of the procedure categories to be covered in detail. The only exception of the system concept of evaluation is in a limited number of "image-in electrical-out" tests. These procedures intercept the system's signal before it reaches the output port.

There are four primary areas in which the procedure development is centered:

- System Responsivity – the objective measures of amplitude transfer, spectral transfer, and contrast transfer response functions of the system under test.

- System Spatial Resolution – the objective measures of system spatial response such as the optical transfer function, modulation transfer function, resolving power, field of view, magnification, etc.

- System Signal-to-Noise – the measurement of the mean and RMS fluctuation of signals at the display of photon-imaging systems. Includes measurements of noise frequently associated with cosmetic effects such as fixed pattern noise, periodic noise, and nonuniformity.

- System Resoltivity Response – Resoltivity refers to observer performance tests that combine the system spatial resolution and sensitivity (responsivity and S/N) to yield the combined observer-system laboratory performance. Examples of candidate procedures to be investigated under this category are Minimum Resolvable Temperature (MRT), Noise Limited Resolution (NLR), and Resolving Power.

The measurements in these areas are separated into 14 categories. These categories are itemized in Table 8 and the DOD agency responsible for each developmental area is

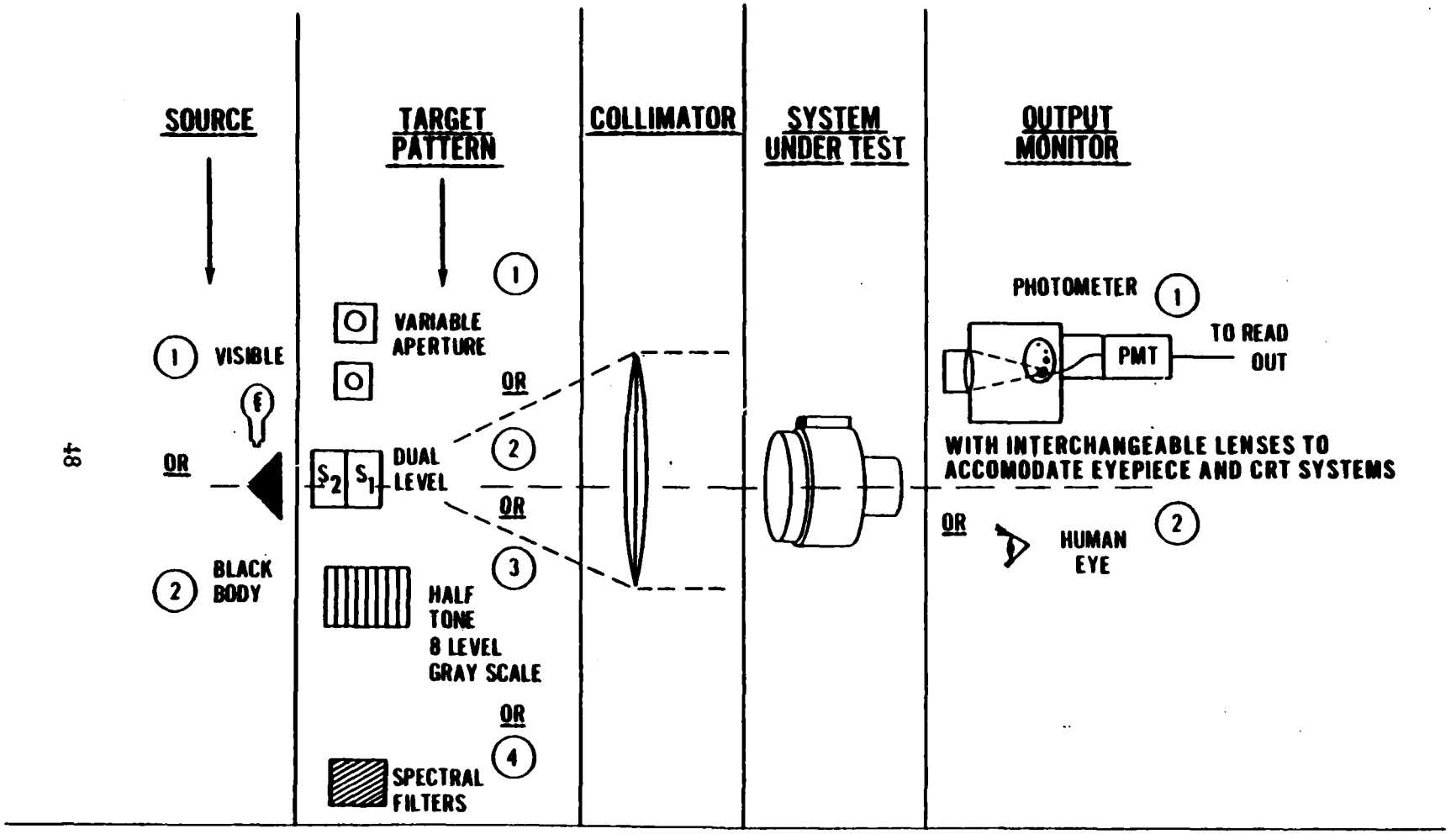

Fig. 15. Basic schematic for system responsivity measurements.

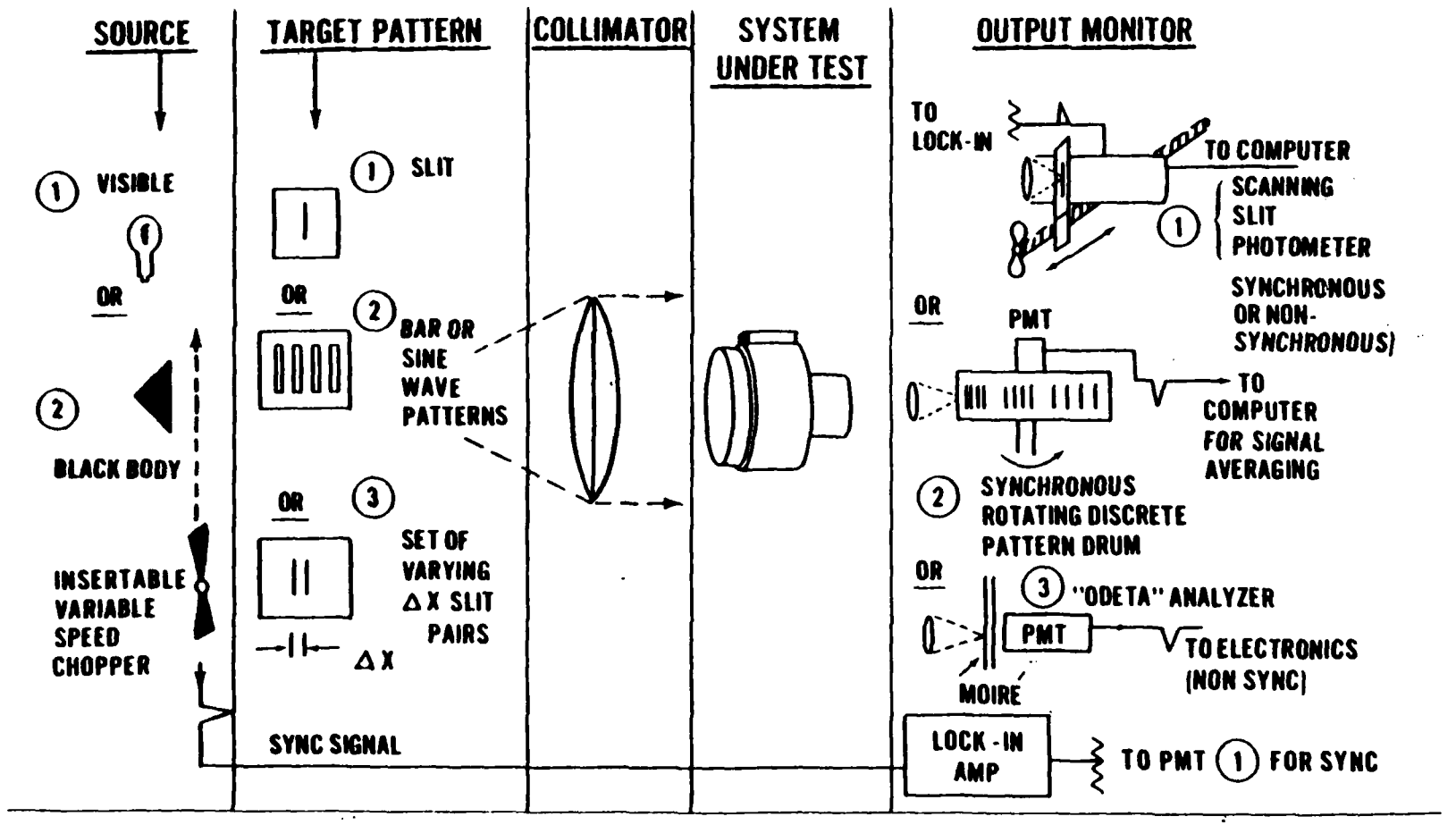

Fig. 16. Basic schematic for system spatial response measurements.

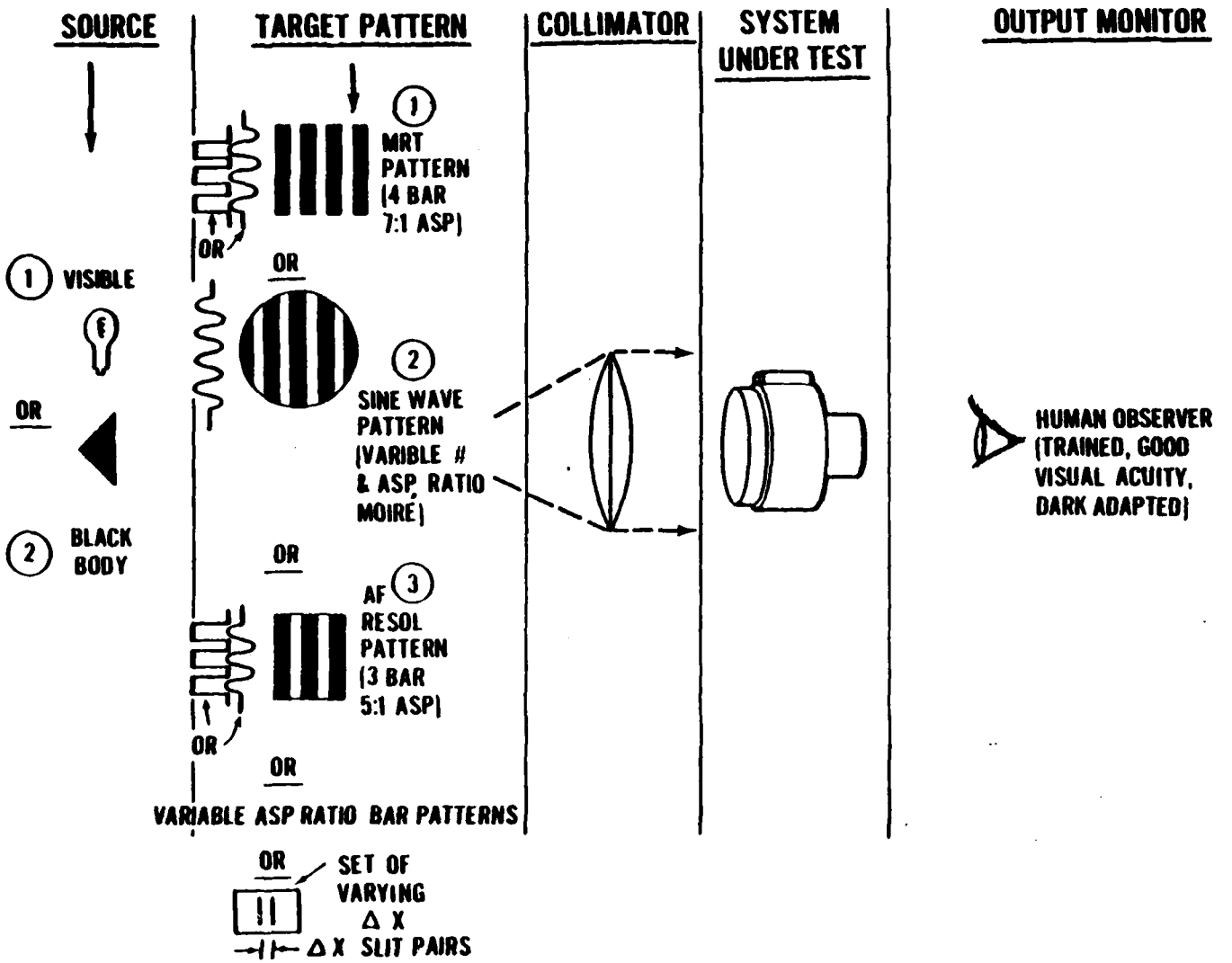

Fig. 17. Basic schematic for system resoltivity response measurements.

Table 8. Candidate Procedures

Para	Category	Procedure
a	System Responsivity[a]	Objective Signal Transfer Function Subjective Signal Transfer Function Spectral Transfer Function
b	System Spatial Resolution[a]	Optical Transfer Function Resolving Power
c	System Resoltivity Response[a]	Visual Resoltivity (Full Dynamic Range) Resolving Power (Limiting Resolution)
d	System High-Signal Response[b]	Image Spreading Saturation Effects
e	System Temporal Response[b]	Image Motion Effects System Time Constant System Jitter
f	System Geometric Response[b]	Magnification and Field of View Off-Axis Distortion
g	System Display Uniformity[c]	Fixed Pattern Noise Raster and Scan Line Effects
h	System Sensitivity Response[c]	Temporal Noise Signal-to-Noise Detective Quantum Efficiency
i	Front-End Sensitivity Response[d]	Signal Level and Noise Level SNR_D
j	Front-End Spatial Response[d]	Optical Transfer Function Resolving Power
k	Front-End Temporal Response[d]	Image Motion and Lag Jitter Response
l	System Responsivity (film readout only)[e]	
m	System Spatial Resolution (film readout only)[e]	
n	System Resoltivity Response (film readout only)[e]	

(a) Procedures contributed by Night Vision Laboratory.
(b) Procedures contributed by Naval Air Development Center.
(c) Procedures contributed by University of Rhode Island.
(d) Procedures contributed by Naval Electronics Laboratory Center.
(e) Procedures contributed by Air Force Avionics Laboratory.

specified. The text following the table describes the candidate procedures of each category in detail. Each category is broken down into its pertinent parameters. For each parameter, there is a definition, a candidate procedure summary, and a review of equipment considerations.

a. System Responsivity.

(1) Objective Signal Transfer Function (Si TF)

(a) **Definition/Discussion.** The Signal Transfer Function of a photon-imaging device is that curve or family of curves which describes the low spatial frequency signal gain of a device over its entire operating range. Typically, the curve as plotted shows output luminance or radiance as a function of input luminance, radiance, or some ΔT (temperature differential). This system characteristic provides information describing the linear regions of operation of the system, system saturation levels, areas of effective gray scale transfer, etc. This information is frequently needed prior to measuring other system parameters.

(b) **Procedure.** Two procedures are proposed. First, for visible itensifier and TV systems, a portion ($\sim$ 10%) of the field of view (FOV) of the photon-imaging system being tested is uniformly irradiated by a 2854°K blackbody (0.4 to 1.2 micrometers) or some other well-specified spectral distribution source (i.e., a night environment radiance distribution).

As the input luminance is changed from low to high magnitudes, the system's output luminance is monitored with a photometer that has a sensing probe which is much greater spatially than the system's output equivalent resolution element. For thermal systems, the source would be a blackbody source, and the output would be monitored as previously described. A parametric set of curves must be generated for systems having display brightness or gain controls as those controls are varied.

The second procedure provides the output information in terms of contrast rather than absolute luminance. The test, primarily designed for systems having brightness and gain controls, determines what control settings give the optimum-output contrast. The input target has dual sources: S_1 and S_2. Consider S_1 as the variable source with S_2 tracking with it but at only a fraction of its output radiance. Also, S_1 is adjacent to S_2. At the output of the system under test, two luminance levels are observed. They are monitored photometrically. For the systems with gain and brightness controls, the test is done in the following manner. S_1 is set to some

level (with $S_2 = fS_1$ where f equals the attenuation fraction). The brightness control is fixed to some fraction of full scale. The gain is then varied over its entire range while the output contrast $\frac{L_1 - L_2}{L_1 + L_2}$ (where L_1 is the output luminance due to source S_1 and L_2 is the output luminance due to source S_2) is monitored. This generates one curve. A family of curves is generated as the value L_1 is varied from low- to high-input values. Other families are generated with different, fixed positions of the brightness control. Similar families can be generated for fixed-gain positions while varying the brightness. When brightness and gain controls are fixed as in a system without variable controls, the test reduces to that described as the first candidate with two inputs.

(c) **Equipment Considerations.** For the first of the procedures described in paragraph (b), a visible source capable of presenting luminances from 10^{-6} to 10^{2} fL uniform and lambertian over the area described is needed. This source must be well calibrated to 2854°K (0.4 to 1.2 micrometers). It should be capable of utilizing wide- and narrow-band spectral filters to simulate real-world conditions when necessary. For the thermal systems, a blackbody of emissivity close to 1 with a range from 273°K to 373°K should be used. It will be necessary for both sources to be capable of covering from approximately 5 degrees to a ½ degree field of view when used with their projection collimators. Further, the background should be uniform over the remaining field of view in both cases. At the output of the system, a photometer will suffice to monitor the output luminance value.

A sufficient variety of coupling lenses and probes is necessary to allow integration over a group of ten or more resolution elements (when referred to the display).

Another approach would be to use the basic equipment mentioned above with one half-tone pattern placed in front of the source. This technique would reduce the time required to execute the test and would eliminate the need to calibrate different pattern/source combinations. By using variable dot densities, eight to ten even increments of density could be applied to a substrate with a range allowing maximum transmission at one extreme and near-zero transmission at the other. This technique would eliminate the need to change the input source temperature or luminance.

The second procedure described in Paragraph (b) would require a dual-level source. This could be accomplished by utilizing either ND filters or half-tone screens for splitting the target format. The basic source and the output monitor would be the same as in the first candidate procedure.

(2) Subjective Signal Transfer Function (SSiF)

(a) **Definition/Discussion.** The Subjective Signal Transfer Function is defined as the number of gray scales an observer can distinguish as a function of system input radiance. If it is assumed that eight shades of gray provide the necessary and sufficient maximum range of output luminance for an observer to perform various field tasks, it is useful to determine if all the eight levels can be exploited over the system's dynamic range.

(b) **Procedure.** The system is set up with an observer monitoring the output display (CRT or eyepiece). The input source is the same as in Paragraph a(1)(c) with the eight-gray-level-density pattern directly in front of it. The sources acting as the radiation emitters are varied from low to high output luminance and radiance values. As the sources are varied, the observer attempts to distinguish the number of gray levels. This number is plotted as a function of peak gray scale luminance or radiance. In the case of systems with brightness and contrast controls, the observer may optimize the controls for maximum gray scale transmission.

(c) **Equipment Considerations.** Again, the equipment required is that described in Paragraph a(1)(c) with the half-tone process utilized to design and fabricate the eight-level-gray scale. It might prove useful to expand the number of gray scale patterns to include lesser and perhaps greater numbers of gray levels thus providing a full gray scale set for presentation to the observer.

(3) Spectral Transfer Function (SpTF)

(a) **Definition/Discussion.** The Spectral Transfer Function is defined as the relative system response to the wavelength of input energy. At some wavelength, the input energy should be specified in absolute units so that an absolute calibration can be assigned to the entire curve.

(b) **Procedure.** For visible I^2 systems in linear operation, a set of narrow bandwidth spectral filters, from 0.4 to 1.2 micrometers, is used in conjunction with a 2854°K source to provide narrow-band input light at various frequencies. The total power transmitted by each filter is adjusted to be equal. The system's output luminance is then measured for each filter. A relative curve is plotted, and the absolute luminance out for a particular input radiance is specified at 1 wavelength. This procedure invites serious problems when nonlinear operation is found in the system under test. It is

essential that the system's gain be constant over the range of apparent input energies utilized during the measurement.

A second procedure which overcomes the linearity problem requires only a narrow linear range. In this procedure, the peak input wavelength light intensity is increased to a value which allows the system to present an output luminance in the center of some linear region (as determined by the SiTF test). The other filters are irradiated by enough energy to allow the output luminance to match that found with the original peak wavelength filter in place. The input changes must be calibrated so that the relative response can be deduced. Again, the output curve demonstrates output luminance as a function of input wavelength with absolute units referenced to a single wavelength.

(c) Equipment Considerations. A well-calibrated source such as that described in Paragraph a(1)(c) is required. In addition to the source, narrowband filters (approximately ten over any of the three ranges, 0.4 to 1.2 micrometers, 3 to 5 micrometers, and 8 to 14 micrometers) are required. Particular care must be taken to insure that blocking is sufficient (usually two orders of magnitude or greater). The output of the system again is monitored by a photometer. The apertures and areas sampled in these procedures must be consistent with the sizes specified in Paragraph a(1)(b).

b. System Spatial Resolution.

(1) Optical Transfer Function (OTF)

(a) Definition/Discussion. The OTF is defined as the Fourier Transform of the line-spread function of the system under evaluation. To be well defined, the line-spread function must be generated by a linear system exhibiting strong stationarity. The modulus of the OTF, when normalized to one, is the Modulation Transfer Function (MTF). The argument of the OTF is the Phase Transfer Function (PTF). The measurement of MTF reveals the ability of the photon-imaging device to transfer information at various spatial frequencies. This is demonstrated by an MTF curve which shows modulation on the ordinate axis (normalized to 1 for 0 spatial frequency) and spatial frequency (usually in cycles/milliradian) on the abscissa axis.

(b) Procedure. There are two primary classes of methodology for analyzing the MTF of a photon-imaging device. First, there is the direct measurement of the edge gradient or line-spread function with its subsequent

computer analysis. And second, there are a number of techniques which either convolve slits with sine or square wave patterns or vice versa. These methods suffer from at least one deficiency. They do not allow measurement of the PTF. However, since the utility of the PTF has not as yet been clearly defined, the loss may be insignificant.

The first category of procedures utilizes a slit target input to simulate an impulse function containing all spatial frequency components (slit is typically ten times less than a resolution element when projected onto the system's basic sensor element). The spread function which is displayed at the system output is then scanned by either a photometric knife edge or a photometric slit. The analog spread function or edge gradient is then digitized and computer fourier transformed or the derivative taken and then fourier transformed. The modulus and argument are then plotted against spatial frequency and phase angle, respectively. This procedure requires careful focusing of all optics, corrections for any degrading lens mechanism MTF's, correction for finite probe sizes, and precise alignment of measuring probe with either the slit or the edge. Alignment and focusing are affected by peaking the PMT output signal while the photometric slit rests on the center of the output spread function. However, it is often difficult with particular types of systems to define accurately the spread function since it is buried in noise. To extract the real signal, synchronous detection must be utilized. For most systems, chopping the input signal and gating the PMT output to a variable integration time lock-in amplifier can effectively solve the problem. The cost, however, is time. In addition, stationarity, which may not be a serious problem for image-intensifier tubes, can be a severe one for framing systems. This implies that system jitter effects become integrated into this slow scan measurement. At present, the only practical method for eliminating the stationarity problem appears to be the incorporation of a well-calibrated, high-resolution storage tube, film, or high-resolution vidicon camera (analyze spread function at the video line) as a final spread function image storage mechanism.

The second group of procedures utilizes slits or bar/sine patterns on the input with bar/sine or slits, respectively, to scan the output image. These procedures naturally break down into the two sub-sections – slit in and frequency pattern in. In the slit case, the input target is identical to that used in the spread function measurements. At the system output, however, the spread function is imaged onto a square wave pattern (corrected later to sine wave) or a sine wave pattern of a particular spatial frequency which chops the slit image. A narrow-band filter around the chopping frequency accepts the PMT's signal, and the modulation is processed and displayed normalized to

some low spatial frequency. Again, alignment and focusing are important. Maximizing the modulation transfer at a particular frequency at high-light-level inputs while making incremental changes in the focus and alignment parameters is the technique assuring optimum performance.

For systems with low luminance outputs and/or poor signal/noise ratios, it is often impossible to define the final MTF. Further signal processing is necessary. As in the spread function case, synchronous detection is used to sample the output. This technique, however, now requires discrete frequency patterns at the output which can provide a precise trigger pulse to the detector to allow sampling. Signal averaging with a storage unit is needed to add the sampled signals which are subsequently displayed with reduced noise. Some of the limitations of this procedure involve again the stationarity problem and interference with the frame rate of framing systems. Further, the actual normalizing point may not be close enough to zero spatial frequency to allow accurate normalization of the final MTF data.

For the case of bar or sine wave patterns on the input, the procedure is similar. Now, the slit scans the output of a particular spatial frequency image. Similar filtering and signal averaging is again necessary to extract the pertinent modulation data.

(c) **Equipment Considerations.** All measurements in the first category require sources, such as described in Paragraph a(1)(c), that must be masked with a narrow slit (approximately 25 micrometers for 1270-millimeter focal length (collimator) etched out of metal with blackened sides and edges matching the physical reflectance-emissive characteristics of the background. However, the system analysis equipment varies widely. When the spread function is measured without synchronous detection for computer analysis, a scanning slit (3 to 5 micrometers) or precise knife edge backed by a PMT is used. The motion must be uniform and continuous. A variety of well-calibrated coupling lenses must be available to handle a range of eyepieces and display CRT's (in fact, for most applications a 25-micrometer slit may replace the 3- to 5-millimeter slit if enough coupling magnification and exit port energy are available). Then, an analog-to-digital converter interfaced to a computer using the Fast Fourier Transfer algorithm is required. If synchronous detection is necessary, a lock-in amplifier with low temporal bandwidth window capability and variable integration time is utilized with a matched chopper for the input radiation. There is also a more stringent requirement on the probe motion. A stepping motor must be used with 1-micrometer resolution. Again, the computer will be needed for transform analysis.

For the second group of procedures where bar and sine wave patterns are used, there are several commercially available analysis units. First, for a slit input (slit must meet same requirements as in previous category), there is available the Aerojet 'Odeta' (Moiré continuous frequency pattern) analyzer, or either of two synchronous detection equipments from OTI or Weiser. The synchronous equipments utilize fixed spatial frequency patterns mounted on a rotating drum. Both devices are available with the necessary computer components to display the MTF. Discrete sine or square bar patterns can also be mounted to a precise linear motion platform if the platform has .1 to .5 micrometer reset reliability. The platform could step the periodic pattern across the final slit image at a relatively high stepping rate. The temporal, modulated PMT output signal could then be filtered and stored by a computer which could subsequently average the stored samples. Similar equipments are also needed for the case of square or sine wave input patterns. In this case, only a slit need be mounted to the stepping platform as in the equipment discussion for the last category. If problems with stationarity cannot be overcome, the equipment would involve some instantaneous storage device whose MTF would have to be precisely calibrated.

(2) Resolving Power

(a) Definition/Discussion. The resolving power is the minimum separation distance of two input impulse functions for which the photon-imaging-device display can meet the Rayleigh Criterion peak-to-valley condition. If the two input pulse functions have different peak intensities, the Rayleigh Criterion would be established for the lower peak-to-valley difference.

(b) Procedure. Two input slits meeting the requirements of the slits in Paragraph b(1)(c) are incrementally moved toward each other until a spread function analysis of the exit port display indicates that the peak-to-valley condition meets the Rayleigh Criterion.

The methods discussed in Paragraph b(1)(b) for extracting the spread function apply to this procedure with the exception that no computer Fourier analysis is necessary. Measurements should be made as the slit intensities are varied – one with respect to the other. This might be done for a half-order and full-order radiance drop in one of the slits. Again, the distance at which the smaller peak-to-valley condition meets the Rayleigh Criterion is noted.

(c) Equipment Considerations. The equipment would be the same as in Paragraph b(1)(c) for the output spread function measurement as

mentioned above. However, a set of incrementally separated slits would be needed as target patterns to insert in lieu of the single slits used in Paragraph (b)(1). Neutral-density filters would also be required to produce the various input, peak-radiance differences.

c. System Resoltivity Response. Resoltivity refers to observer performance tests that combine the system spatial resolution and sensitivity (responsivity and S/N) to yield the combined observer-system laboratory performance.

(1) Visual Resoltivity (Full Dynamic Range)

(a) Definition/Discussion. Visual Resoltivity is defined as the maximum resolution (spatial maximum frequency input pattern referred to object space) the eye can perceive when viewing the display of a photon-imaging device operating over its full expected range of input target radiances and contrasts. This implies that a visual resoltivity measurement demonstrates the performance of the system-observer combination from conditions where the system is noise limited to conditions where it is resolution limited. When properly trained observers are utilized and care is taken that the eyes have reached the correct level of dark adaptation, this measurement brings together the interaction of a number of the parameters measured objectively in a system evaluation. It can also serve to provide a critical link with field performance and thus act to validate various performance models.

(b) Procedure. A periodic resolution pattern is back radiated by one of the sources described in Paragraph a(1)(c). This source-pattern combination is placed at the focal point of a collimator which projects the pattern to a photon-imaging device under test. Two observers with normal visual acuity and trained for repeatability in this type of testing view the output monitor or eyepiece coupled to the display of the system under test. A pattern of low spatial frequency (usually ten times less than the maximum spatial frequency) is presented to the system-observer combination. The observer then increases the back-radiating intensity until he first discerns the existence of the periodic pattern image. This radiation level and the brightness/gain control positions (optimized by the observer if adjustable) are recorded for that spatial frequency. The measurement continues as higher frequency patterns are presented until the system reaches its resolution limit. This procedure is carried out for various input contrast settings where contrast is defined as the difference in the radiance of the peak of the periodic pattern and that of the valley of the pattern divided by the sum of the two. The measurement described could also be run using the spatial frequency of the periodic pattern as the observer variable rather than the back-radiation level.

A number of candidates exist for the actual periodic input patterns. They include the following: MRT resolution patterns (constant aspect ratio 7:1 with four bars); AF resolution patterns (constant aspect ratio 3:1 with three bars); square or sine wave patterns with varying aspect ratio; MRT patterns or AF patterns with sinusoidal wave forms; Moiré generated varying aspect ratio quasi-sine wave patterns (NLR, or Noise Limited Resolution Patterns); and true sine wave monochromatic varying aspect ratio patterns.

(c) **Equipment Considerations.** As noted in the above text, the basic sources would be the same as those described in Paragraph a(1)(c). The patterns, however, are generated in a variety of ways. In the case of the MRT, AF, or varying respect ratio square wave patterns, an etching process is used on various metal substrates to form the bars. These can be easily mounted in front of the visible or thermal source. If sine wave patterns are needed, they generally must be computer processed on film for either varying or constant-aspect ratio varieties. For the Moiré patterns, two gratings are needed. As they are counter-rotated and the angle between the gratings departs from zero, an interference pattern forms a near sine wave which increases in frequency as the angle is increased. Although the methods just described cover the majority of patterns that might be used, there are two other processes which could handle most of the above requirements. One is depositing patterns on IR-tran materials (front-surface reflection must be controlled). Another involves a half-tone process where dots are deposited in various densities on properly transmitting substrates. This process is limited only by the half-tone screen resolutions available and in some cases by the substrates themselves.

In cases where an absolute sine wave is needed at a particular spectral wavelength, an interferometer can be utilized to project patterns directly onto sensing layers. One such interferometer has been designed and built by NELC and is reviewed in the Appendix.

The only other major equipment consideration concerns contrast control in the visible region. This can be handled by dual light paths and beam splitters or by depositing various contrast patterns on quartz glass. The beam splitter method has the advantage of providing continuous contrast control.

(2) **Resolving Power (Limiting Resolution)**

(a) **Definition/Discussion.** Resolving power is defined as that

spatial separation of two impulse functions which allows an observer viewing their image at the system output to just discern their separation. If the radiation forming the two input slits is varied, the measurement has strong similarities with limiting resolution field measurements where adjacent target details have different apparent radiances.

(b) Procedure. The test would be run with an observer arrangement as in Paragraph c(1)(b). One would begin the test with two slightly separated identical radiance slits. They would then be incrementally moved apart until the observer could just distinguish their dual nature. This separation would be recorded as well as the optimized gain and brightness control positions. This procedure would then be repeated for a range of input target radiances and/or radiance differences between the two input slit targets.

(c) Equipment Considerations. The necessary equipment would consist of the basic sources previously described and the slit patterns referred to in Paragraph b(2)(c).

d. System High Signal Response.

(1) Image Spreading

(a) Definition/Discussion. Image spreading is herein defined as the gross increase in image size occurring when the system is exposed to a source whose radiance is outside of the linear range of operation. Image spreading can best be measured using a point source. Image spreading can then be described in terms of a point-spread function at each condition of overload. The absolute radiant intensity levels of the point source should be indicative of levels likely to be encountered by the system in an operational environment. In general, the degree of image spreading exhibited will depend on the average radiance of the scene. At low background radiance levels, the system will require high gains and will, therefore, be more susceptible to image spreading. Thus, it will be necessary to adjust background radiance independent of point source radiant intensity. Fig. 18 is an example of the spreading of a point source in a scene as imaged on a low-light-level television system.

(b) Procedure. Point source radiant intensity J is adjusted to the desired level. A uniform background is adjusted to a desired level of radiance N. The system variables are adjusted to prescribed values previously determined to optimize the system over the range of operation or for a specific

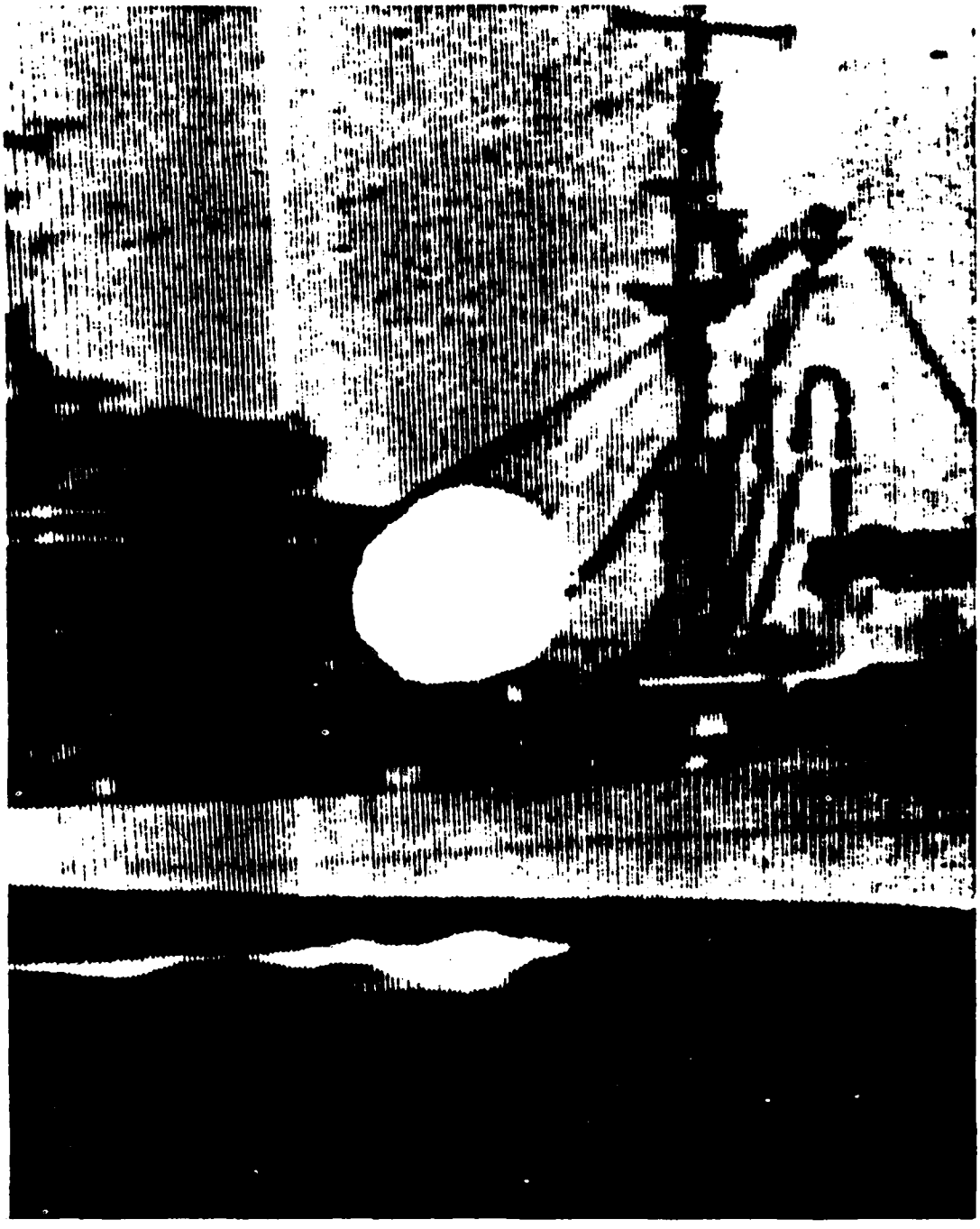

Fig. 18. Example of point source spreading.

input condition. The center of the output image is identified, and a circular sampling aperture is scanned along a line passing through the center in the direction of the maximum spreading.

The procedure will be repeated with the point source positioned at various locations in the field of view.

The degree of image spreading can be expressed in terms of a figure of merit θ_s defined as the diameter of the image spread function at an intensity level 10% above or below the background intensity level. The diameter is expressed in terms of an equivalent angular subtense. θ_s will, in general, be a function of N, J, θ_H, and θ_V where the latter two parameters are the angular displacement of the point source from the center of the field of view in the horizontal and vertical direction, respectively.

(c) **Equipment Considerations.** The spectral distribution of the background and point-source radiation will, of course, influence the results. One or more standardized distributions will be required for all of the system tests. For sensors responding to visible and near IR radiation, a 2854°K source is an excellent standard. For infrared responding sensors, radiance is controlled by varying the blackbody temperature rather than by spectrally neutral attenuation. The range of background radiance required will depend on the specific system being evaluated. In general, for systems responding to visible and near infrared radiation, background radiance levels can vary from 10^{-6} to 10^{+4} w st^{-1} m^{-2}. For infrared sensors, background temperature can range from 250 to 350°K. In practical situations, point-source radiant intensity can range as high as that of the sun. More typically, the problem source is likely to be man-made. A 100-watt incandescent source can emit up to 1 watt st^{-1}. The simulated source radiant intensity J_s can be expressed in terms of J_o the simulated object radiant intensity by:

$$J_s = \frac{fl}{R} \; J_o$$

where fl is the focal length of the collimator, and R is the actual range to the target being simulated. Thus, to simulate a 1-killowatt incandescent lamp at 300 meters with a 3-meter collimator, a small incandescent bulb using about 1/10th watt could be used. Subminiature lamps with bulbs smaller than 1/16th inch are available for this purpose. If the source is to approximate a point, it should subtend a small fraction of the total field of view. A good working relation for the bulb size d is

$$d < \frac{fl\,\theta}{100}$$

where fl is the collimator focal length and θ is the system diagonal field of view. For a 120-inch collimator, a 1/16th inch bulb would be adequate for systems with θ as small as 3 degrees.

It remains to define a means of superimposing the point source on the background. Pellicle beam splitters exhibit flat transmission out to over 2 microns and are, therefore, suitable only for the sensor working in the visible region. In Fig. 19, this implementation of the image-spreading test is shown schematically. For testing in the infrared, a blackbody source simulating the thermal emission from man-made sources could be located directly in front of the background. In this instance, the source would have to be carefully baffled to prevent stray radiation on the background.

The readout aperture should be circular, subtending less than 0.5% of the picture diagonal.

(2) Saturation Effects

(a) **Definition/Discussion.** Image spreading is sometimes not the only degradation due to a localized point of saturation. Saturation could also affect image sharpness in areas away from the point source. A localized point of saturation may also affect the operation of an automatic gain control. In a moving scene, a saturated point often leaves a residual trail that could obscure images in its wake. In general, saturation will affect every measurement normally performed on a system. To completely characterize the effects of saturation, it would, therefore, be necessary to repeat many of the system measurements over a range of point-source radiant intensity levels as in the image-spreading case. A more practical approach would be to make a single subjective measurement of limiting resolution as a function of background radiance, point-source intensity, and distance to the source. Limiting resolution will be strongly dependent on MTF, veiling glare, smearing, reduced sensor gain, and other effects caused by localized saturation.

(b) **Procedure.** The point-source radiant intensity and background highlight radiance are adjusted as in Paragraph d(1)(b). The appropriate limiting resolution pattern prescribed in Paragraph c(1) is used in place of the uniform background. The test pattern is positioned at varied distances from the point source, and limiting resolution is measured. The location of the point source is varied as in Paragraph d(1).

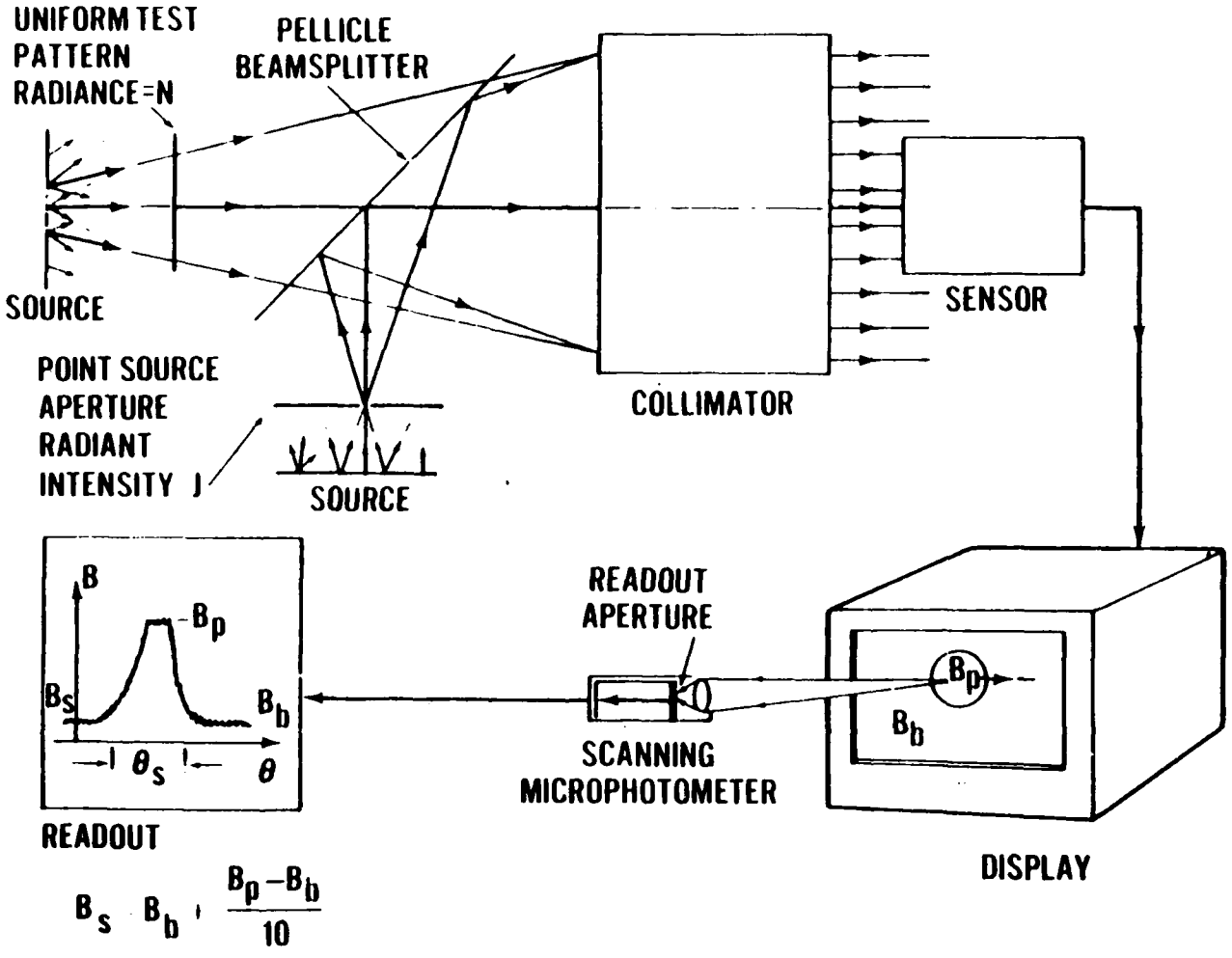

Fig. 19. Image spreading test.

To test for smearing, the camera is panned as in Paragraph e(1), and the limiting resolution is measured as a function of distance behind the point source.

A figure of merit describing the saturation effects could be the ratio of the limiting resolution in the presence of the point source to the resolution measured without the source as in Paragraph c(1).

(c) Equipment Considerations. The range of J and N required is the same as in Paragraph d(1); thus, the same instrumentation can be used.

A resolution test pattern is required. The same pattern used in Paragraph c(1) can be used, or the pattern can be redesigned specifically for this test.

e. System Temporal Response.

(1) Image Motion Effects

(a) Definition/Discussion. Image quality in virtually all imaging devices suffers when there is relative motion between the scene and the field of view. Image smearing or signal mixing reduces modulation in a manner very difficult to treat analytically. It will, therefore, be necessary to characterize image smearing with a subjective test. The measurement of limiting resolution in the dynamic condition, where the test pattern is moving relative to the camera field of view, has been performed on television systems at the NAVAIRDEVCEN for many years. While it is not always possible to relate limiting resolution to performance in the field, dynamic resolution is often a useful descriptor of image lag.

(b) Procedure. System resolution is measured as in Paragraphs c(1) and c(2) with the system scanning in a uniform rotation about either the vertical or transverse horizontal axis. The subjective assessment of the resolution or MRT limit is determined during scanning. The highest spatial frequency that can be resolved is then determined as a function of N, C, ΔT, θ_V, θ_H, θ_V, θ_H, etc. as required. A figure of merit could be the ratio of the resolution at a given speed θ to the resolution at $\theta = 0$.

(c) Equipment Considerations. A platform with two degrees of rotational freedom is required. To keep the system lens within the collimated beam, the system must be rotated on an axis passing very close to the center of the first objective element. An upper limit or angular rate would

be on the order of 10°/sec for normal image motion testing. The maximum deflection should be at least ± 10°. Masks can be used to obscure the display in areas where the direction is reversed so that the observer is not clued by the static image.

It is desirable to be able to impart arbitrary sensor movement as well as uniform scanning to simulate the equipment's actual operating vibration environment. It is recognized, however, that the cost and size of the "shake table" thus required may be prohibitive.

(2) System Time Constant

(a) Definition/Discussion. The transient response of an imaging system is an objective measure of the image smearing measured in Paragraph e(1). By exposing the system to a time-varying source and measuring the resultant time-varying signal, the degree of image lag can be assessed. At present, there is no model that utilizes such data to predict dynamic performance. However, it is felt that this data is fundamental and should be measured to provide a means of comparison between systems.

(b) Procedure. A portion of the field of view (10% to 30%) is irradiated with a uniform source which is pulsing on and off in synchronization with the system's framing cycle. The time on and time off the square wave of radiation is adjustable in multiples of frame times. A point on the display is viewed with a circular sampling aperture. This point is made to coincide with the transition of the radiation from the on to off condition and from the off to on condition. The source radiance is adjusted to a given level. At each radiance level, the output of the sampling detector is recorded as the system signal builds up and decays during the repetitive radiation cycling.

A figure of merit for decay lag that has been used is the signal at a given time after the off transition expressed as a percentage of the steady-state on signal. The buildup lag is described as the difference between the signal at a given time after the on transition and the steady-state on signal also expressed as a percentage of the steady-state on signal.

An alternate procedure would use a constant radiation source. The transient would be introduced at a given point in the field of view by scanning the system past a step transition in space. The problem with this method is that the transition cannot be readily synchronized in phase with the system framing. However, the transition envelope should be the same as that derived for the synchronous measurement. In Fig. 20, the sampled

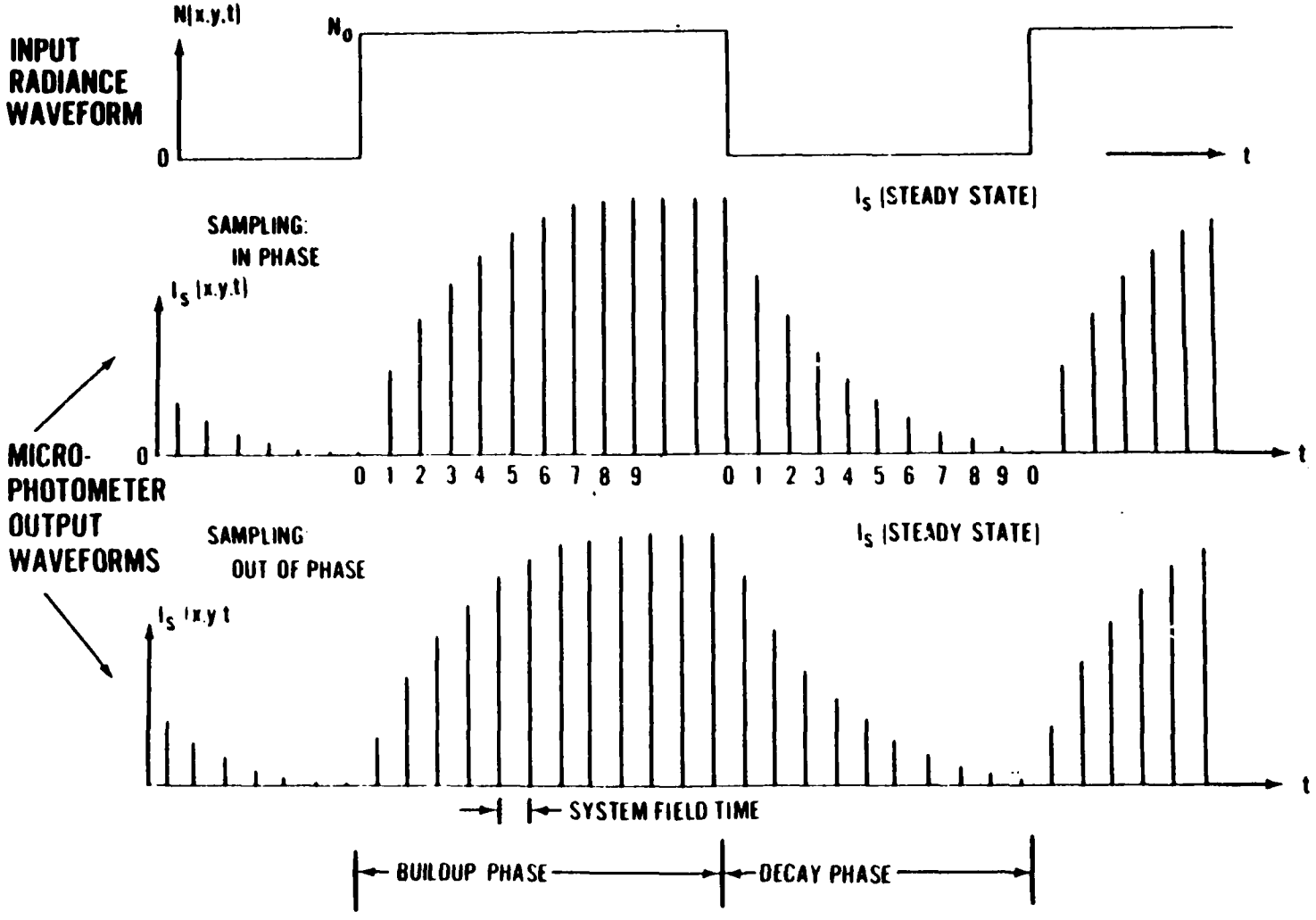

Fig. 20. Time constant test.

waveforms generated using both techniques are shown.

(c) **Equipment Considerations.** The main consideration is the means of modulating the source. At NAVAIRDEVCEN, several techniques have been tried including a mechanical shutter and a pulsed fluorescent source. The most successful approach has been the use of light-emitting diodes. An array of these diodes can be used to generate a uniform field of radiance for working with visible systems. A logic circuit has been recently designed at NAVAIRDEVCEN to separately control the on time, off time, and phasing of the modulation. A complete description of the logic and driver circuitry used at NAVAIRDEVCEN is being prepared and will be made available for possible use in the prototype evaluation facility being constructed at NVL.

For work in the infrared, a mechanical chopper would be required. The chopper could possibly be comprised of a mirror made to oscillate so that a point in the field of view is switched back and forth between two blackbody temperatures. The pulse train from the sampling detector can be used to synchronize the modulation with the system framing rate.

The method of using the spatial rather than the temporal step has some distinct advantages. The same radiation source used in other tests can be directly applied making pulsing and chopping unnecessary. Some analysis and experimentation will be required to determine the accuracy of this method.

(3) System Jitter

(a) **Definition/Discussion.** System jitter is defined herein as a displacement of the field of view as seen at the display which occurs independently of relative scene/sensor displacement. The effect of jitter on the observer will depend on the amplitude frequency (absolute spectral) characteristics of the jitter. Jitter will also affect objective system measurements made at the display. It is, therefore, desirable to characterize jitter prior to making other measurements so that the techniques can be adapted to the degree of jitter present.

(b) **Procedure.** Three methods are proposed: the first method is to generate a linear gradient of radiation as a source and to image the microphotometer pickup at some point on the display where this gradient is linearly transformed to a spatial-brightness gradiant. Then, by "slope detection," jitter will result in an a-c microphotometer output as the gradient moves back

and forth causing lighter and darker areas to be imaged. Measurement signal-to-noise can be improved by measuring jitter along one axis at a time and letting the gradient pattern and measurement slit extend along the orthogonal axis to increase signal. For accuracy, the gradient should be as steep as possible, assuming small amplitude jitter, but steepness will be limited in amplitude by the system's linear transfer range and spatially by the system's ability to image small targets. This measurement is liable to signal-to-noise problems due to the small area measured and the wide bandwidth needed to preserve the spectrum of the jitter.

A second method involves placing at the collimator focal plane a "grating" or extended bar target consisting of many parallel square wave bars each subtending a few resolution elements. This target may subtend 20% to 30% of the system field of view along each axis with the bars oriented perpendicular to the measured axis. A second similar bar mask is placed in front of the photometer so that its apparent period equals that of the displayed mask. The two masks, aligned with their bars parallel, form a kind of "moiré pattern" whose transmission depends on the relative displacement of the two masks. In this way, the average brightness of a large area of the display may be made to vary with system jitter, and a considerably higher signal-to-noise can be achieved. This method has several practical drawbacks including system distortion which would destroy the matching of the patterns. This could in turn be alleviated by "custom-building" the display mask using opaque tape when a suitable display is used.

A third potential approach uses a multichannel sensor to improve the signal-to-noise of the display measurement. A photosensor consisting of many small adjacent pickups is imaged onto the display face such that several (10 to 50) sensors view an area equal to that of a line-spread function on the display. One way to implement such a sensor is to use a fiber optics bundle partitioned into separate small bundles: the small bundle ends are molded into a "focal plane" to form the array of adjacent pickups, and each small bundle is coupled to a separate photosensor. A line source is imaged by the sensor system, and the resultant LSF is imaged onto the pickup array. The outputs of the separate photosensors are then polled automatically to determine the location of the peak of the LSF in real time. An alternative way to implement this same idea would be to procure one of the new solid-state optical line scanner arrays developed for optical character recognition applications. These devices combine the pickup and readout functions in a single package requiring only power and clock to produce video. Readout speed is limited by the serial nature of the video output but would probably suffice for sensors having typical frame rates.

When the movement of the imaged scene relative to the physical display is known as a function of time, the spectral characteristics of the jitter may be inferred with appropriate band limitation assumptions. Note that significant lag occurring after jitter is introduced would make this measurement overlap MTF considerations.

(c) Equipment Considerations. Three methods for measuring jitter were proposed above. The first requires the means for generating a linear radiation gradient of adjustable ΔT and adjustable size. Representative values would be $\Delta T \simeq 5°C$ with slopes ranging from 1 to 20°C/mr. Source linearity should be such that the system's linearity is limiting.

The second method requires a fairly standard bar target consisting of several tens of bars, the pattern extending 20% to 30% of system field of view in both dimensions, backlighted as usual.

The third method utilizes the usual slit source. (Where jitter measurement is being used to correct an LSF measurement, two slits on the same horizontal plane are required – one for each measurement.)

For output measurement, the first method requires the standard slit photometer using a wide enough bandwidth to capture the jitter's spectral content and provision for automatic "capture" of successive (frame by frame) measurements.

The second method requires the grating in front of the display, as described in the procedure above, as well as a large-area photometer with the requisite bandwidth and "signal capture" provisions.

The third method requires the particular multichannel sensor chosen to detect the position of the LSF on the display face. Supporting this sensor are the optics needed to image the LSF onto the sensor array, and the electronics required to extract the information about LSF position from the array outputs.

f. System Geometric Response.

(1) Magnification and Field of View

(a) Definition/Discussion. Magnification and magnifying power are two parameters useful in describing a system's geometric response. Magnification can best be defined as the ratio of the angle (or distance) defining

the position of a point in image space to the angle defining the corresponding position in object space. Distortion is a measure of how magnification across the field varies with respect to the paraxial magnification. The effects referred to as barrel and pincushion distortion in electro-optical systems are due to the decrease and increase, respectively, in magnification with radial position.

Magnifying power is used to describe the microscopic or small-scale transfer of an object through a system. It is defined as the ratio of the angle subtended by a given object at the eye with the imaging system to the angle subtended by the same object without the imaging system. At the center of the field of view, the magnifying power will be numerically equal to the magnification. In electro-optical systems, the magnifying power will often depend on how close the viewer stands to the display. In such systems, magnifying power can be uniquely expressed only if the viewing distance is specified. The magnifying power can, in principle, be calculated from the magnification. In practice, though, it may be more accurate to do the measurement independently.

In general, both the magnification and magnifying power will not vary in the same manner for all orientations about the center. Therefore, a point mapping of the object to image plane is required to completely characterize distortion.

The field of view is the total angular object extent presented on the display.

(b) Procedure. A point source is centered in the collimator field of view. A rectangular reticle is superimposed on the display. The gradations of the reticle are in fractions of the display diagonal. The system is aligned so that the point is imaged at the center of the display. The system is then rotated in the field of view so that the point is imaged at each intersection. The horizontal and vertical angle of the rotation is recorded at each point. The extremes of the display now define the overall field of view. This technique saves the time of measuring distances off the display.

An alternate procedure would have the system image a known-sized input square in the center of the field of view. The size and location of the image are measured as the system is rotated within the field of view. This technique may be preferable for those systems for which it is excessively difficult to superimpose a reticle on the display.

(c) Equipment Considerations. The point source used in making

image-spreading tests can be used. Square targets will be needed if the second method is used. Two degrees of rotational freedom are required. An accurate determination of the angle of rotation is required. At the output, a transparent overlay with a rectangular grid is required. The operator will need sufficient magnification to determine the point of coincidence between the grid intersection and the point-source image. For the second method, the operator will require a cross-hair reticle in his magnifying optics. The data may be fed directly to the computer for manipulation for a desired figure of merit.

(2) Off-Axis Distortion

(a) **Definition/Discussion.** System performance will, in general, vary over the field of view. It is, therefore, desirable to perform many of the tests at points off-axis. Of particular importance is the MTF measurement.

(b) **Procedure.** The system will be rotated in the collimated beam in aximuth and elevation to a given off-axis point. The test patterns will be positioned on-axis to the collimator, and measurements will be performed as in the on-axis case.

Performing off-axis testing by rotating the system in the collimated beam is equivalent to real-world, off-axis testing of the system. The image plane irradiance produced off-axis by a source of a given size and given radiance will be the same for the source in the real world or in the collimator focal plane. The position of the source in the test system's image plane will be identical in both cases as well. The only difference in the two test methods occurs when the linear size or extent of the object is considered. A given-sized object in the focal plane of the collimator does not subtend the same angle as an identically sized object would off-axis in the real world (for a flat object plane). Thus resolving a 1-mm square target at the focal plane of the collimator with the system tilted 30° is not equivalent to resolving a 1-mm square target 30° off-axis. However, if angular extent or subtense of the object is considered, the two test situations are identical. Resolving a 1-mr-square target at the focal plane of the collimator with the system tilted 30° is equivalent to resolving a 1-mr-square target 30° off-axis in the real world.

(c) **Equipment Considerations.** Of prime importance, once again, is the ability to rotate the system about two axes. The extent of rotation should be sufficient to handle most practical systems. A total angular coverage of at least 60° would be required to handle most systems. For direct-viewing systems, the readout sensor must be rigidly attached to the platform that is rotating the system.

The performance of most electro-optical systems at any point in the field of view will depend on the conditions existing over the entire field of view. In both visible and infrared devices, the operating point can vary as the average scene radiance varies. It is, therefore, necessary to control conditions over the entire field of view. This is particularly difficult for infrared systems since the temperatures of the room surrounding the collimator cannot always be maintained. Making off-axis measurements further increases the problem.

It will, therefore, be necessary to fill all of the system field of view with a source of controlled radiance. One possible configuration would utilize baffles or "shrouds," placed in the vicinity of the sensor, having an aperture through which the sensor can view the collimator aperture. For infrared imaging, the temperature of the shroud must be controlled or at least held constant and uniform in time and space. For off-axis testing, the shrouds should extend over more than twice the system field of view.

g. **System Display Uniformity.**

(1) **Fixed-Pattern Noise**

(a) Definition/Description. *The uniformity of the output display of photon-imaging devices is determined by such stationary variations in display brightness as shading, mottling, blemishes, and granularity. They are commonly called fixed-pattern noise. Figures 21, 22, and 23 will help to visualize the imperfections under consideration.*

1 **Shading.** Shading is a large-area, low-spatial-frequency type nonuniformity. It usually appears on the display as a gradual increase or decrease in brightness from one part of the display to another (very often center to edge).

2 **Mottling.** Mottling is a medium-area, medium-spatial-frequency type nonuniformity. It usually appears as an area of higher or lower brightness than its surroundings. The brightness change is usually sharp rather than gradual.

3 **Blemishes.** Blemishes are a small-area, high-spatial-frequency type nonuniformity on a scale of the smallest detail resolved by the sensor. A blemish appears as an isolated bright or dark point with high contrast compared to the surrounding area.

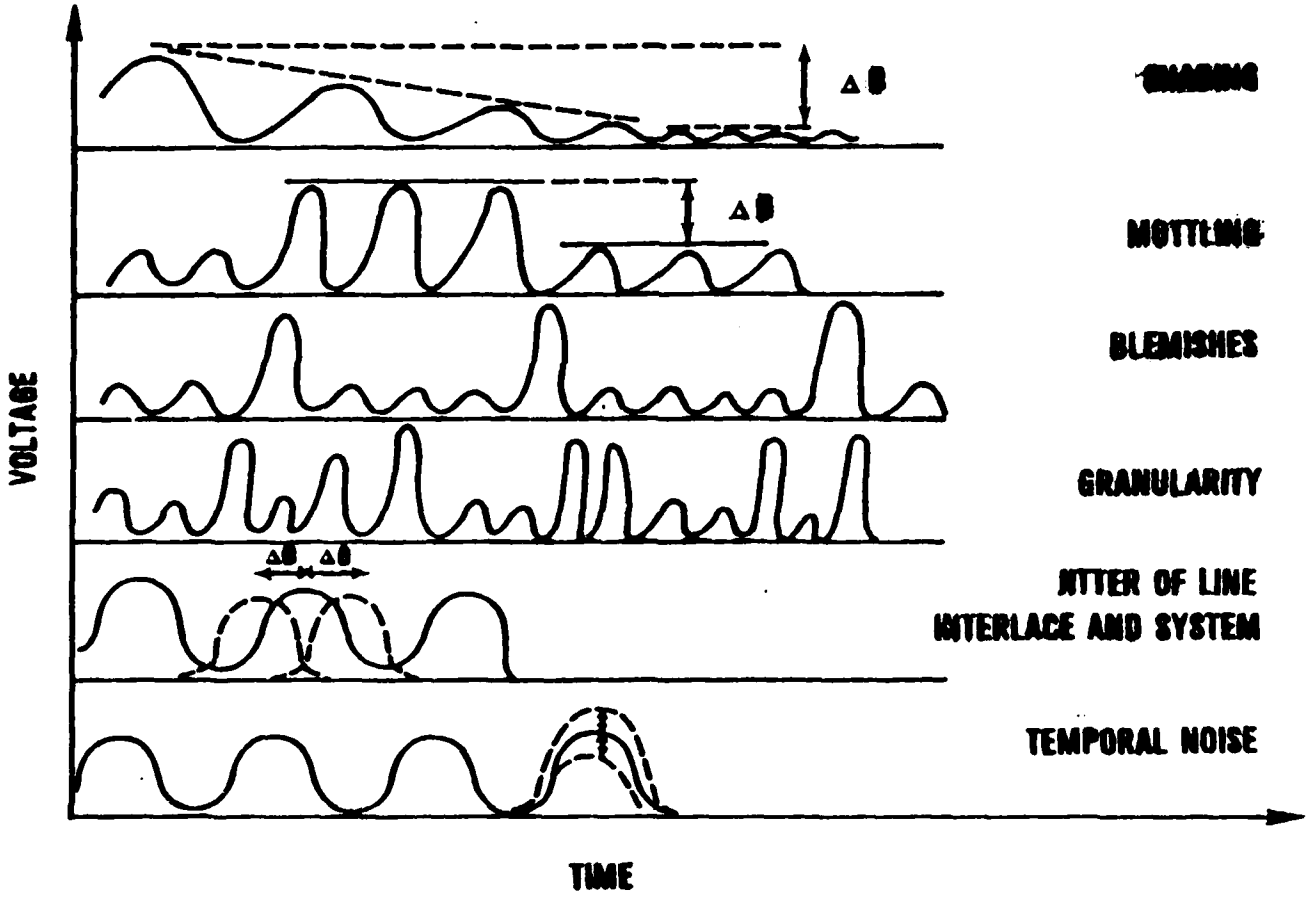

Fig. 21. Illustration of display nonuniformities as observed on an Image Orthicon video line in the high-resolution case.

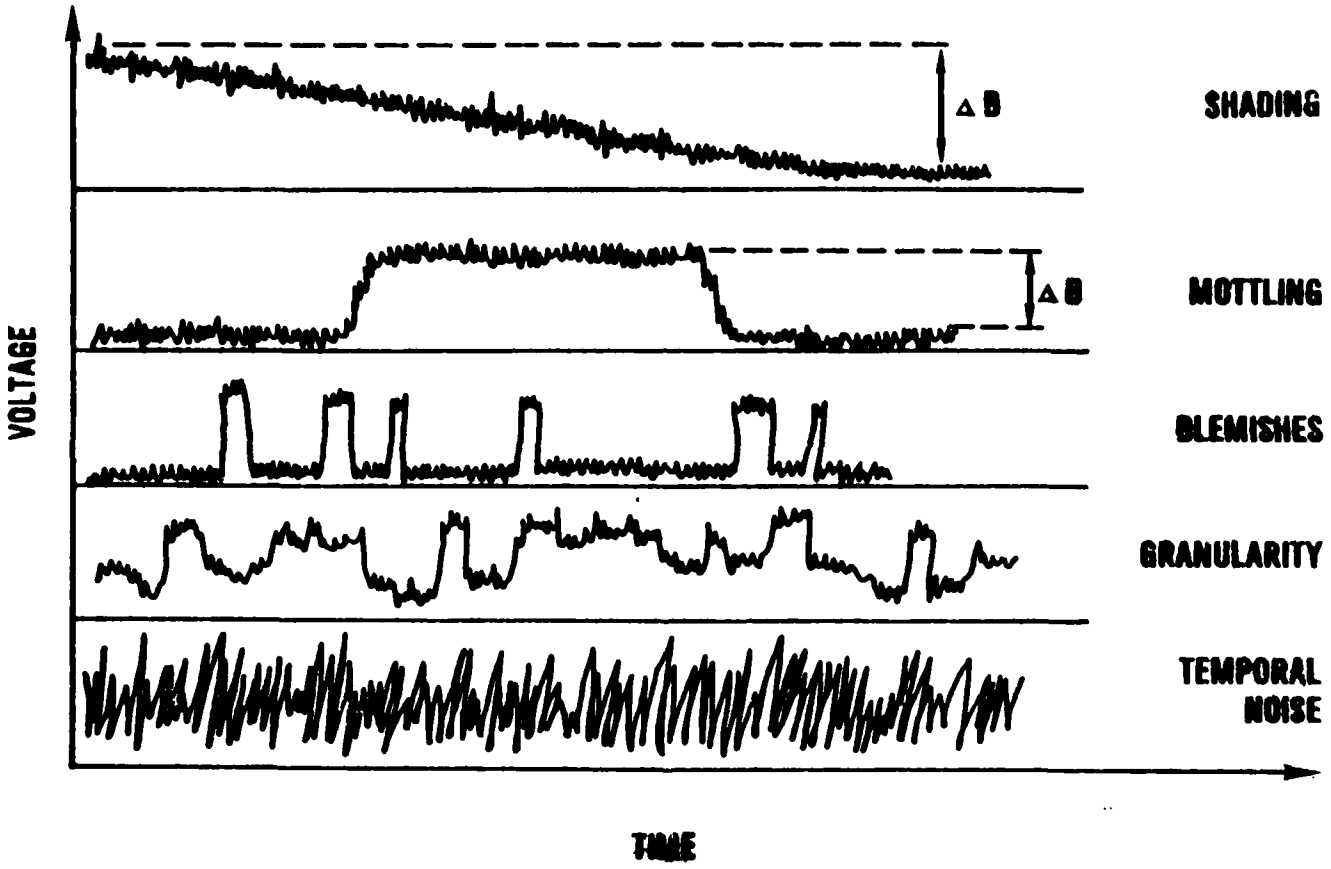

Fig. 22. Illustration of display nonuniformities as observed on an Image Orthicon video line in the low-magnification case.

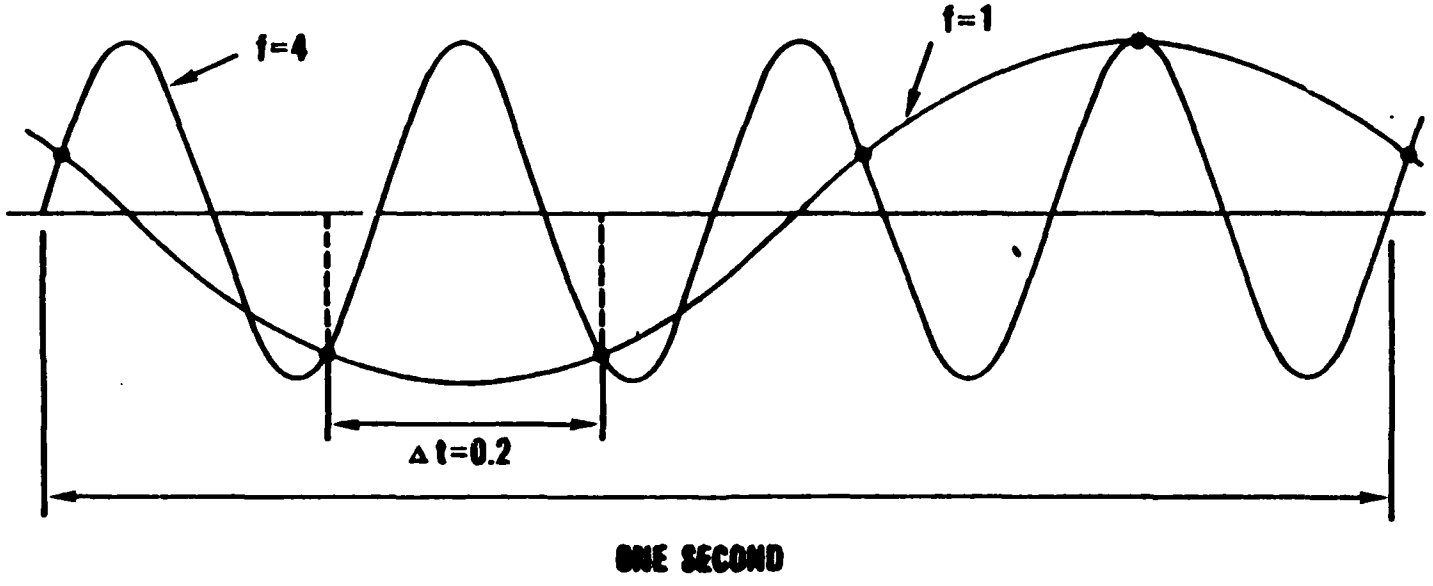

Fig. 23. Sampling of sinusoidal wave (high frequency) and resulting aliasing (low frequency).

4 Granularity. Like blemishes, granularity is a small-area, high-spatial-frequency type brightness variation on a scale of the smallest detail resolved. However, one does not consider isolated points but rather the very closely spaced, randomly arranged and sized areas of random brightness variation (like those one observes on extremely magnified photographic prints).

These spatial nonuniformities result in patterns which range in size from as large as a display diameter to one tenth of a percent of that diameter. The smallest detail of interest for the human observer may be on the order of 2.5×10^{-2} mm for the output of a first-generation image intensifier. This corresponds to 20 cycles/mm or nominally 3×10^{-1} mrad or 1.6 cycles/mrad as this type display is commonly viewed by the observer through an eyepiece. However, for a directly viewed 8-in.-diameter cathode ray tube display, scanned at standard U.S. TV rates, the smallest detail of interest may be 3×10^{-1} mm or 1.6 cycles/mm.

The mean brightness of the display can be as low as 10^{-4} lumens/cm^2 ster (for a Generation I Image Intensifier to be viewed by the dark-adapted human eye) and as high as 10 lumens/cm^2 ster or higher for an 8-in.-diameter cathode ray tube display to be viewed under normal daylight environment.

The variations about these mean-brightness values to be of interest for the human eye are at the most one order of magnitude below and one order of magnitude above this mean value.

(b) Procedures. Measurement procedures to evaluate these nonuniformities consist basically of examining the display brightness at different points and at different times with a photo-sensitive device having known characteristics, whose effective aperture is variable, and which can be made comparable to or even smaller than the size of the brightness pattern being examined. Simultaneously, the sensor of the imaging system under evaluation is viewing a uniformly bright test pattern, filling its entire field of view.

As most of the imaging systems to be evaluated have a tendency to be nonlinear, it is recommended to determine first of all their signal-transfer curves. Most likely, there will be different signal-transfer curves for different operating conditions. It is desirable to evaluate the systems at different positions along the signal-transfer curves with operating conditions chosen to be at least one each in the linear and in the nonlinear region. From the multitude

of transfer curves, one should choose at least three – one corresponding to optimum viewing conditions to the eye, one above that condition, and one below. All procedures for fixed pattern noise evaluation have to include temporal averaging to eliminate temporal effects.

The sampled brightness data are then processed by a computer to determine the desired uniformity characterizations such as contour plots, relative brightness change, Δ B/B, RMS and amplitude distribution, and spatial and temporal noise power density spectra.

The candidate procedures for the above considered fixed-pattern noises follow.

1 **Shading.** The procedure is to scan an aperture across the shading pattern, possibly along a major axis of the display, or a maximum diagonal across the shaded area. The effective aperture diameter need not be smaller than 1 percent of the display diameter.

In the ideal case, where there is only a gradual brightness change across the display from one side to the other or from center to edge, the relative brightness change of interest is given by the brightness at the beginning and at the end of the diagonal or major axis.

In the case of an abrupt brightness change or even several such changes, a contour plot is recommended at 4 to 5 brightness levels. This contour plot can be displayed on a cathode ray tube storage display and then photographed. It can also be obtained by connecting a hard copy machine to the computer.

2 **Mottling.** The proposed procedure is to scan a sampling aperture across the display covering an area slightly larger than the mottled area. The diameter of the sampling aperture need not be smaller than one-tenth of the diameter of the mottled area. Usually, aperture sizes of 1 to 2 mm in diameter are sufficient, which takes into consideration a slightly higher resolution requirement for taking contour plots in the presence of abrupt brightness changes.

In the case of an abrupt brightness change encircling the mottled area, one determines the mottled area and the relative brightness change ΔB/B. In the presence of gradual and abrupt brightness changes, a contour plot is recommended; and one is interested also in the maximum Δ B/B. The contour plot can be displayed on a CRT display

storage tube or given in hard-copy form as explained above.

3 **Blemishes.** Blemishes are a small-area, high-spatial-frequency disturbance with an extremely high $\Delta B/B$. If there are a few blemishes, say 5 to 10, they can be located and counted with the eye. Otherwise, it is necessary to scan with an aperture having a diameter smaller than the size of the blemish (usually around .1 mm to 1 mm) in small increments across the display. The increments have to be on the order of magnitude of the aperture size. As the $\Delta B/B$ is extremely high, it is not necessary to average over 2 sec. Averages over .2 sec and even less are ample.

This procedure allows calculation of the total number of the blemishes and their distribution across the display area. This information is added to the hard-copy contour plots describing shading and mottling.

4 **Granularity.** The proposed procedure is similar to that used commonly in photographic circles to evaluate film granularity. It is based on the observation that if one scans a very small aperture across the photographic area disturbed by granularity, one obtains brightness variations. The RMS of these brightness variations is taken as a measure of the granularity.

The sampling aperture should be very small. However, there exists no unique requirement, since over a large range of aperture sizes the RMS value is inversely proportional to the aperture size. This is known as Selwyn's law. Aperture sizes commonly used in the film industry are 2.4×10^{-2} mm.

Additional characterizations are the amplitude distribution and the power-density spectrum. The latter is obtained from the equi-spaced sampling data (brightness at various locations) by correlation and Fourier transformation techniques as described in the literature. The important consideration for planning the experiment is the desired range of the spatial frequencies covered and the total number of points to determine the frequency resolution from the power spectrum.

(c) **Equipment.** The equipment to perform these measurements must meet the above-mentioned experimental conditions. It must have a resolution $\cong$ the effective aperture of 2.5×10^{-2} mm in diameter or an angular resolution of 3×10^{-1} mrad. It must be sensitive to brightness levels

of 10^{-5} lumen/cm^2 ster and must be linear over two orders of magnitude.

The following equipment can be used to meet these requirements:

- Spotphotometer.
- Signal generating camera tube with a good storage target like Image Orthicon (I.O.), Image Isocon, SEC.
- Peripheral equipment including a high-speed A/D converter and a computer.

The operation of the equipment is as follows:

1 **Spotphotometer.** As an example, we will choose a Spectra-Pritchard Spotphotometer, Model 1980, mounted on a mechanical x-y and possibly z translation unit. Depending on the effective aperture size which depends on physical apertures within the photometer and the imaging optics, smaller or larger areas of the display under investigation are imaged onto the phototube. The output signal from the spotphotometer is a measure of the average light level of the sampled area. In the case of a scanned display, the output from the photometer is taken directly at the phototube and consists of a pulse or a burst of pulses representing the total brightness of the sampled area (Fig. 24). Variations in display brightness then show up as variations in the area under the pulses. The determination of the total brightness (adding the areas) will be done digitally with an A/D converter and computer. The brightness can also be measured using the photometer's built-in averaging electronics with a time constant of .1 sec and its analog meter or, again, an A/D converter and a computer. Areas of constant brightness are measured by xy scanning and the recording of position data taken from the xy translation unit.

The technical data of the Spectra-Pritchard Spotphotometers are as follows:

Spectral range:	Matched to the human eye
Sensitivity:	10^{-5} - 10^{7} fL scene brightness.
Effective aperture:	Variable in steps from 16 35 mm to .02 mm in diameter.

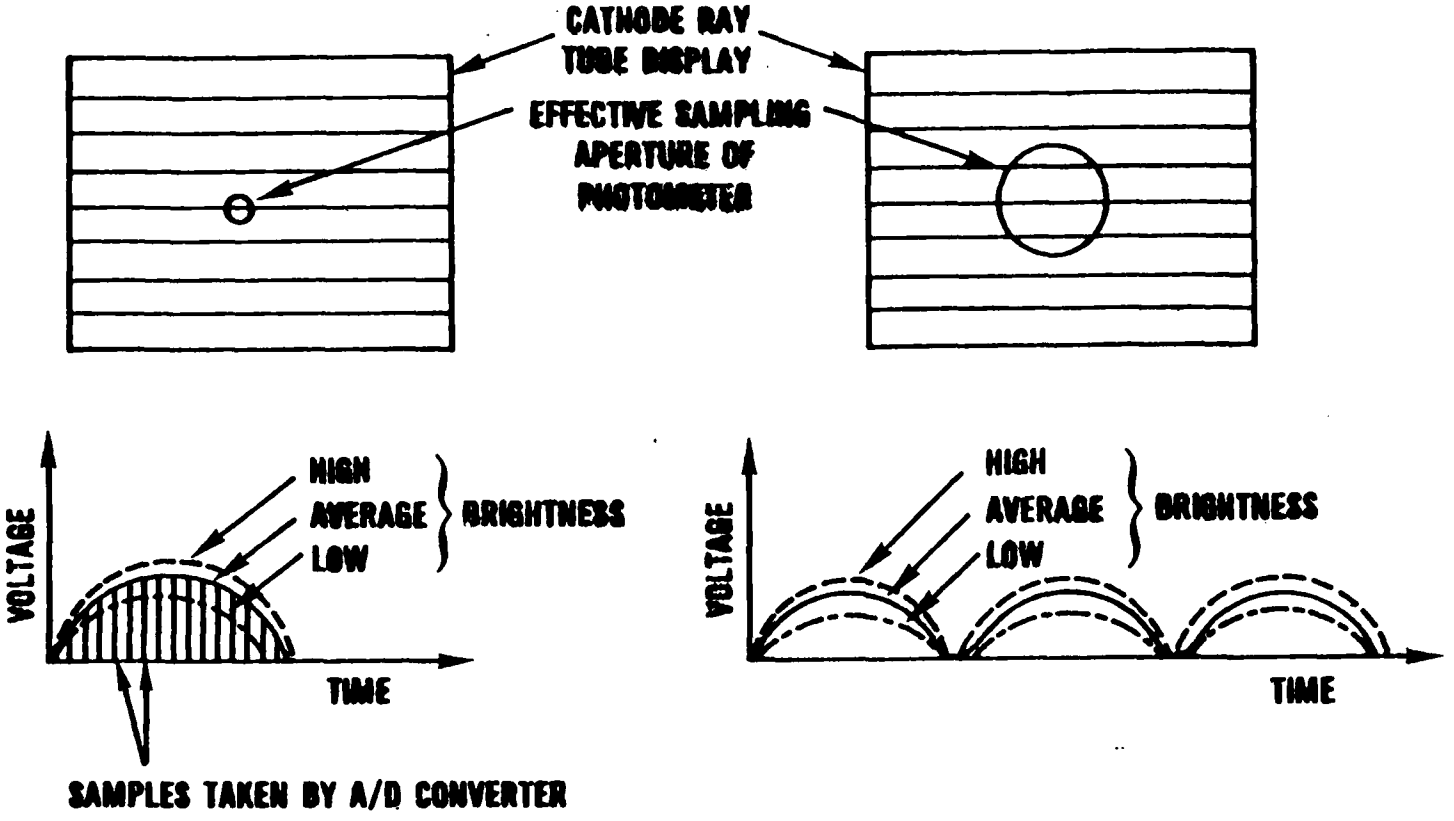

Fig. 24. Sampling of cathode ray tube display with spot photometer of various aperture sizes and resulting photometer signals.

Time Response: Matched to the human eye if built-in electrical circuits and meter are used; better than 10^{-7} sec if output of phototube is taken directly.

Dynamic Range: At least 3 orders of magnitude.

2 **High Resolution TV Camera Tube Image Orthicon.** A typical example is the Image Orthicon Model RCA 7198A.

The display under investigation is imaged completely or partly onto the camera tube face. The effective aperture sampling the display is determined by the electron beam of the camera tube, the target characteristics, the imaging lens, and the raster system. Depending on the camera MTF for horizontal and vertical resolution, the aperture shape can be square or rectangular. It is calculated from the limiting resolution horizontally and vertically which effectively determines the picture element size.

In order to avoid alignment problems and Moire disturbances, the camera tube is adjusted such that its scanlines are perpendicular to the scanlines of the display under investigation. If the effective I.O. sampling aperture is small compared to the display raster, then the output signals of the camera tube appear as indicated in Fig. 25. The peak amplitudes of the pulses are indicative of the brightness of the display lines; variations in brightness will result in variations of the amplitudes. The locations of the peaks of the pulses are indicative of the location of the scanline on the display. Areas of constant brightness will be measured by locating peaks of constant amplitude on the camera tube face and by knowing the imaging data of the lens.

The determination of the peak amplitudes, their temporal and spatial variations, and their location and the determination of the size of the disturbance pattern will be made with the aid of a digital computer.

If the effective aperture size is large compared to the line structure of the display, then the display lines are no longer distinguishable and the I.O. video line appears as in Fig. 25. The disturbance pattern is again evaluated from the video lines with the A/D converter and computer. However, it is no longer necessary to locate the peak amplitudes corresponding to the individual display lines. In this case, TV tube evaluation procedures can be applied as described in the Appendix.

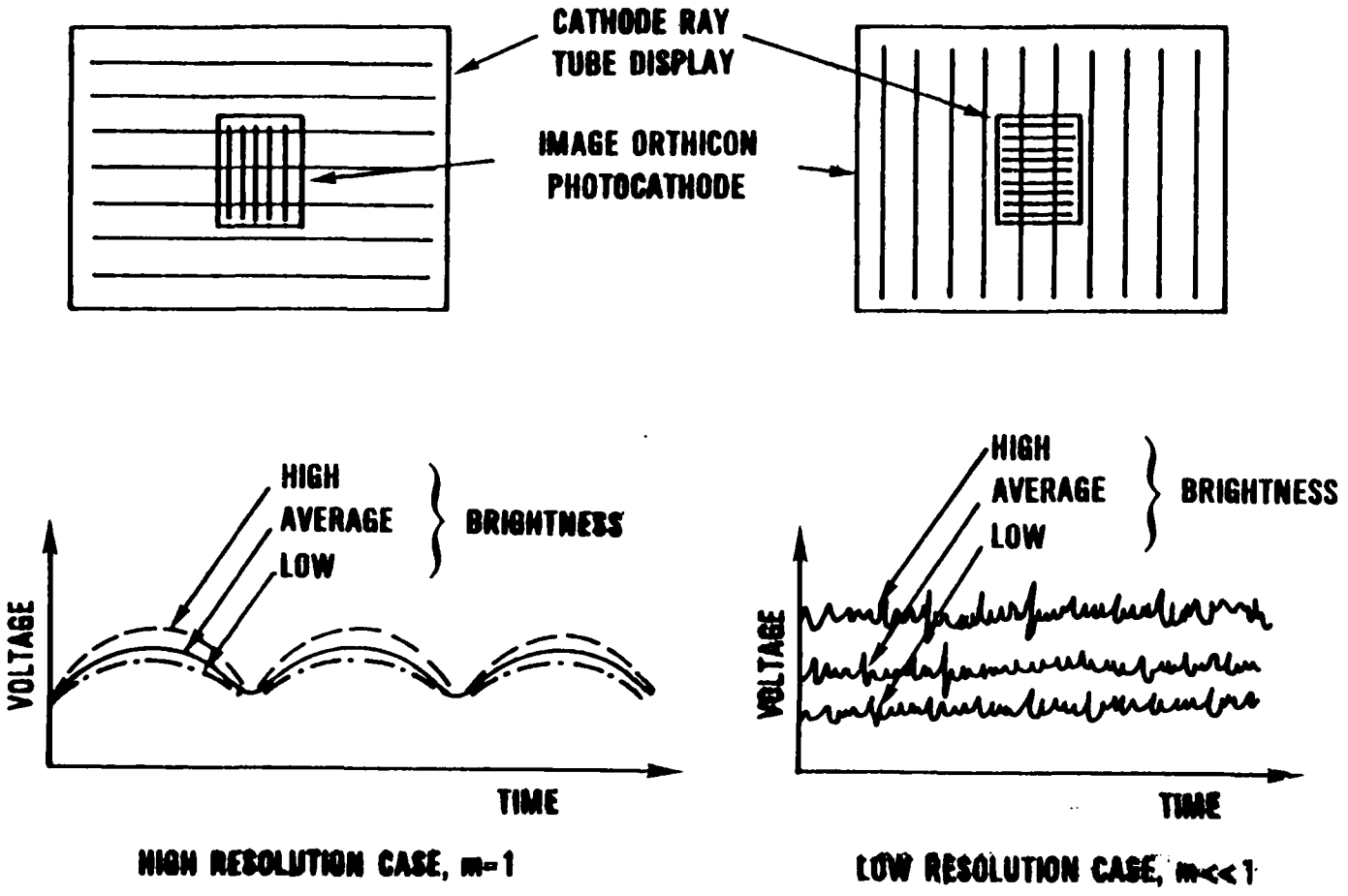

Fig. 25. Sampling of Cathode Ray Tube Display with Image Orthicon at various magnifications (m) and resulting Image Orthicon video lines.

Normally, the I.O. is operated continuously at standard U.S. TV rates. The data on the brightness of the display are then given as averages over 1/30 sec, neglecting for the moment any I.O. lag. However, if it is intended to determine brightness variations averaged over periods longer than 1/30 sec, the I.O. can be operated in the so-called snapshot mode. The photocathode is exposed to the display for the desired integration time while the readout beam is blanked. Then the photocathode is blanked and the readout beam is started.

The technical data of the Image Orthicon Model RCA7198A are:

Spectral sensitivity: S-20 cathode.

Sensitivity, given by illumination on tube face:

3×10^{-3} footcandle – Signal to noise 23:1.
3×10^{-4} footcandle – Signal to noise 9:1.
3×10^{-5} footcandle – Signal to noise 3:1.

Spatial resolution:

550 TV lines at 3×10^{-3} footcandle.
350 TV lines at 3×10^{-4} footcandle.
115 TV lines at 3×10^{-5} footcandle.

Effective aperture diameter on display for 1:1 imaging:

$2{:}1 \times 10^{-2}$ mm at 3×10^{-3} footcandle.
3.5×10^{-2} mm at 3×10^{-4} footcandle.
1.4×10^{-1} mm at 3×10^{-5} footcandle.

Time response: .1 sec (including lag).

Dynamic Range: Two orders of magnitude, linear.

(2) Raster and Scan Line Effects

(a) Definition/Description. Imaging systems working with a sampling process such as TV systems or multiple-element scanners show temporal brightness variations like jitter of scan lines, jitter of interlace, jitter of system, and jitter of scene. Over and above, there is aliasing which can be a

stationary as well as temporal disturbance (Figs. 21, 22, and 23).

1 **Jitter of Scanlines.** Jitter of scanlines is a temporal variation in the location of the scanlines about an average location.

2 **Jitter of Interlace.** Jitter of interlace is a simultaneous. temporal variation in the location of all the scanlines of one field about an average location.

3 **Jitter of System.** Jitter of system is a simultaneous, temporal variation in the location of all the scanlines of a frame about an average location.

4 **Jitter of Scene.** Jitter of scene is a relative movement of the image of the scene appearing on the display about an average location.

5 **Aliasing.** Aliasing is a common phenomenon in sampling data systems. It always occurs when the Nyquist frequency $\frac{1}{2T_s}$, given by the sampling period T_s, is smaller than the frequency of the sampled waveform in the temporal-frequency domain. The same holds for the spatial-frequency domain when the spatial frequency determined by the detector or sample spacing is smaller than the apparent spatial frequency projected by the lens onto the detector array (or sampling system). Then, one obtains spurious signals at frequencies lower than the sampled frequency (Fig. 23).

The temporal-brightness variations described above range in frequency from almost DC level (.001 Hz) up to the Nyquist frequency of the system under investigation (usually 15 Hz). This upper limit in temporal-brightness variation may also be determined by size and decay characteristics of the display phosphor which can be around 10^{-1} sec as used in direct-viewer image intensifiers or 10^{-4} sec as used in cathode ray tube displays. However, most displays are viewed by humans and, therefore, the highest temporal-frequency range of interest is mostly determined by the time constant of the human eye which is around 2×10^{-1} sec.

The lowest brightness levels of interest and also the dynamic range of levels of interest are determined as discussed under Paragraph g(1).

(b) **Procedures.** Measurement procedures consist basically of periodically examining the display brightness, possibly simultaneously at different points, with a photo-sensitive device described under Paragraph g(1)(b). In addition, it has to meet the above-discussed, time-constant requirement; that is, its time constant should be at the most 2×10^{-1} sec and possibly smaller.

1 **Jitter.** All types of jitter, as discussed above, can be evaluated simultaneously with the Image Orthicon while the sensor of the system under investigation is viewing some scene – possibly a bar pattern. Even though the bar pattern is visible on the display, the I.O. in its high-resolution mode is able to locate the individual display lines (Fig. 21). It, therefore, can determine any movement of the display lines or the scene. The desired jitter characterization is RMS and amplitude distribution of the display line or scene displacements (Fig. 21).

2 **Aliasing.** The proposed procedure is to expose the system under test to frequencies (spatial as well as temporal) higher than the Nyquist frequency (spatial and temporal case) of the system. The resulting low frequencies are analyzed, their power spectrum being a measure of the degree of aliasing (spatial as well as temporal domain).

The power spectrum is obtained by periodically sampling the brightness of the display with a photometer or an I.O. and analyzing these samples by correlation and Fourier transform techniques.

h. **System Sensitivity Response.**

(1) **Temporal Noise**

(a) **Definition/Description.** The most widely known disturbance interfering with the recognition of signals in imaging devices is temporal noise. It is a temporal-brightness fluctuation for a viewer determined display area and sampling time.

Due to the statistical nature of photon emission average, the photon flux carrying the information on the scene is modulated by a random, temporal fluctuation. This temporal (photon) noise is the ultimate limitation of imaging systems.

However, in most cases this ultimate limitation is hardly ever achieved. There are temporal noise sources other than the photon noise.

such as processes associated with the photon-photoelectron conversion, the electrical readout, the electrical circuits, and the means of presenting the information on a display to the human observer, which may be responsible for the temporal-brightness fluctuations on the output display of an imaging system. Temporal noise is commonly characterized by its RMS value, its amplitude distribution, and its power density spectrum. Also temporal noise as it appears on the output display of imaging devices is associated with a geometrical pattern, like granularity, except that this pattern is varying in a random fashion. This affects performance since, as one knows from threshold recognition experiments for the human eye, the recognition of patterns is dependent on size and amplitude of the pattern. It is, therefore, expected that the time-dependent granularity associated with temporal noise is an additional important characterization of the temporal noise. This granularity per unit time will be characterized by the spatial power density spectrum.

(b) **Procedure.** The proposed procedure is to sample the brightness of the display at one location in equi-spaced periods and to analyze the data by correlation and Fourier transform techniques which will result in the temporal power density spectrum as described in the literature. The test pattern to be viewed by the system under test is a well-calibrated, uniform, large-area radiator.

It is assumed that temporal noise is independent of the location on the display – an assumption which one may want to test. The sampling aperture should be on the order of magnitude of the smallest detail recognized by the human eye. The evaluation of the spatial pattern of the temporal noise follows the same example as outlined in the procedure to evaluate granularity. However, as this pattern varies with time, it is important to have a multichannel system to evaluate that pattern, since only in this way is one able to evaluate different parts to the display simultaneously.

(c) **Equipment.** The procedure can be implemented with both the Spotphotometer and the Image Orthicon as described in Paragraph g. However, the evaluation of the spatial effects with the Spotphotometer has to include a storage medium to "freeze" the spatial effects for the time of the evaluation.

(2) **Signal-to-Noise**

(a) **Definition/Description.** Recent theories predicting observer performance of imaging systems are based on an assumed signal-to-noise ratio at the display. The basic assumptions are that the systems are linear and that

the noise is temporal and due to the photon-photoelectron conversion process.

Both assumptions have to be challenged. First of all, imaging systems are only partly linear – particularly thermal systems. Many of them even achieve their optimum performance in the extremely nonlinear portion of their signal transfer curve.

Secondly, there are temporal noise sources other than the ones associated with the photon-photoelectron conversion process within the system contributing to the total temporal noise as discussed in Paragraph h(1)(a). It is, therefore, of importance to evaluate signal-to-noise at the display directly.

Signal is the difference in the average brightness for two adjoining small areas – of course, averaged over the above-treated stationary nonuniformities. It is commonly given in peak-to-peak; however, it can also be given in RMS.

Noise is the time-varying brightness fluctuation for a viewer-determined display area and sampling time. It is usually given in RMS.

(b) **Procedure.** The proposed procedure is to determine peak-to-peak signal and RMS noise separately and then to perform the division.

The procedure to determine peak-to-peak signal is to scan an aperture across the display while the system under investigation is exposed to a well-calibrated, large-area radiator whose brightness is spatially modulated by a sine wave. The pattern on the display is again a sine wave. Of course, the spatial frequency of the sine wave should be smaller than the Nyquist frequency of the effective resolution in the system under investigation and larger than the one determined by the display diameter. The aperture diameter should be small compared to the spatial period of the sine wave. The aperture is scanned across the sine wave in the direction of the wave which can be adjusted to be parallel to the scan lines of the display.

RMS noise is determined as described under Paragraph h(1)(a). The division of signal and noise can be done by calculator or can automatically be given by the computer.

(c) **Equipment.** Both the Spotphotometer and the Image Orthicon can do this measurement in a straightforward manner.

(3) Detective Quantum Efficiency (DQE)

(a) Definition/Description. Determination of the signal-to-noise ratio, both at the input and output ports, permits evaluation of the Detective Quantum Efficiency (DQE). Its application to display systems and displays is being examined. This quantity, conceived by Rose and named by Jones, is a number designed to provide the measure of device quantum efficiency when limited by noise.

It is being commonly referred to and increasingly used by the British as "effective quantum efficiency" (EQE). As such, DQE, or EQE, directly indicates the efficiency of the device in providing an absolute rating of usable "signal out" per "signal in."

(b) Procedure. The proposed procedures on signal-to-noise will also allow verification of current interpretation of DQE which is still being developed. The performance of several devices will be measured in terms of DQE, and the overall performance of widely different imaging systems will be compared to indicate how DQE serves to indicate comparative imaging quality.

(c) Equipment. Apparatus required will be the same as for the foregoing items.

i. Front-End Sensitivity Response.

(1) Signal Level and Noise Level

(a) Definition/Discussion. In image devices that are provided with an electrical output, the purpose of the electrical output is to provide the picture information in a convenient form for transmission to a remote display. A typical example is the standard television vidicon tube which provides an electrical signal by electron beam scanning at standard U.S. broadcast rates. The amplifiers, transmitters, and receivers must have frequency responses of at least 4.5 MHz in order to convey the highest resolution image information at these standard rates.

This brings us to the most pervasive problem in making even moderately precise measurements from the electronic video signal: namely, the noise associated with this large bandwidth. The best signal-to-noise ratios (SNR) that can be obtained are on the order of 500 to 1 for a high-contrast, low-spatial-frequency optical signal, large beam currents, and state-of-the-art amplifiers. Very often, the signal-to-noise ratio in the electronic signal will

be as low as 2 to 1 even though the final picture at the display will look quite good to the eye. The reason for this apparent contradiction is that the human eye has a very small bandwidth (roughly 5 MHz) and does not respond to the rest of the noise in the roughly 5 MHz video bandwidth. More exactly, the noise is generally proportional to the square root of the bandwidth so that there is an increase in SNR of

$$\frac{SNR_D}{SNR_V} = \sqrt{\frac{1/\Delta f_D}{1/\Delta f_V}} = \sqrt{\frac{\Delta f_V}{\Delta f_D}} = \sqrt{\frac{5 \times 10^6}{5}} = 1000$$

when the transmitted information is displayed. Here, the subscript D stands for display and V stands for video signal (the same as electrical signal).

The origin of these different bandwidths lies in the idea of scanning. There are N resolution elements in the entire picture, and all elements are sensed and displayed at the same time, e.g., in parallel. However, the elements are scanned and transmitted one after the other, e.g., serially. This means that only 1/N of a frame time is spent on each element, or, equivalently, the bandwidth must be N times larger in the video channel. For a standard 525-line system, N is roughly $(525)^2 \simeq 0.28 \times 10^6$ which is close to the bandwidth ratios mentioned earlier. In any scanning system, therefore, the SNR will be very poor and signal measurements very difficult without some form of integration.

Another major signal measurement problem is nonlinearity. Many of the components of imaging systems are *nonlinear*: that is, their output is not directly proportional to their input but to some power of their input. A typical example is a vidicon tube in which

$$I = \alpha H^{\gamma}$$

where I is the current (in amperes) out of the tube with a uniform irradiance H in watts/cm^2 at its input, and α is a constant of proportionality. If $\gamma = 1$, the tube is linear. However, if $\gamma \neq 1$, then for small changes in irradiance dH,

$$dI = \alpha \gamma H^{\gamma-1} \, dH = f(H)dH.$$

and the change in current (which the eye would eventually be sensing as an image) depends on the average irradiance level H and not only the change in irradiance dH. It is important to account for these nonlinearities when

making any image-evaluation measurements. If the system is known to be nonlinear and procedures assuming linearity are used, then all operating conditions must be specified so that the measurements can be understood and repeated.

(b) Procedure. With a suitable image focused on the system, the controls are adjusted while the display is observed for proper operation and maximum resolution. A typical image source would be a Limansky chart in the visible or its equivalent in the infrared.

This source is convenient because it can also be used for MTF measurements. The noisy electronic signal is then averaged by a variety of techniques and the peak-to-peak amplitude of the signal is recorded. The simplest and most popular averaging and recording technique is to photograph the recurrent trace of an oscilloscope. An alternative method is to feed the signal again and again into an analog-to-digital converter and store the results in a computer. If peak-to-peak signal were the only measurement of interest, the scope and camera would be simpler and cheaper though less precise than the computer.

However, the computer offers great improvement in speed, accuracy and precision over the oscilloscope when the measurement of rms noise is considered. Various methods have been investigated for making noise measurements with the oscilloscope.[4] A method which is more precise than the common visual estimation procedure and much less complicated than the method of Jensen and Fawcett is the comparison of known and unknown noise waveforms on a split-screen oscilloscope. In this method, the noisy video waveform is displayed on one-half of the oscilloscope screen, and the output of a random noise generator is displayed on the other half. The output of the noise generator is then adjusted until both waveforms have about the same amplitude, and this noise level is read from the generator and taken to be equal to the noise in the video waveform.

The computer analysis for noise measurement is fully described by Don Fisher in the NELC Phase I ARPA Order 1938 Report (see Appendix).

(c) Equipment Considerations. Two candidates are generally proposed for each category. The first method will in all cases use an oscilloscope with photographic averaging to improve the SNR. The second method will use analog-to-digital conversion followed by data manipulation in a small computer.

[4] L. M. Biberman, and S. Nudelman: *Photoelectronic Imaging Devices.* Vol. II. Plenum Press, N. Y., 1971, Chapter 4.

(2) SNR_D

(a) **Definition/Discussion.** If an image of area a is observed at a display by the eye, which has a time constant t ($t \simeq 0.2$ sec), then

$$SNR_D = \sqrt{(t)\ (\Delta f)\ (a/A)}\quad SNR_V$$

where A is the area of the entire display, Δf is the bandwidth of the video channel, and SNR_V is the "broad-area" video SNR.

This concept has been developed by Rosell and others.

(b) **Procedure.** Having measured SNR_V, then SNR_D can be derived if t, Δf, a, and A are known.

SNR_D will not be specified directly since it will depend on the integration time of the eye, which changes from observer to observer, and on the ratio of image area to total picture area which will change from one picture to the next. Rather, SNR_V, D, and Δf will be measured, and the calculation of SNR_D will be left to be made according to the particular system under consideration.

(c) **Equipment Considerations.** No special equipment will be required in addition to that needed to measure SNR_V.

j. **Front-End Spatial Response.**

(1) Optical Transfer Function (OTF)

(a) **Definition/Discussion.** OTF is defined as the Fourier Transform of the line-spread function of the system being tested. This function is not defined for a nonlinear device since the Fourier Transform is itself only defined for linear systems. The OTF is a complex quantity possessing both a modulus and a phase. Physically, the modulation transfer function (MTF) describes the reduction in amplitude that a purely sinusoidal image of spatial frequency F and infinite extent would undergo in transmission through the system. The phase transfer function (PTF) describes the spatial displacement of a pure sine wave as it is transmitted. A phase shift of 180°, for example, would describe a situation where the contrast was reversed at a given point such as the axis of the system: the sine wave would enter bright on-axis and emerge dark on-axis.

(b) Procedure. Normally, only MTF is measured for imaging devices. MTF should be measured across the picture height and across the picture width since, in general, the resolution will not be the same in both directions. MTF can be measured by the Limansky technique which images a pattern of bars (the optical analog of square waves) onto the image tube and measures the reduction of the amplitude of the video signal as the bar frequency increases. A correction is applied to convert the data to the response the system would have if the bars were sinusoidal, but no correction is made for the fact that the bars are not infinite in extent. Alternatively, an almost infinite irradiance pattern that is sinusoidal can be produced with a Michelson interferometer. With this source, the reduction in video amplitude with increasing spectral frequency will give the MTF directly. An additional advantage of a pure sinusoidal image is that harmonic analysis of the video output gives immediate indication of any nonlinearities present in the system.

A third possibility would be to use the computer system already mentioned to calculate the Fourier Transform of the line-spread function. This would be done by means of the Fast Fourier Transform algorithm and would give both MTF and PTF.

(c) Equipment Considerations. The Limansky chart for the visible and its infrared analog will be required for MTF analysis. A Michelson interferometer has already been developed at NELC and is described in the Appendix. For OTF measurement by computer, a slit or edge source with dimensions much less than a resolution element would have to be designed. The computer would also have to be equipped with FFT capability.

(2) Resolving Power

(a) Definition/Discussion. Resolving power is defined as that spatial separation of two identical point or line images at the input of an optical system which is needed to just discern (according to various criteria) their separation at the output. One of these criteria is Rayleigh's which says that the dip between the peaks of the two line (or point) spread functions should be 19% of the common peak height.

(b) Procedure. An oscilloscope or computer could be used to average the line-spread function of two identical slit images. The image separation would have to be continuously varied until Rayleigh's criterion was met at the output. The separation would also have to be measured or calculated from lens magnification, collimator settings, and so forth.

(c) **Equipment Considerations.** Rather than the expense of developing a double slit source of equal intensity and continuously variable separation, a rougher estimate from a bar chart might be acceptable. In all probability, the chart would contain bars which bracketed those exactly meeting Rayleigh's criterion. For the greatest accuracy, signal averaging would be mandatory.

k. Front-End Temporal Response.

(1) Image Motion and Lag

(a) **Definition/Discussion.** Lag, defined as the ratio of the transient signal to the steady state signal in the n^{th} frame, and the effects of image motion such as smearing of leading and trailing edges are both transient response measures. Measurement of the two quantities would be equivalent if the pattern moved in steps only during the retrace periods. Candidate procedures will be proposed for both measurements while anticipating a unification of the approach.

(b) Procedure

1 **Lag.** The average value of a line in successive frames after turning on the source will give the buildup lag. Doing the same after the source is turned off will give the decay lag. Averaging along the selected line will be done to improve S/N. The light source should come on immediately after the first set of samples is taken (which defines the quiescent state) and turn off after an appropriate time has elapsed coincident with the taking of samples in that frame.

2 **Image Motion.** To indicate the effects of image motion (or dynamic lag), the MTF as a function of $\dot{\theta}$ will be determined. This will be accomplished in the same manner as the static MTF measurement.

(c) **Equipment Considerations.** A computer interfaced to a Biomation 100 MHz A/D converter will be required. To trigger the A/D converter, a jitter-free line selection pulse must be provided. A pulsed source of irradiance (such as LEDS in the visible) will be required for buildup and decay lag measurements. For image-motion measurements, it is adequate to have the system on a rotating table. This technique does not, however, lend itself to doing signal averaging in a concise manner.

(2) **Jitter Response**

(a) **Definition/Discussion.** Jitter, as used herein, is the time variation between an otherwise static picture and the field of view probably introduced by the framing system. A framing-imaging system is very dependent on the synchronizing pulses that initiate the vertical and horizontal scans. In a well-designed LLLTV system, high noise immunity is maintained by the use of separate, external synchronizing signals. In this way, the camera and display will trigger together providing a jitter-free display (assuming a stable, noise-free sweep follows the trigger). A possibly less stable system becomes necessary when it is no longer possible to use external sync making the derivation of these signals from composite video mandatory.

The only timing that the eye is aware of is from the display. Using the left edge of the display as a reference, i.e., the pulse which initiates the sweep in the display, would be most ideal. A more convenient and equally valid point is to use the horizontal drive pulses discussed above.

(b) **Procedures.** An edge or impulse will be imaged by the system, and its position relative to the left edge reference will be determined. The variation could then be given as a percent of some spatial frequency – say 100 TV lines.

(c) **Equipment Considerations.** The equipment required is the same as that described in Paragraph k(1)(c).

l. **System Responsivity (Film Readout Only).** The definition and procedure here are the same as in Paragraph a with the following exception. Photographic film is used as the system output detector rather than a photomultiplier tube. A microdensitometer trace of the exposed and processed film can be analyzed to determine the signal-transfer-function curve. In the case of the spectral-response curve, density comparisons must be traced back through the film characteristic D-Log E curve.

m. **System Spatial Resolution (Film Readout Only).** The definition and procedure are the same as in Paragraph b with the exception that the output information will be recorded on film. The film information is then scanned by a microdensitometer, traced back through the film D-Log E curve, and analyzed.

n. **System Resoltivity Response (Film Readout Only).** The definition and procedure are basically the same as in Paragraph c. In this case, however, information from Paragraph l will be utilized to determine at what system contrast and brightness settings the hard film copy should be made. Observers will then analyze the film.

BIBLIOGRAPHY

AAS-25 (NVS) Acceptance Test Procedure. Hughes Aircraft Company, Report No. NVS2, 1970.

Biberman, L. M., ed.: *A Guide for the Preparation of Specifications for Real-Time Thermal Imaging Systems.* Institute for Defense Analysis, Paper P-676, 1971.

Biberman, L. M., et al.: *Low-Light-Level Devices: A Designers' Manual.* Institute for Defense Analysis, Report R-169, 1971.

Biberman, L. M., and Nudelman, S., eds.: *Photoelectronic Imaging Devices.* Vols. I and II. Plenum Press, 1971.

Campana, S., et al.: *Response to Image Evaluation Survey* (ARPA Order 1938). Naval Air Development Center, 1971.

Electro-Optical Viewing System Equipment Specification. Boeing Company, D3-7505-1, Revision D, 1971.

Goodman, M.: *Introduction to Fourier Optics.* McGraw-Hill, 1968.

Hodges, J.: *Infrared Image Test Program - Variable Analysis (Interim Report).* Electro-Optical Systems, Technical Report AFAL-TR-71-362, February 1972.

Kingberg, C. L., Elworth, C. L., and Filleau, C. R.: *Image Quality and Detection Performance of Military Interpreters.* Boeing Company, Air Force Office of Scientific Research Contract F44620-69-C-0128, 1970.

Lavin, H.: "Image Quality Considerations of Low Light Level Television." Society of Photographic Scientists and Engineers, 1970.

Lavin, H., et al.: *Survey of Image Evaluation Facilities and Techniques for Image Intensifier, Television Sensors and Systems, Infrared Detectors and Systems.* General Electric Company, Aircraft Equipment Division, 1972.

Lee, Y. W.: *Statistical Theory of Communications.* John Wiley and Sons, 1961.

Lloyd, J. M.: "The Optical Transfer Function of Real-Time Infrared Imaging Systems." Presented at the 18th National Infrared Information Symposium, May 1970.

BIBLIOGRAPHY (Cont'd)

Modified Advanced FLIR Program Oral Presentation Report. Hughes Aircraft Company. Report No. P70-391, 1970.

Modified Advanced Forward Looking Infrared (MAFLIR) System Integration and Test Program. Hughes Aircraft Company, Technical Report AFAL-TR-71-311, 1972.

Moulton, J. R., and Wood, J. T.: "Two Port Evaluation Techniques Applied to Commercial Imaging Thermographs." Proceedings of the Electro-Optical Design Conference. September, 1970.

Neiswander, R. S.: *Considerations of Forward Looking Infrared (FLIR) Optics.* Te Company, Technical Report AFAL-TR-71-174, January, 1972.

NOD-LR Acceptance Test Report System 101. Hughes Aircraft Company. Contract No. DAAK02-70-C-0162, 1971.

Proposal for an Advanced Low-Cost Forward Looking Infrared System (FLIR). Electro-Optical Systems, Proposal No. 1008, 1969.

Proposal to Develop a Night Viewer for the Mini-Sensor Night Designator. Texas Instruments Incorporated, Proposal No. EG72-100, 1972.

Rosell, F. A.: "Resolution-Sensitivity Model for FLIR." Presented at the Imaging Specialty Group, Infrared Information Symposium, 1971.

Scade, O. H., Sr.: "Resolving Power Functions and Integral of High-Definition Television and Photographic Cameras – A New Concept in Image Evaluation." RCA Review, Vol. 32, December, 1971.

Schwartz, M.: *Information Transmission, Modulation, and Noise.* McGraw-Hill, 1959.

Sendall, R. L.: "The Definition and Analysis of the Noise-Limited Performance of an Infrared Imaging System." Presented at the 17th National Infrared Information Symposium, May 20-22, 1969.

Wood, J. T., and Moulton, J. R.: "System Evaluation Techniques for Image Intensifier Devices." Proceedings of the Electro-Optical Design Conference. September, 1970.

APPENDIX

ELECTRONIC MATERIALS SCIENCES DIVISION

CODE 2600

NAVAL ELECTRONICS LABORATORY CENTER
SAN DIEGO, CALIFORNIA 92152

PHOTOELECTRONIC IMAGING DEVICE EVALUATION PROGRAM

A Report to the Advanced Research Project Agency on the Progress in Image Device Evaluation achieved during Phase I of ARPA Order 1938.

PREFACE

This report describes the work accomplished under the direction of Dr. Roy F. Potter at NELC during Phase I of the Photoelectronic Imaging Device Evaluation Program. Phase I began on August 17, 1971, and ended on February 29, 1972. The report consists of three separate sections.

Section I describes a very precise method for measuring the signal and noise in a video waveform with a very low signal-to-noise ratio. This work was done by H. D. Fisher, III. as a continuation of work begun at the University of Rhode Island during the summer of 1971. The project has been completed.

Section II describes the design and construction of a laser interferometer to be used as a source for image tube resolution measurements. This effort is still in progress: preliminary results are reported in this section along with suggestions for future refinements. The interferometer was designed by Dr. Carl R. Zeisse and built by John C. Daley.

Section II describes a method for measuring the absolute spectral response of image tubes. This technique has been developed for image tubes by Dr. Stephen A. Miller. The detailed technical approach is given herein; the actual equipment for the measurements will be set up during Phase II of the evaluation program.

CONTENTS

ILLUSTRATIONS

TABLES

I. VERY PRECISE SIGNAL AND NOISE MEASUREMENTS OF VIDEO WAVEFORMS

INTRODUCTION

Present methods being used for the evaluation of the peak-to-peak signal and RMS noise are perhaps satisfactory at high signal-to-noise levels; but at low signal-to-noise levels, where many low light level tubes operate, these methods are inadequate. Even at large light levels, signals which can ultimately be detected by the human eye (which integrates for periods of up to 1/5 second) will be buried in the noise of the video waveform (which is usually determined by the noise of the large bandwidth of about 10 MHz in the video channel). Any routine image tube measurement, such as spectral response or spatial resolution, will therefore need an averaging technique of one kind or another to eliminate the video noise and permit an accurate measurement over the entire useful range of signal levels. In addition, certain applications also require a knowledge of the noise itself. For instance, the amplitude distribution of the noise[1] is very important in determining the "false alarm rate" of a system designed to detect a specific target. At the limiting resolution of the system, a large noise pulse would be indistinguishable from the target itself. The noise pulse would be a "false alarm." The false alarm rate of a system can only be predicted if the amplitude distribution of the noise is known. In the analysis of photoelectronic imaging devices, the present methods for measuring signal and noise[2] include those where a time exposure of an oscilloscope trace is taken, allowing the film to average out the noise. The width of the "grass" displayed (assumed to indicate the $\pm 3\,\sigma$ value of a Gaussian distribution) is divided by six and used as an estimate of the RMS noise value. Peak-to-peak signal is determined by measuring the positive extremes of the noise envelope. An improvement on this, while still subjective in nature, involves using a split-screen presentation on the oscilloscope with the unknown signal on one side and a known RMS value on the other. By varying the known waveform amplitude until a match between the two sections is achieved and then reading the value from the known source, the RMS value can be determined.

While the last method described is far superior to the others indicated, they all have drawbacks, not the least being that they are subjective in nature. What is desired is a mathematically rigorous quantitative measure of known accuracy whose validity could not be subject to debate. Additional noise statistics such as the mean signal level and probability density and distribution histograms were also determined.

---

[1] The amplitude distribution of the noise is the same as the probability density of the noise. It gives the probability of detecting a noise pulse of a given height.

[2] L. M. Biberman and S. Nudelman, *Photoelectronic Imaging Devices*, Vol. II, Plenum Press, N.Y., 1971, p. 95.

THE MEASUREMENT TECHNIQUE

Consider the raster area to be divided into a matrix of resolution elements $R_{V,H}$, where V and H indicate the address in the vertical and horizontal directions, respectively. We now confine our attention to one of these resolution elements and record the signal plus noise (X_i) on N successive frames. This ensemble of X_i's can then be used, assuming stationarity, to calculate the desired noise statistics.

A block diagram of the experimental setup is given in Fig. A-1. The vertical address of R_{VH} is selected by a Tektronix 547 oscilloscope operated as a "line selector" scope such that an "A" gate[3] is generated once the selected line is reached. This "A" gate is then used to trigger first a Hewlett-Packard 1400 series sampling oscilloscope and subsequently the A/D converter. Responding to the leading edge of the "A" gate pulse, the sampling scope delaying and delayed[4] time bases select the horizontal resolution element where the sample is to be taken. The sampled value (normalized to a value between 0 and 1 volt) is available at the chart recorder output approximately 2 μsec after the sample is taken. By selecting the length of the "A" gate (equal to the A sweep duration) so that it is at least 2 μsec longer than the line of interest, we can make use of the falling edge of the "A" gate to enable the A/D converter.

The chart recorder output is amplified to make it compatible with the A/D converter input. The A/D converter output is stored in successive locations in memory the number taken determined by software control.

The parameters that are presently being evaluated include RMS noise, peak-to-peak signal and probability density, and distribution histograms. The RMS value of the noise is determined by evaluating the expression

$$\hat{\sigma} = \left[\frac{1}{N} \sum_{i=1}^{N} (X_i - \bar{X})^2 \right]^{1/2} \qquad (1)$$

where

X_i = value of sample in frame i

$\bar{X}$ = average value of X_i

---

[3] The "A" gate is an output from a Tektronix 547 oscilloscope enabled coincident with the initiation of the A sweep and disabled with its termination.

[4] The delayed sweep is initiated after a selected percentage of the delaying sweep has expired.

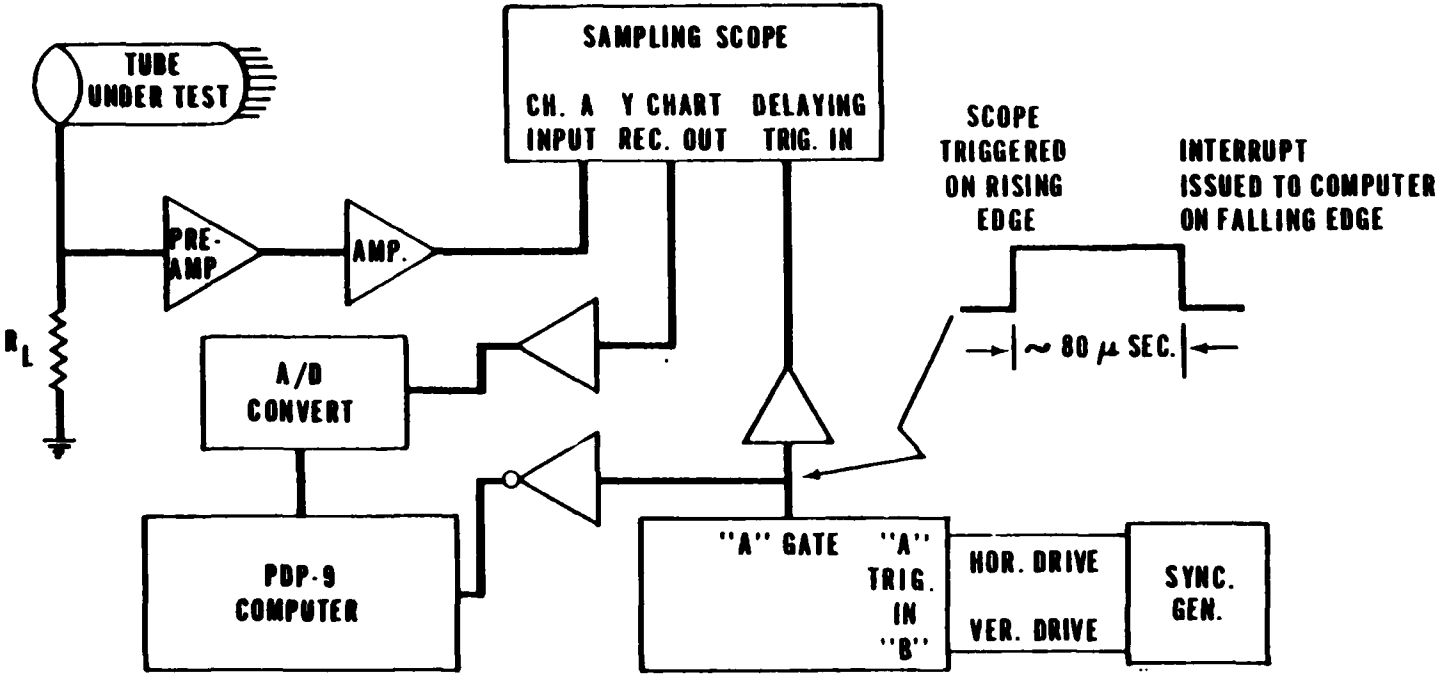

Fig. A-1. Experimental arrangement for making precise signal and noise measurements on the waveform coming from an image tube.

N = the number of samples (frames)

$\hat{\sigma}$ = the standard deviation of the X_i's (RMS value of the noise)

Equation (1) can be rewritten in a form more suitable for computation yielding

$$\sigma = (\overline{X^2} - \overline{X}^2)^{1/2} = \left[\frac{1}{N} \sum_{i=1}^{N} X_i^2 - \left(\frac{1}{N} \sum_{i=1}^{N} X_i \right)^2 \right]^{1/2} . \qquad (2)$$

Equation (2) is the expression presently being used to evaluate the RMS noise magnitude.

The second term in the brackets of Eq. (2)

$$\left[\overline{X} = \frac{1}{N} \sum_{i=1}^{N} X_i \right]$$

also has significance since from it the peak-to-peak signal can be determined. Since the signal was assumed to be stationary, it would appear as a constant level to which is added the noise in any one resolution element. Assuming Gaussian noise with zero mean, the average calculated in Eq. (2) is the signal level of that resolution element. If V_I and V_D represent the values of signal at an illuminated and dark portion, and C is a constant due to DC positioning, then

$$V_{pp} = \left(V_I + C \right) - \left(V_D + C \right) = V_I - V_D$$

gives the peak-to-peak signal.

A histogram of the probability density $f(X_i)$ of the noise can be obtained in a straightforward manner. This is accomplished by forming an array of bins V_i, each of which represents a certain range ΔV of the possible input, and incrementing the bin V_i which corresponds to the magnitude of the X_i. The probability distribution histogram is obtained by summing the V_i of the probability density histogram.

The ensemble of points X_i stored in memory is a subset of a parent set which could have an infinite population. What we would like to determine is the mean, μ, and RMS value, σ, of the parent set – not of our sampled subset. The error in our estimation decreases as the number of samples N increases. The average of N samples of X_i is given by

$$\bar{X} = \frac{1}{N} \sum_{i=1}^{N} X_i.$$

The expected value of $\bar{X}$ is μ – the parent population average. The standard deviation of $\bar{X}$ about μ is given by

$$\frac{\sigma}{\sqrt{N}} \tag{3}$$

which can be used to determine the uncertainty of our knowledge of X. The variance of our sampled subset is given by

$$\hat{\sigma}^2 = \frac{1}{N} \sum_{i=1}^{N} (X_i - \bar{X})^2.$$

This is related to the parent set by

$$\sigma^2 \cong \frac{N}{N-1} \hat{\sigma}^2.$$

The variance of $\hat{\sigma}^2$, an indication of our uncertainty of $\hat{\sigma}^2$, is given by

$$S^2 = \mathrm{Var}\, \hat{\sigma}^2 = \frac{2\sigma^4}{N} \tag{4}$$

where N, the number of samples to be taken, can be determined using Eqs. (3) and (4) with a knowledge of the statistical accuracy desired.

MEASUREMENTS OF A WHITE NOISE GENERATOR AND A VIDICON TUBE

Fifty-two sets of measurements, each measurement with N = 2000, of band limited white noise generator producing 0.1V RMS were made. Figure A-2 shows a computer plot of the probability density and the probability distribution of one such set.

Equation (4) indicates that the standard deviation of these 52 measurements ($S = (\mathrm{var}\, \hat{\sigma}^2)^{1/2}$) would be 3.1×10^{-4}. Assuming the noise has a Gaussian distribution, Table A-1 shows the expected vs measured values of the 52 samples.

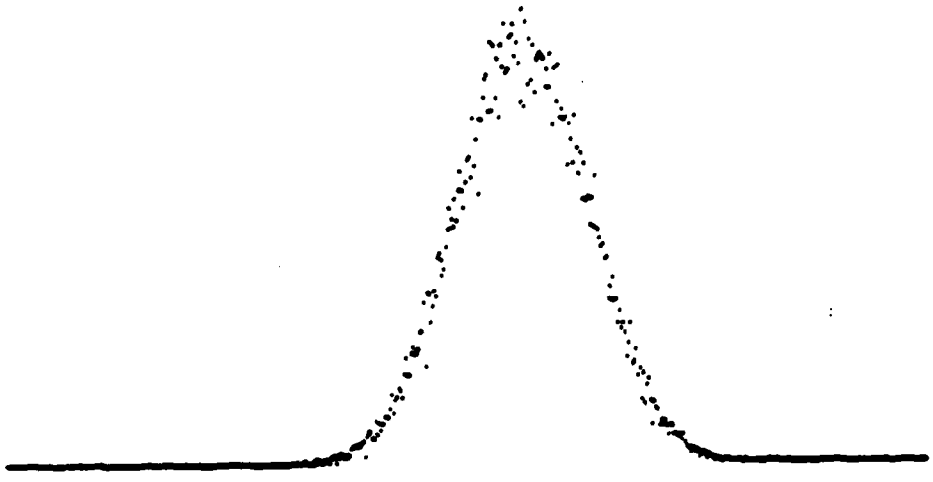

PROBABILITY DENSITY HISTOGRAM

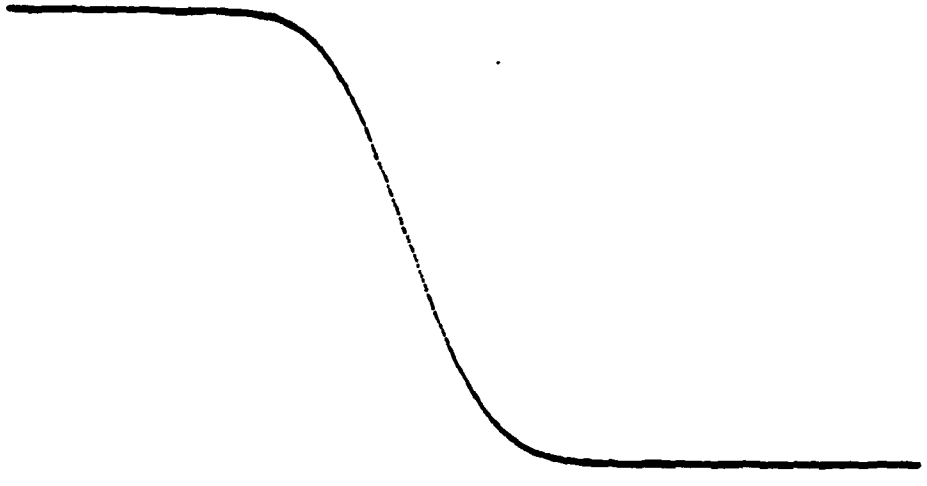

PROBABILITY DISTRIBUTION HISTOGRAM

Fig. A-2. Signal and noise measurement technique results:
(20 MHz Band Limited White Nose).

Table A-1. Number of Expected vs Measured Values

Range of S	Expected Number of Measurements Within Range of S	Actual Number of Measurements Within Range of S
$0 \leq S \leq 1$	36	37
$1 \leq S \leq 2$	13	10
$2 \leq S \leq \infty$	3	5

The discussion of the statistical uncertainty above this has made no mention of the accuracy of the measuring apparatus. The three components which comprise the signal path in Fig. A-1 (scope, amplifier, and A/D converter) determine this accuracy.

The A/D converter used (Digital Equipment No. AF01 B) is specified to be within 0.025% with 12 bit resolution giving 4096 quantization levels. The oscilloscope, acting as a sample and hold module rather than being used as the manufacturer intended, makes the furnished specifications invalid. (They are far too conservative.)

An empirical evaluation, using a square wave input of known magnitude (to 1%), indicated an accuracy of greater than 2% for values ranging from 0.5V RMS to 0.0025V RMS.

With a vidicon type of tube, the video system is preamplifier noise limited. Since practically all of this noise comes from the first stage of the preamplifier, it can be estimated from

$$I_N = \sqrt{\frac{4KT\Delta f}{R_L} + \frac{4\pi^2 \, Req \, C^2 \, \Delta f^3 \, 4KT}{3}} \qquad (5)$$

which is the quadrature sum of the Johnson noise of the load resistor R_L in bandwidth Δf and the shot noise of the input tube. C^2 is the capacitance of the input circuit and $Req = \frac{2.5}{Gm}$ is the equivalent resistance of the input triode. Equation (5) was evaluated using values typical for the type of preamplifier in the URI test facility (Westinghouse Model SEC MARK III RI). Table A-2 shows a comparison between values calculated from Eq. (5) above and those measured.

Table A-2. Comparison Between Values Calculated and Measured

Bandwidth	Calculated Value	Measured Value
10 MHz	6.0 nA	6.5 nA
15 MHz	10.9 nA	12.0 nA

Considering the uncertainties of many of the parameters in Eq. (5), the measured and calculated values agree very well indicating that for this particular setup the sensitivity of the system is limited by the noise of the preamplifier.

Similar measurements were also made confirming that the peak-to-peak signal measurements would be as expected. The results for a few of the measurements taken are shown in Table A-3.

Table A-3. Signal Value Comparison

Spatial Frequency	PAR Box Car Integrator	Sampling Oscilloscope
300 TVL/PH	23.2 nA	23.7 nA
400 TVL/PH	15.8 nA	15.2 nA

CONCLUSION

The above data demonstrate a quantitative measure of peak-to-peak signal and RMS noise to accuracy not before achievable. Since the bandwidth of the oscilloscope is so high (12.4 GHz), the upper bound placed on the useful frequency response is determined by trigger stability. There are still some areas where minor work needs to be done. One of these becomes evident when we try to make N large to decrease statistical error. The experiment time becomes large causing the assumption about stationarity to become invalid. The DC drift comes partially from the lack of temperature compensation in the oscilloscope output and the external electronics.

Aside from these minor problems, the system does work, is fairly simple to implement, and gives accurate results. The new, inexpensive A/D converters and digital calculators make this method attractive also from an economic viewpoint.

II. THE DESIGN OF A LASER INTERFEROMETER FOR IMAGE TUBE RESOLUTION MEASUREMENTS

INTRODUCTION

The optical transfer function of an optical component such as a lens or image tube is of great importance because this one function, together with any scene entering the lens, can be used to predict the scene leaving the lens. The concept of the optical transfer function, which is the product of a phase transfer function and a modulation transfer function (MTF), has been well described in the literature.[5] The analogous situation

[5] L. M. Biberman and S. Nudelman: *Photoelectronic Imaging Devices*. Vol. I. Plenum Press. N.Y., 1971. p. 291.

in electronics is that of an arbitrary waveform entering a linear electronic black box. Armed only with the transfer function, the engineer can predict the output waveform in the following way: the input waveform is decomposed into its Fourier components, each component is multiplied by the value of the transfer function at that frequency, and the result is summed over all frequencies. The transfer function changes the amplitude and shifts the phase of each Fourier component.

In the optical case, the spectral components are now light intensities that vary sinusoidally in space and can be used in a similar fashion to compose an arbitrary scene in two dimensions.

Many instruments have been designed to measure the MTF of lenses, but the measurement of image tube MTF has relied on the use of charts made up of equally spaced black and white bars. The spatial frequency of the bars varies across the chart. These patterns are generally back-illuminated with white light and imaged through a lens onto the faceplate of the image tube. A single line of the video signal is displayed on an oscilloscope and photographed. In practice, the optical signal is assumed to have constant amplitude, and the relative amplitude of the video output is recorded as a function of spatial frequency. This plot is then assumed to be the MTF of the tube under test.

An obvious objection to this approach is that the black and white bars are a spatial square wave, whereas a spatial sine wave should be used in order to compute the MTF from a simple ratio of output to input. In recognition of this fact, a technique has recently been developed to compute the MTF from the bar chart data.[6] A more serious objection is that the lens in front of the tube will have a lens MTF of its own: and this MTF is generally not known because a lens MTF can change significantly with small changes in aperture, focus, and alignment.[7] Thus, the MTF at both lens and tube is obtained this way, and the proper approach would be to use a precisely adjusted lens whose MTF was either well known or negligible compared to the tube MTF.

It has been suggested by Kelsall[8] that a simple Michelson interferometer, used with a laser light source, is an elegant way of projecting a pattern of sinusoidal fringes directly onto the face of an image tube. The irradiance is sinusoidal, eliminating the need for any mathematical conversion process, and the light beam is well collimated, eliminating the need for a lens in front of the tube. If carefully designed, it is capable of generating high spatial frequencies, on the order of a hundred cycles per mm, and can be made small enough to be portable. Its main disadvantage is that monochromatic

---

[6] L. Limansky: *The Electronic Engineer* 22, 50, 1968.

[7] M. Born, and E. Wolf: *Principles of Optics*. Second Ed., Macmillan Co., N.Y., 1964, p. 484.

[8] D. Kelsall: *Proc. SPIE 14th Annual Technical Symposium* 2, 3, 1969.

light is used for the MTF measurement instead of white light. Since it is conceivable that the MTF varies with the wavelength of the light, the MTF measured with the Michelson interferometer may not apply when the tube is irradiated with white light which contains many wavelengths. This drawback is offset by the ability of the interferometer to operate at a great number of single wavelengths in the ultraviolet, visible, and infrared (even at 10.6 μm, for example).

The remainder of this report will describe the design of such an interferometer source. A convenient MTF measurement procedure for image tubes will be chosen. This procedure will require constant fringe visibility and peak irradiance as the spatial frequency is varied. These requirements will be examined to see what constraints are imposed on the design of the interferometer. A list of commercially available components will be given with some design hints that have guided their assembly. The performance to be expected from the interferometer will be calculated and some preliminary observations will be made on its use in image tube measurements.

THE MEASUREMENT PROCEDURE

The simplest possible source would consist of a sinusoidal irradiance pattern whose amplitude and visibility (or contrast) are constant in space and independent of the spatial frequency f_o:

$$E(x, y) = 2E_o \left[1 + \alpha \cos (2 \pi f_o x) \right] . \tag{1}$$

The peak-to-peak amplitude is $E_{max} - E_{min} = 4E_o \alpha$ and the visibility is

$$V \equiv \frac{E_{max} - E_{min}}{E_{max} + E_{min}} = \alpha . \tag{2}$$

Decomposing this input irradiance E(x, y) into its spatial spectrum E(f, g)

$$E(f, g) \equiv \int_{-\infty}^{\infty} \int_{-\infty}^{\infty} E(x, y) e^{2 \pi i (fx + gy)} \, dx dy$$
$$= 2E_o \, \delta (g) \left[\delta (f) + \alpha \frac{\delta (f_o + f) - \delta (f_o - f)}{2} \right] .$$

Multiplying by the transfer function of the image tube, K(f, g) will give the output current I(f, g):

$$I(f, g) = K(f, g) \; E(f, g).$$

Taking the inverse Fourier transform to reconstitute the output waveform

$$I(x, y) = \int_{-\infty}^{\infty} \int_{-\infty}^{\infty} I(f, g) e^{-2\pi i(fx + gy)} \, df dg$$

we find that

$$I(x, y) = 2E_o \, [K(0,0) + \alpha \, K(f_o, 0) \cos(2\pi f_o x)] \, . \tag{3}$$

Because amplifiers are generally ac coupled to the image tube, it is difficult to establish a true zero level for the current at the output of the tube. In other words, only differences in current due to changes in irradiance can conveniently be measured. We can therefore measure

$$I_{max} - I_{min} = 4E_o \, \alpha \, K(f_o, 0). \tag{4}$$

If it is assumed[9] that

$$\lim_{f_o \to 0} K(f_o, 0) = K(0, 0)$$

then a plot of $I_{max} - I_{min}$ as a function of F_o, normalized to 1 as $f_o \to 0$, will be the same as the transfer function $\frac{K(f_o, 0)}{K(0, 0)}$ of the image tube.[10]

This procedure imposes the following simultaneous constraints on the irradiance pattern emitted by the interferometer:

1. The maximum spatial frequency should be 50 cycles/mm to accommodate the highest resolution vidicons.[11]

2. The value of the maximum irradiance E_{max} should be adjustable from 10^{-7} to 1 W/m^2 (from a 2854°K source, refer to Table A-4) to fall within the dynamic range of all image tubes.

3. The maximum irradiance E_{max} should be constant across the image tube as the spatial frequency f is varied.

---

[9] The pitfalls inherent in this assumption are discussed by Biberman and Nudelman, *Photoelectronic Imaging Devices*, Vol. II, P. 107.

[10] The fact that K(f, g) is completely specified by K(f, o) is proven by Born and Wolf, *Principles of Optics*, p. 487.

[11] L. M. Biberman and S. Nudelman: *Photoelectronic Imaging Devices*, Vol. II, Plenum Press, N.Y., 1971, p. 81.

4. The fringe visibility V should be constant across the image tube as f is varied.

The optical setup of the Michelson interferometer and the characteristics of laser radiation will now be presented in order to see how well these constraints can be met.

Table A-4. Conversion of Sensitivity to a 2854°K Source into Sensitivity to a Laser Source*

1. Cycles/mm = line pairs/mm = $\frac{5}{6D}$ (TV lines/picture height) where D is the tube diameter in mm.

2. 1 ampere/lumen = 20 amperes/watt for a 2854°K blackbody source. This equation means that for each watt radiated by a 2854°K blackbody throughout the entire spectrum from ultraviolet to infrared, the eye will see 20 lumens.

3. For an image tube with an S-20 photocathode, an He-Ne laser is 11.4 times more efficient than a 2854°K blackbody. The integrated response of a photocathode (where integrated means "over all wavelengths") is given by

$$\frac{\int E_\lambda \, 6_\lambda \, d_\lambda}{\int E_\lambda \, d_\lambda} \quad \frac{ma}{watt}$$

where 6_λ is the photocathode spectral sensitivity in ma/watt and E_λ is the spectral irradiance of the source in watts/μm · cm^2. For a 2854°K blackbody, E_λ is given by Plank's distribution; for a laser, $E_\lambda \simeq E_o \, \delta (\lambda - \lambda_o)$. An S-20 photocathode, as taken from an RCA wall chart, has an integrated response of 2.45 ma/watt for the blackbody and 28 ma/watt for the He-Ne laser.

* Conversions are different because many of the watts emitted by a blackbody source consist of infrared radiation to which the tube cannot respond.

MICHELSON OPTICS

The Michelson interferometer is a simple two-beam interferometer. A beam splitter is used to separate a single-incident beam into two separate beams which emerge from the instrument to interfere at the detector. The optical layout is shown in Fig. A-3. In general, there is a separation e and an inclination θ between the reference mirror, which is considered fixed, and the image in the beam splitter of the movable mirror. The optical paths of the two beams are identical everywhere until they reach the air wedge of central thickness e and wedge angle θ. Thereafter, they diverge at angle 2θ. Whenever the optical path difference between these two beams is a whole number of wavelengths, there will be a maximum in the intensity of the combined beams:

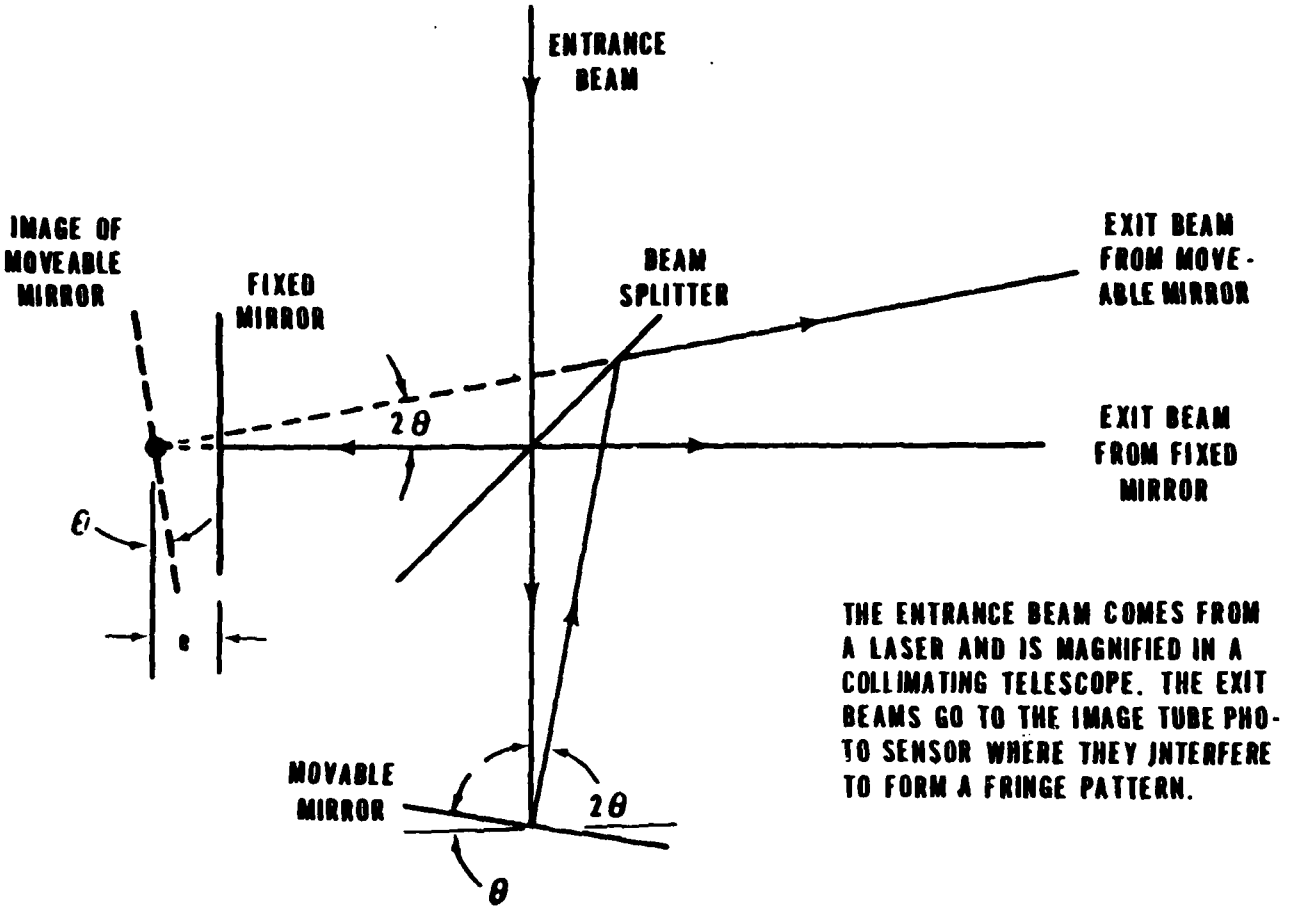

Fig. A-3. Schematic diagram of the Michelson interferometer.

whenever the difference is a half-integral number of wavelengths, there will be a minimum in the combined intensity.

Generally, θ is set to zero, the beams emerge superimposed and colinear, and the entire field of view lightens and darkens as the mirror separation e is changed by turning a screw. This is the technique used, for example, in gaining precise information about the spectrum of an unknown source and in making very accurate length measurements. However, in our case we are interested in creating a pattern of maxima and minima throughout the plane transverse to the exit beam. Hence, we need the complementary situation where e is set to zero and θ is adjusted by turning a screw. For a fixed value of θ (which will be on the order of one degree), the beams will diverge slightly; and, where they overlap, a sinusoidal fringe pattern will appear whose intensity and visibility depend on the intensity and optical path of the individual beams.

THE LASER DISTRIBUTION

We will, therefore, need to know how the amplitude and phase of the entrance beam varies in space. This beam originates in a laser. For a laser beam operating in the TEM_{00q} mode, the irradiance across a wavefront is Gaussian:

$$E(x, y) = E_o \exp\left[-2 \frac{(x^2 + y^2)}{W^2} \right] \tag{5}$$

where E_o is the irradiance in watts/m^2 at the center of the beam and W is called the "beam radius." W is the distance at which the power per unit area has fallen to $1/e^2$ of its value at the center. It will later be convenient to have a relation between the total beam power, Φ, and the central irradiance, E_o, in case the beam is magnified to a different value of W:

$$\Phi = \int_o^\infty \int_o^\infty E_o \, e^{-2 \frac{x^2 + y^2}{W^2}} \, dx \, dy$$

$$= 2\pi E_o \int_o^\infty e^{-2 \frac{r^2}{W^2}} \, r \, dr$$

$$\Phi = \frac{\pi}{2} E_o W^2. \tag{6}$$

The laser beam also diverges so that very far from the laser the wavefront is spherical. We will assume, however, that the wavefront is planar because the divergence angle is

generally so small (usually about 1 milliradian) and because beam magnification, if any, reduces this divergence even further.[12] We will call a plane wave with a Gaussian irradiance along its wavefront a Gaussian plane wave.

THE INTERFERENCE OF TWO TILTED GAUSSIAN PLANE WAVES

We now have the problem of calculating the interference at the image tube between the two Gaussian plane waves emerging from the interferometer and propagating with an angle 2θ between their rays. For this purpose, Fig. A-4 shows a system which is optically equivalent to that shown in Fig. A-3. A coordinate system has been chosen whose origin is in the center of mirror 1 (the fixed reference mirror) with the x axis horizontal, the y axis vertical, and the z axis perpendicular to the mirror. The figure illustrates the case for which the image of the movable mirror, mirror 2, has its center at (0, 0, e), e being a negative number, and is inclined at an angle θ to the z axis. The image tube will be located outside the interferometer, centered on the z axis, and oriented perpendicular to it. A Gaussian plane wave, heading in the -z direction and centered on mirror 1, can then reach the point (x, 0, z) on the image tube in two different ways: via immediate reflection in mirror 1 at (x, 0, 0), or via a continuation from the point (x-T, 0, 0) to mirror 2 where it undergoes a delayed reflection and emerges at angle 2θ. In the language of interferometry, 2e is the "lead" and T is the "tilt." The irradiance at the image tube, after these two beams interfere, is given by the familiar formula[13]

$$E = E_1 + E_2 + 2\sqrt{E_1 E_2}\,\cos\left(2\pi\,\frac{\Delta_2 - \Delta_1}{\lambda}\right) \qquad (7)$$

where E_1 is the irradiance in beam 1, E_2 is the irradiance in beam 2, and $\Delta_2 - \Delta_1$ is the optical path difference between beams 2 and 1. The general behavior of this function can be seen by considering the case $E_1 = E_2 = E_o$. The E varies from a maximum of $4E_o$ to a minimum of zero as $\frac{\Delta_2 - \Delta_1}{\lambda}$ goes from some integer m to the next half-integral value m + ½.

According to Fig. A-4

---

12 In an optical system without any transmission or reflection losses, the image area at a point multiplied by its divergence angle at that same point remains constant. This quantity is called the throughput or entendué of the system. To the extent that losses can be neglected, therefore, magnification of a 1-mm, 1-milliradian laser beam to a 100-mm beam would be accompanied by a reduction in beam divergence to 0.01 milliradian.

13 M. Born and E. Wolf: *Principles of Optics*, 2nd Ed., Macmillan Co., N.Y., 1964, p. 259.

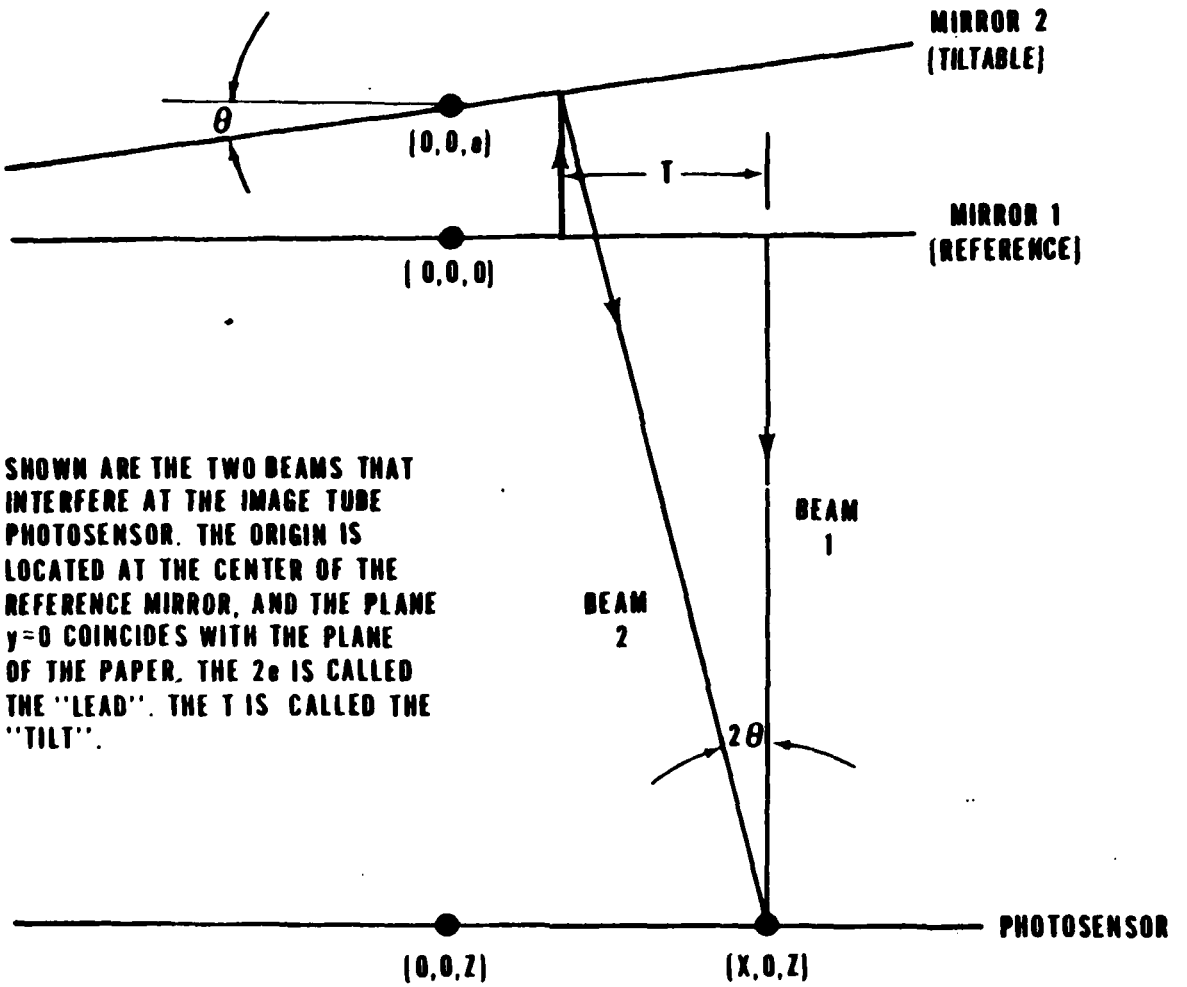

Fig. A-4. Equivalent optical system of the Michelson interferometer.

$$E_1 = E_1(x, y, z) = E_{10} \exp\left(-2\,\frac{x^2 + y^2}{W^2}\right)$$
$$E_2 = E_2(x, y, z) = E_{20} \exp\left[-2\,\frac{(x-T)^2 + y^2}{W^2}\right]. \qquad (8)$$

Because of the symmetrical way in which each beam traverses the beam splitter, $E_{10} = E_{20} = E_0$.[14] At very low spatial frequencies, T will approach zero, and the irradiance pattern will appear as shown in Fig. A-5. There will be a system of straight fringes underneath a Gaussian envelope that falls off along any radius on the image tube face.

In general, however, T will not be close to zero. Substituting Eq. (8) into Eq. (7) and letting $x' = x - \frac{T}{2}$, we find that

$$E = 2E_0 \exp\left(-2\,\frac{x'^2 + \left(\frac{T}{2}\right)^2 + y^2}{W^2}\right)\left[\cosh\left(\frac{x'T}{W^2}\right) + \cos\left(2\pi\,\frac{\Delta_2 - \Delta_1}{\lambda}\right)\right].$$

E_{max}, the value of E when the cosine term equals +1, is symmetrical about $x = \frac{T}{2}$, $y = 0$:

$$E_{max} = 2E_o \exp -2\left(\frac{x'^2 + \frac{T^2}{4} + y^2}{W^2}\right)\left[\cosh\left(\frac{x'T}{W^2}\right) + 1\right].$$

The visibility is

$$V \equiv \frac{E_{max} - E_{min}}{E_{max} + E_{min}} = \operatorname{sech}\left(\frac{x'T}{W^2}\right) = \operatorname{sech}\left[\frac{\left(x - \frac{T}{2}\right)T}{W^2}\right]$$

and is also symmetrical about $x = \frac{T}{2}$. The individual beam irradiances, E_{max} for the combined beams, and V have all been plotted in Figs. A-6, A-7, and A-8 as a function of $\frac{x}{W}$. Three values of the parameter $\frac{T}{W}$ have been chosen to show how the tilt affects these functions. As the tilt is increased in an effort to go to higher spatial frequencies, the second beam "walks off" the image tube face. The entire design problem is to make W large enough so that the tilt introduced at $f \cong 50$ cycles/mm will not seriously

[14] Beam 1 is reflected, then transmitted; beam 2 is transmitted, then reflected. For the special case of an ideal beam splitter with R = T = ½ each beam is attenuated by a factor of 4. For an arbitrary R, each beam will have a central irradiance of RTE_0 LASER.

THIS FIGURE SHOWS THE STRAIGHT FRINGES FALLING ON THE TUBE FACE. THEIR INTENSITY FALLS OFF RADIALLY IN A GAUSSIAN MANNER

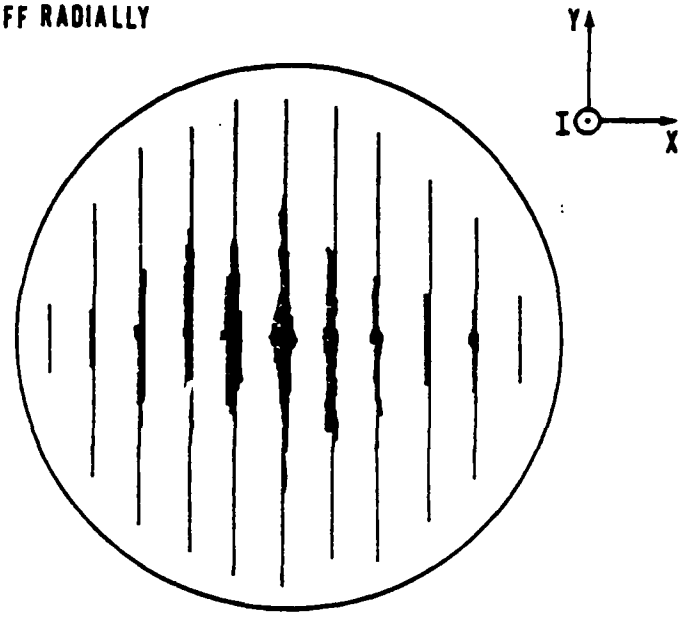

THIS FIGURE SHOWS THE SINUSOIDAL NATURE OF THE FRINGES. A SINGLE VIDEO LINE WOULD HAVE THIS APPEARANCE FOR A PERFECT IMAGE TUBE.

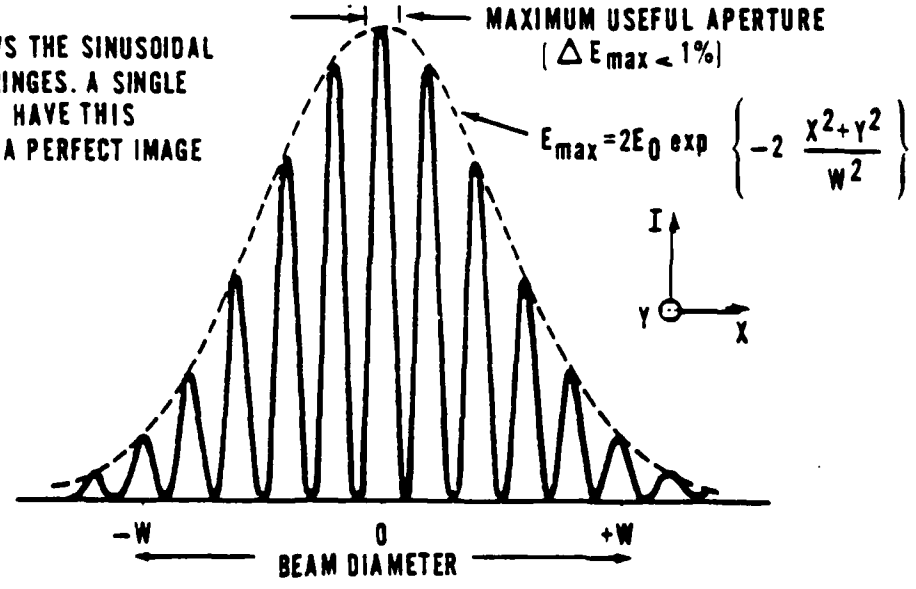

Fig. A-5. Pattern projected on the image tube at very low spatial frequencies.

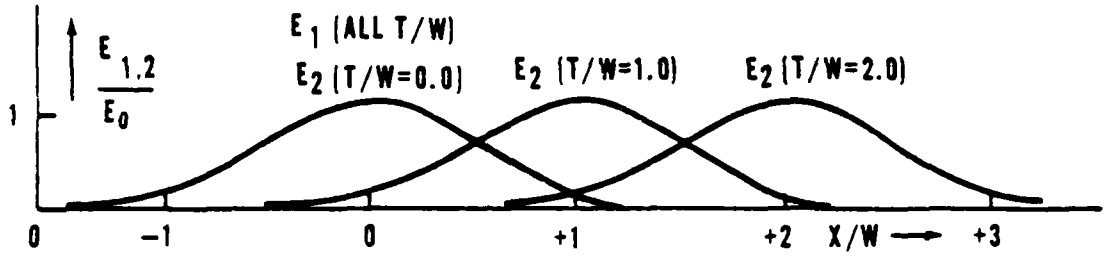

Fig. A-6. Individual beam irradiances, E_1 and E_2.

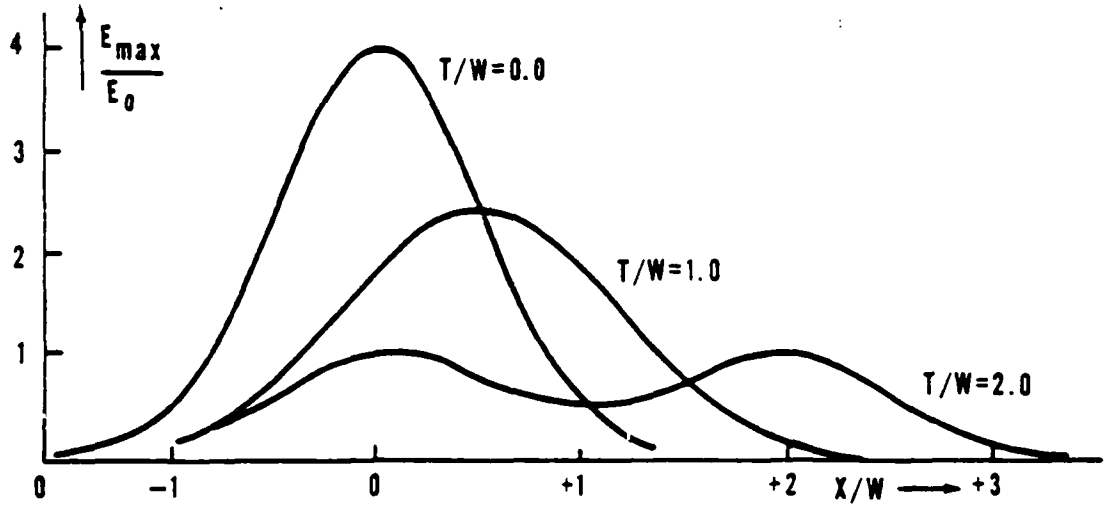

Fig. A-7. Fringe envelope of the combined beams, E_{max}.

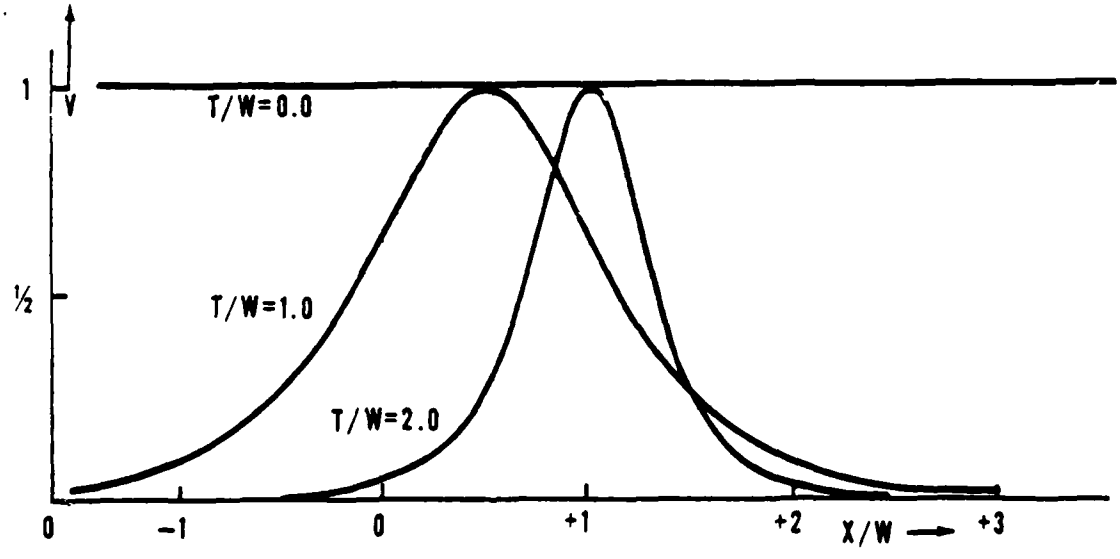

Fig. A-8. Fringe visibility, V.

degrade E_{max} and V below their values of $4E_o$ and 1, respectively. To examine how large W must be to keep E_{max} and V within, say, a few percent of their values at low spatial frequencies, we will need to expand these functions about $\frac{x}{W} = 0, \frac{y}{W} = 0$, and $\frac{T}{W} = 0$. Carrying out this expansion, we find that

$$E_{max} \cong 4E_o\left[1 - \frac{2}{W^2}\left(x^2 - xT + \frac{T^2}{2} + y^2\right) + \ldots\right] \tag{9}$$

$$V \simeq 1 - \frac{1}{2W^4}(xT - T^2)^2 + \ldots \tag{10}$$

T and $\Delta_2 - \Delta_1$ have yet to be evaluated. A moderate amount of trigonometry applied to Fig. A-4 shows that the tilt

$$T = z\tan(2\theta) + [-e + (x - T)\tan(\theta)]\tan(2\theta)$$

or

$$T = \frac{(z - e)\tan(2\theta) + x\tan(\theta)\tan(2\theta)}{1 + \tan(\theta)\tan(2\theta)} .$$

The optical path for beam 1 is simply

$$\frac{\Delta_2}{n} = z$$

where n is the index of the intervening medium. The optical path for beam 2 is

$$\frac{\Delta_2}{n} = \frac{z}{\cos(2\theta)} + [-e + (x - T)\tan(\theta)]\left[1 + \frac{1}{\cos(2\theta)}\right].$$

If these trigonometric expressions are replaced by their small angle expansions, then to order θ^2

$$T \simeq 2(z - e)\theta + 2x\theta^2 + \ldots \tag{11}$$

$$\frac{\Delta_2 - \Delta_1}{n} \simeq -2e + 2x\theta - 2(z - e)\theta^2 + \ldots \tag{12}$$

The interferometer can be mechanically arranged so that $e = 0$. For this case, and neglecting the θ^2 of terms, we have the simple formulae

$$T \simeq 2z\theta, \tag{13}$$

$$\frac{\Delta_2 - \Delta_1}{n} \cong 2x\theta . \tag{14}$$

Formula 12 can be used to locate the fringe maxima in space and along the face of the image tube. The spatial frequency in direction dr is given by the component of $\nabla \frac{\Delta_2 - \Delta_1}{\lambda}$ in that direction. This is because the magnitude of a scalar gradient can be thought of as the reciprocal of the shortest distance that must be traveled to increase the scalar by one unit. In that distance, then, $\frac{\Delta_2 - \Delta_1}{\lambda}$ would increase from m to m + 1. This is identical to the definition of the spatial frequency in that direction. To travel along the fringe maxima, dr must be oriented so that

$$\nabla\left(\frac{\Delta_2 - \Delta_1}{\lambda}\right) \cdot dr = 0$$

or

$$2\theta dx - 2\theta^2 dz = 0$$

$$\frac{dx}{dx} = 0. \tag{15}$$

The fringe maxima are seen to be oriented at an angle θ to the z axis. Along the image tube, dr = dx so

$$f = \nabla_x \left(\frac{\Delta_2 - \Delta_1}{\lambda}\right) = \frac{2n\theta}{\lambda} . \tag{16}$$

We can now collect those formulae pertinent to the constraints imposed by the measurement procedure:

1. $f \cong \frac{2n\theta}{\lambda}$ (17)

2. $E_o = \frac{1}{4} E_o^{\text{LASER}} = \frac{1}{4}\left(\frac{2\Phi}{\pi W^2}\right)$ (18)

3. $E_{max} \approx 4E_o \left[1 - \frac{2}{W^2}\left(x^2 - xT + \frac{T^2}{2} + y^2\right) + \ldots\right]$, (19)

$T \approx 2z\theta$

4. $V \cong 1 - \frac{1}{2W^4}(xT - T^2)^2 + \ldots$ (20)

A PRACTICAL SYSTEM

With the foregoing considerations in mind, components were bought and the interferometer was assembled. A scale drawing of the system is shown in Fig. A-9, and a photograph is shown in Fig. A-10. A parts list is given in Table A-5. The laser generates a Φ = 5mW beam of red light at 633 nm. The beam radius w is 1/3 mm and the beam divergence is 1:7 milliradians at the $\frac{1}{e^2}$ points. It is also linearly polarized to better than 1 part per thousand. If the beam were unpolarized, there would be an independent interference pattern from each polarization component (namely, perpendicular and parallel to the plane of incidence of the beam splitter). In general, the fringes from the two patterns would not exactly superimpose, and the total fringe visibility would be decreased in unpolarized light.

Table A-5. Interferometer Components

Component	Description
Laser	Spectra-Physics Model 120 Stabilite Gas Laser with Model 126 Exciter
Beam Bender	Coherent Optics, Inc., Model 340 Beam Director.
Attenuation Filters	Jener Glaswerk Schott & Gen, Type ND419 Optical Glass filters
Spatial Filter & Expanding Telescope	Tropel, Inc., Model 261-D Pre-expansion Lens, Model 261 Spatial Filter, and Model 280-50 Laser Collimator
Iris Diaphragm	Ealing Corp. Catalog Number A22-3537 Iris Diaphragm.
Angular Orientation Device	Coherent Optics, Inc. Model 58 Magnetic Gimbal Suspension Optical Mount.
Optics	Oriel Optics Corp. One Model A-43-564-80 substrate with one 60% Reflectivity Coating and one anti-reflective coating and three Model A-33-264-00 First Surface flat reflectors with Aℓ/SiO coatings
Base Plate	½-inch thick Aluminum Tooling Plate

The beam is turned around and sent through a series of neutral-density filters which are slightly canted to prevent reflections from reentering the system. The beam bender

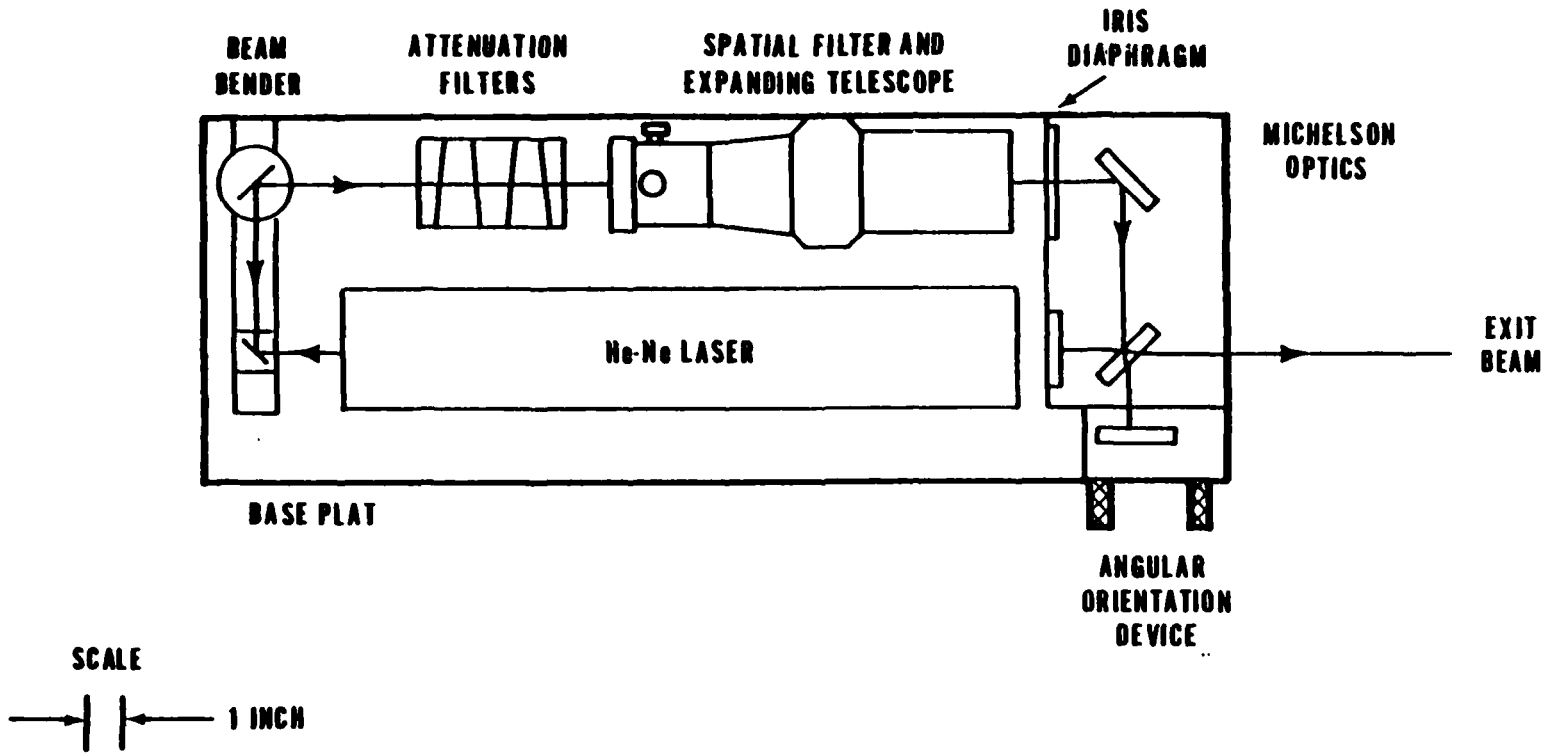

Fig. A-9. Scale drawing of the NELC-URI Michelson interferometer system.

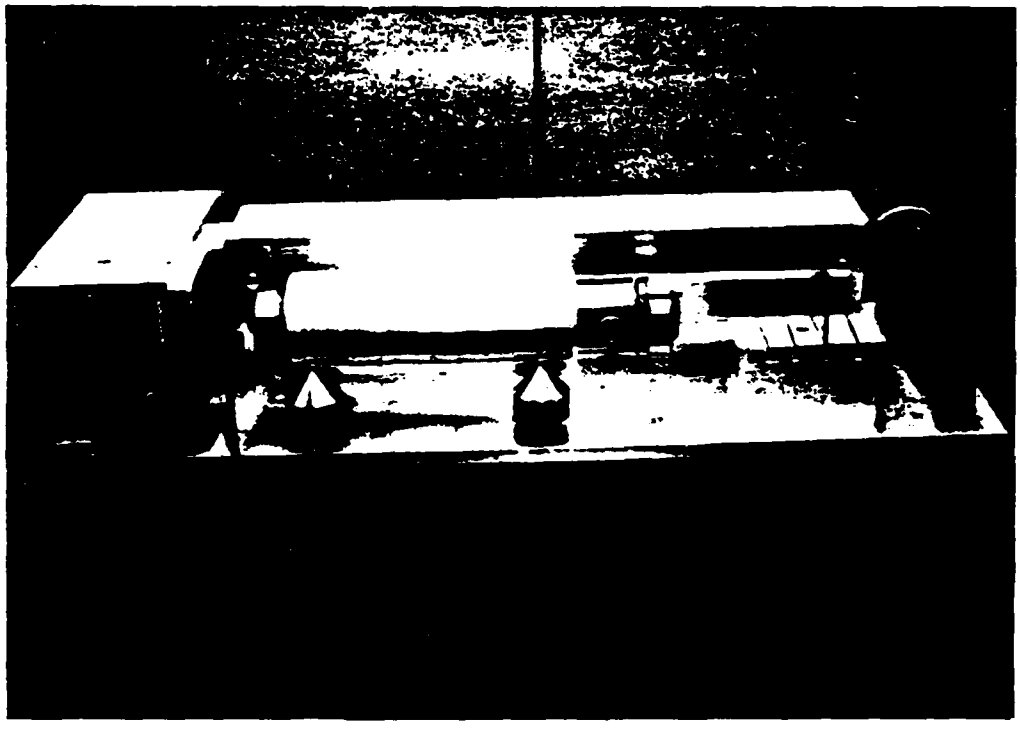

THE COLLIMATING TELESCOPE CAN BE SEEN IN FRONT OF THE LASER.
THE OPTICS ARE HOUSED IN THE ALUMINUM BOX ON THE FAR LEFT.

Fig. A-10. Interferometer system.

and filters are relatively poor optical surfaces and are, therefore, located in front of the spatial filter which will remove any irregularities they produce.

After entering the telescope, the beam is focused to a point, passed through an 8 μm diameter hole which acts as a spatial filter, and allowed to expand until it is re-collimated by a 50-mm-diameter lens. The purpose of the spatial filter is to remove unavoidable irregularities, such as reflections from the sides of the laser plasma tube, from the beam. Only the Gaussian plane wave can be focused to a small enough spot to pass through the hole. The magnification of the telescope is adjustable from 40X to 83X so that the final beam radius W can be varied from 13.3 to 27.7 mm. The adjustable iris diaphragm stops the beam down to confine it to the center of the following optics and to prevent unwanted reflections from mirror holders and so forth. The optical surfaces are flat to $\lambda/20$ over the central 80% of their 51-mm diameter. The collimating objective on the telescope and the second beam splitter surface are antireflection coated to minimize interference patterns that might originate at their surfaces. The smallest practical value of z in this system is 120 mm.

THE EXPECTED PERFORMANCE

With this system at maximum magnification, a spatial frequency of 50 cycles/mm could be generated across a large portion of the image tube face. Within a central spot 2 mm in diameter, the maximum irradiance would be constant to within 3% and the visibility would be above 99.9%. The value of the maximum irradiance would be 1.04 watts/m^2 without additional filtering.

PRELIMINARY PERFORMANCE

Preliminary performance checks have been carried out at the University of Rhode Island. The interferometer was built at NELC, carried to URI in pieces, reassembled, and substituted for their conventional source. The interferometer and camera head are shown in Fig. A-11 and the entire test set is shown in Fig. A-12. The instrument is easy to assemble and align, and the fringes are immediately apparent where the beams overlap. The spatial frequency could be simply changed by turning the micrometer screw on the angular orientation device in which the movable mirror is mounted. The fringes could be easily oriented in the horizontal or vertical direction. Fig. A-13 is a photograph of the CRT monitor displaying the fringes falling on an experimental RCA vidicon. The fringes do not look sinusoidal in the display because the display itself, and very probably the vidicon as well, is nonlinear.[15]

[15] The whole problem of analyzing a nonlinear tube will be theoretically investigated in Phase II of this program.

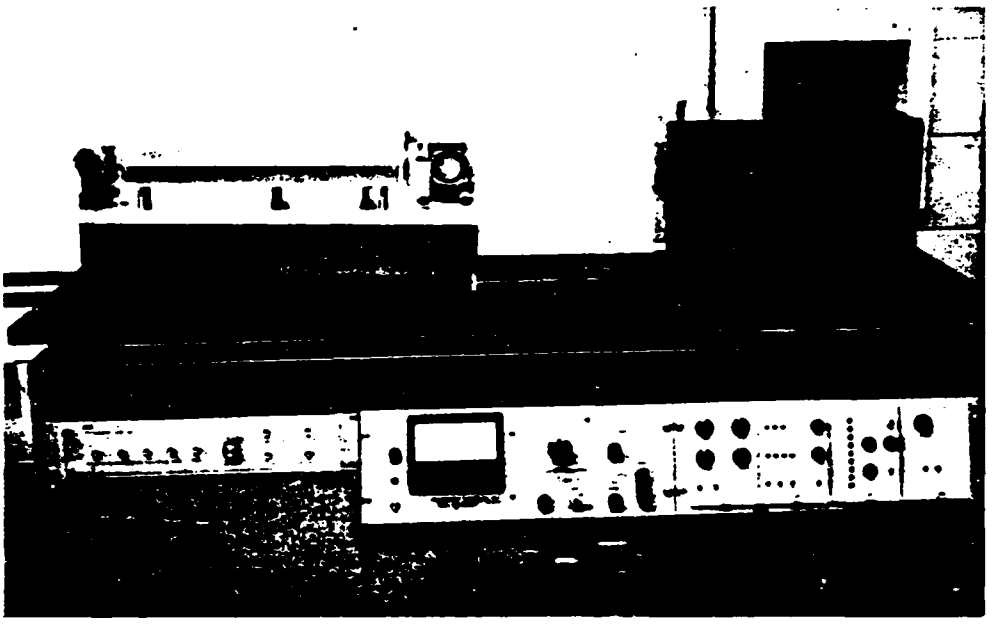

Fig. A-11. Interferometer, camera head, and associated electronics in the URI test set.

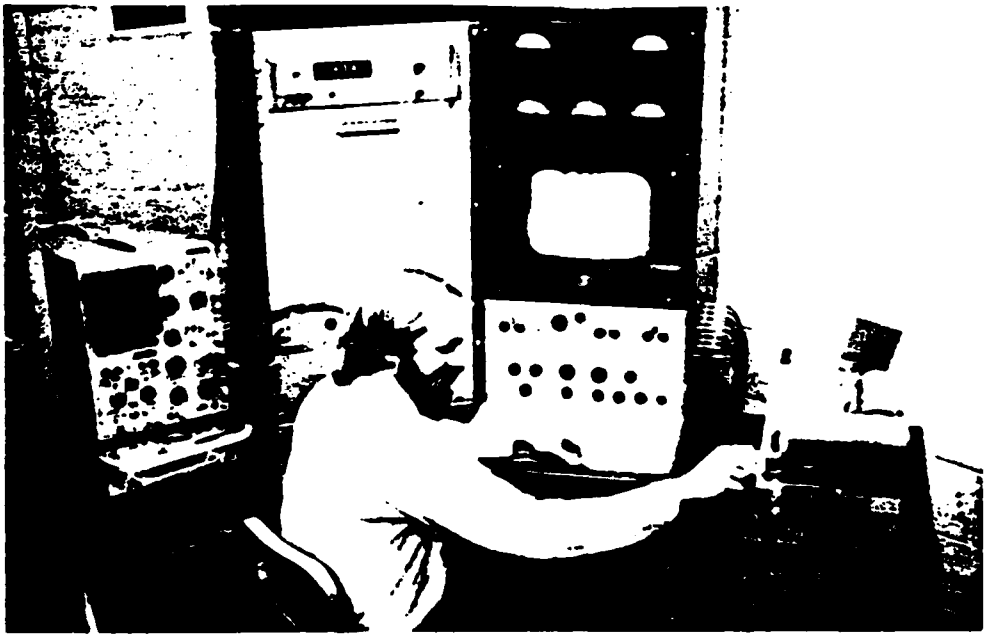

Fig. A-12. URI test system.

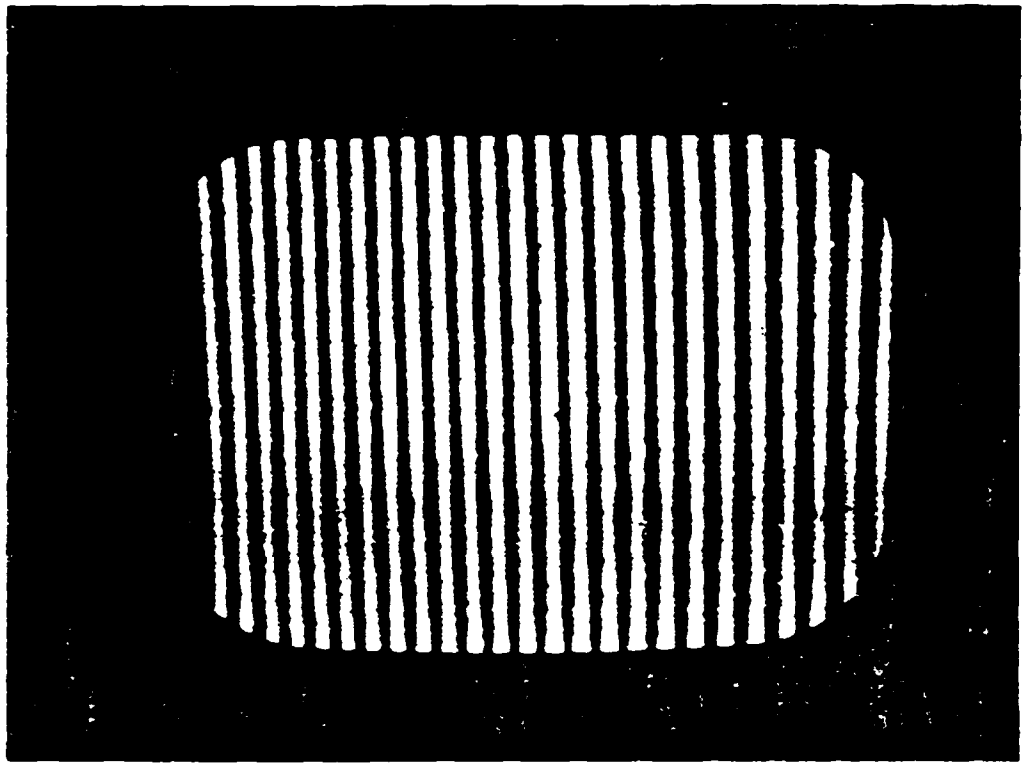

Fig. A-13. CRT display monitor photographed while on an experimental vidicon tube was being irradiated by the interferometer.

Although Fig. A-13 does not show them, there are two annoying effects that were immediately apparent and quite unexpected. Both are due to the very long coherence length of the laser and can occur even when only one beam strikes the tube. One effect is a random array of diffraction rings that resemble "owl's eyes" scattered over the tube face. These are due to diffraction of the plane waves by tiny pinholes in the mirror coatings or pieces of dust on any of the optics after the spatial filter. These can be completely eliminated by recoating the mirrors and keeping them clean. The other effect is an interference pattern caused by multiple reflections in the approximately 1-mm-thick glass faceplate on the front of the image tube.[16] These fringes are "fringes of equal thickness." Each tube presents its own special pattern. If the faceplate has a slight wedge, the fringes will be straight and parallel. If the faceplate is slightly bowed on one side, a Newton's rings pattern will appear. The only way of eliminating these fringes that is evident to us at this time is to coat the face of the tube with an antireflection coating. This problem will continue to be studied.

[16] F. A. Jenkins and H. E. White: *Fundamentals of Optics*. 3rd Ed., McGraw Hill, N. Y., 1957, Chapter 14.

A method must also be devised to quantitatively evaluate the performance of the interferometer. The constant visibility, the constant maximum irradiance, and the sinusoidal nature of the fringes should be checked. Following this, a series of measurements will be made on linear and nonlinear image tubes. This approach will be compared to Limansky's approach; both methods should give the same result. Any discrepancy will be due to some systematic error in one of the methods or a variation of MTF with the color of the light.

III. A METHOD FOR MEASURING THE ABSOLUTE SPECTRAL RESPONSE OF IMAGE TUBES

INTRODUCTION

The sensitivity of a particular imaging device to a scene depends, among other things, jointly upon the spectral distribution of the radiation from the scene and the absolute spectral responsivity of the device. Given the characteristics of the scene, the device's performance is predictable to the extent that its absolute spectral responsivity is known. For reasons of experimental convenience, the absolute spectral responsivity is often measured in two steps: first, a relative spectral responsivity measurement; and, second, an additional measurement to make the data from the first measurement absolute.

SPECTRAL RESPONSE

The relative spectral response of an image tube is its response to radiation of different wavelengths relative to the response at some particular wavelength. If $R(\lambda)$ is the absolute responsivity (expressed, for example, in microamps per microwatt/cm^2) at wavelength λ, then the spectral response will be written $kR(\lambda)$, where k is a factor independent of λ whose value depends on the measurement conditions. Measuring $kR(\lambda)$ and k independently allows the absolute responsivity $R(\lambda)$ to be calculated.

Using a suitable source and filter to give narrow-band radiation, the signal $S(\lambda)$ from the device under test is compared with the signal $S_s(\lambda)$ from a standard "grey" detector, whose response is known to be independent of λ, with the same incident radiation intensity at wavelength λ. The spectral response is given by the ratio of these signals measured over a range of wavelengths:

$$kR(\lambda) = S(\lambda) / S_s(\lambda).$$

The experiment arrangement for the spectral response measurements is shown schematically in Fig. A-14. The light from a tungsten lamp is focussed onto the entrance slit of a Jarrell-Ash 0.5-meter Ebert monochromator. The slit width is chosen to give

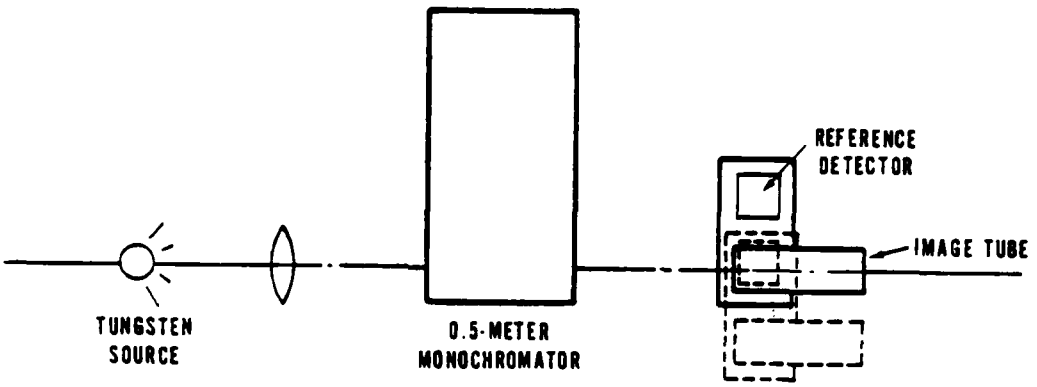

Fig. A-14. Experimental arrangement for image tube spectral response measurements made over a wide range of wavelengths.

adequate energy on the device under test while preserving the necessary spectral resolution.

The approximately monochromatic light leaving the monochromater is allowed to fall alternately on the device under test and on a Reeder radiation thermocouple which serves as reference detector. Since the thermocouple response is very nearly independent of wavelength, the ratio of image tube signal to thermocouple signal at each wavelength represents the spectral response.

The image tube is masked so that only part of the photocathode is illuminated. The signal is taken to be the difference between the video levels corresponding to the clear and dark areas of the mask on each scan line as shown in Fig. A-15.

When the signal is sufficiently greater than the noise in the video channel, the signal is determined directly from photographs of a monitor scope. Under poor conditions, the video signal is sampled synchronously and averaged using a Princeton Applied Research Model CW-1 boxcar integrator.

ABSOLUTE RESPONSIVITY

Once the spectral response of an image tube is determined for some wavelength range, the absolute responsivity need be measured at only one wavelength λ_o. Two methods are practical: using a calibrated source, or using a calibrated reference detector.

- **Calibrated source** – If the spectral distribution $I(\lambda)$ of a source is known and if the peak transmittance $T(\lambda_o)$ and effective bandwidth $\Delta\lambda$ of a narrow-band filter are known, then the absolute responsivity at λ_o is

$$R(\lambda_o) = S(\lambda_o) \; / \; I(\lambda_o)T(\lambda_o)\Delta\lambda$$

where $S(\lambda_o)$ is the detector signal.

- **Calibrated reference detector** – If the absolute responsivity $R_s(\lambda_o)$ of a detector is known and if its signal $S_s(\lambda_o)$ is compared with the signal $S(\lambda_o)$ of the device under test with the same incident narrow-band radiation at wavelength λ_o, then the unknown responsivity is given by

$$R(\lambda_o) = R_s(\lambda_o)S(\lambda_o) \; / \; S_s(\lambda_o).$$

Once $R(\lambda_o)$ is known, then the factor k can be calculated from the previously measured spectral response curve $kR(\lambda)$ at the wavelength λ_o.

The experimental arrangement for absolute responsivity measurements is based on a calibrated source as shown schematically in Fig. A-16. An Eppley Model EPI tungsten-filament quartz-iodine certified standard of spectral irradiance, or a working standard calibrated from the certified standard, irradiates the image tube through a calibrated narrow-band filter at λ_o. The image tube is partly masked, as in the spectral response measurements, and the bandwidth of the filter together with the lamp calibration are used to compute the irradiance at λ_o on the device under test. The ratio of the signal to the irradiance is the absolute responsivity at λ_o.

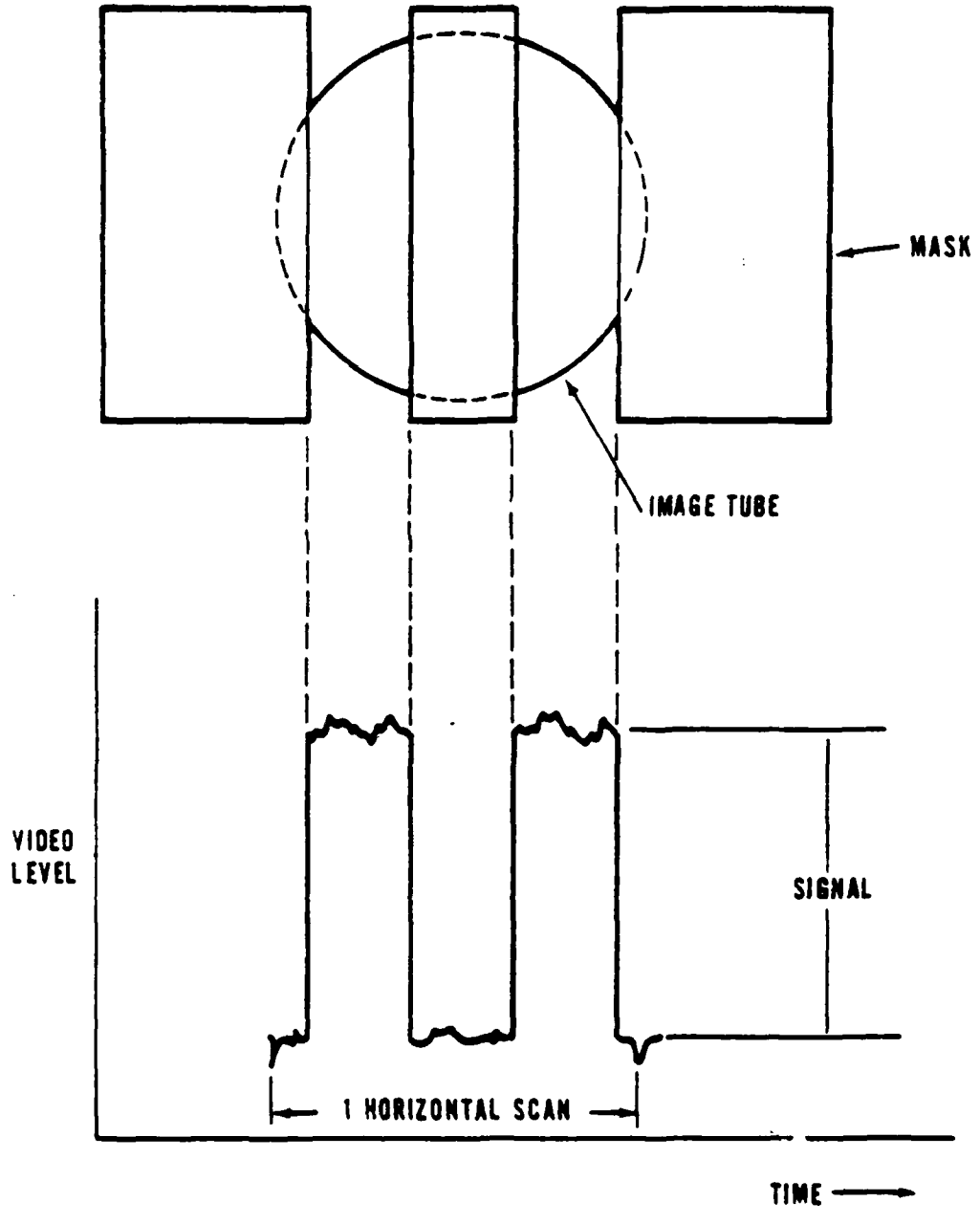

Fig. A-15. Details of spectral response measurement.

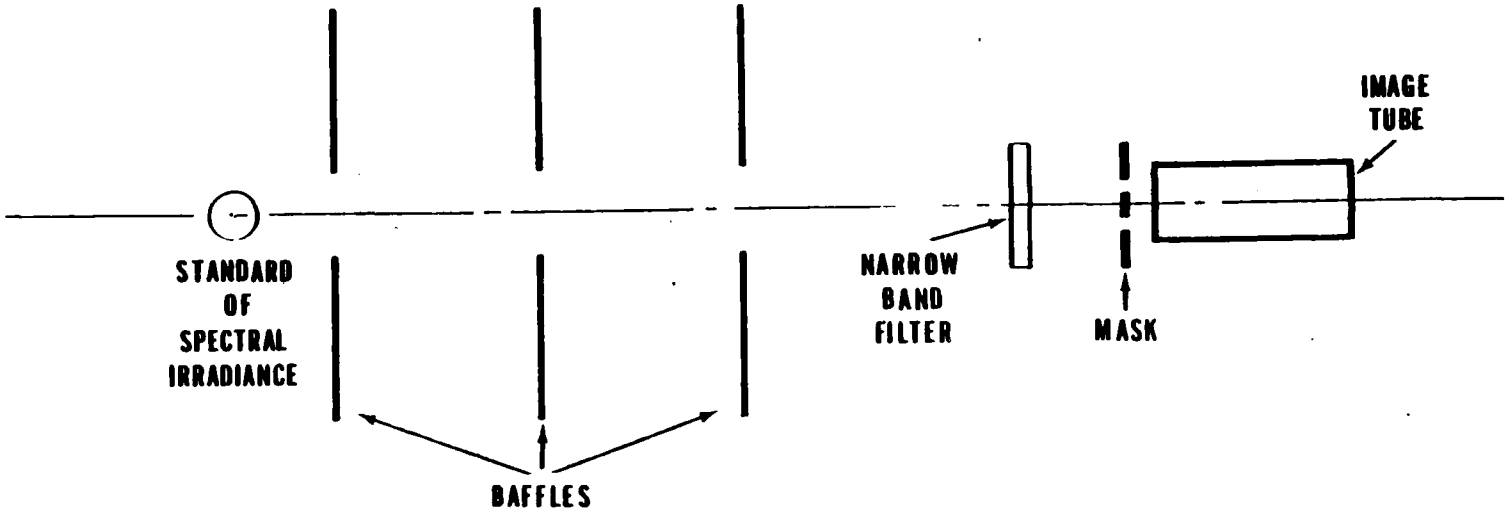

Fig. A-16. Experimental arrangement for the absolute responsivity measurement made at a single wavelength.

DISTRIBUTION FOR NVL REPORT ECOM-7034

No. Copies	Addressee
	Department of Defense
101	Defense Documentation Center ATTN: DDC-TCA Cameron Station (Bldg 5)
012	Alexandria, VA 22314
107	Director National Security Agency ATTN: TDL
001	Fort George G. Meade, MD 20755
109	Advanced Research Projects Agency 1400 Wilson Boulevard
001	Arlington, VA 22209
	Department of the Navy
201	Commander, Naval Ship Systems Command Technical Library, Rm 3 S-08 National Center No. 3
001	Washington, DC 20360
204	Department of the Navy Chief, Office of Naval Research
001	Washington, DC 20350
205	Director Naval Research Laboratory Code 2627
001	Washington, DC 20390
206	Commander Naval Electronics Laboratory Center ATTN: Library
001	San Diego, CA 92152
207	Commander U.S. Naval Ordnance Laboratory ATTN: Technical Library
001	White Oak, Silver Spring, MD 20910
209	Commander Naval Electronic Systems Comd Hq ATTN: Code 0563
002	Washington, DC 20360
210	Commandant, Marine Corps Hq, U.S. Marine Corps ATTN: Code A04C
001	Washington, DC 20380
212	Communications-Electronics Division Development Center Marine Corps Development & Educ Comd
001	Quantico, VA 22134
218	Marine Corps Ln Officer Bay 2C214A, Hex Bldg ATTN: John W. Everett
001	China Lake, CA 93555
219	Naval Weapons Center Code 5525 ATTN: Henry Blazak
001	China Lake, CA 93555
	Department of the Air Force
301	Rome Air Development Center ATTN: Documents Library (TDLD)
001	Griffiss AFB, NY 13440
307	Hq ESD (TRI) L. G. Hanscom Field
001	Bedford, MA 01730
309	Air Force Avionics Laboratory ATTN: AFAL/DOT, STINFO
002	Wright-Patterson AFB, OH 45433
310	Recon Central/RSA AF Avionics Laboratory
001	Wright-Patterson AFB, OH 45433
311	U.S. Air Force Avionics Lab ATTN: AVRO
001	Wright Patterson AFB, OH 45433
313	Armament Development & Test Center ATTN: SSLT
001	Eglin Air Force Base, FL 32542
314	Hq, Air Force Systems Command ATTN: DLTE Andrews AFB
001	Washington, DC 20331
317	Tactical Air Reconnaissance Center Army Liaison Office
001	Shaw AFB, SC 29152

No. Copies	Addressee
	Department of the Army
400	HQDA (DAMI-ZA)
002	Washington, DC 20310
403	HQDA (DACE-ED)
001	Washington, DC 20314
406	HQDA (DARD-DDC)
001	Washington, DC 20310
408	HQDA (DARD-ARP/Dr. R. B. Watson)
001	Washington, DC 20310
409	Commander U.S. Army Materiel Command ATTN: AMCMA-EE 5001 Eisenhower Ave
001	Alexandria, VA 22304
413	Commander U.S. Army Materiel Command ATTN: AMCRD-FW 5001 Eisenhower Avenue
001	Alexandria, VA 22304
415	Commander U.S. Army Materiel Command ATTN: AMCRD-H 5001 Eisenhower Avenue
001	Alexandria, VA 22304
419	Commander U.S. Army Missile Command ATTN: AMSMI-RR, Dr. J.P. Hallowes
001	Redstone Arsenal, AL 35809
421	Commander U.S. Army Missile Command Redstone Scientific Info Center ATTN: Chief, Document Section
002	Redstone Arsenal, AL 35809
423	Commander U.S. Army Weapons Command ATTN: AMSWE-REF
001	Rock Island, IL 61201
424	Commander U.S. Army Weapons Command ATTN: AMSWE-RER-L
001	Rock Island, IL 61201
442	Commander Harry Diamond Laboratories ATTN: Library
001	Washington, DC 20438
443	Commander, USA Foreign Science & Tech Center ATTN: AMXST-ISI 220 Seventh St., N.E.
002	Charlottesville, VA 22901
444	Commander, USA Foreign Science Div ATTN: AMXST CE Division 220 7th St., N.E.
001	Charlottesville, VA 22901
447	Commander, U.S. Army Picatinny Arsenal ATTN: SMUPA-VC5 (Mr. P. Kisatsky) Bldg 350
001	Dover, NJ 07801
449	Commander Picatinny Arsenal ATTN: SMUPA-RT-S, Bldg 59
002	Dover, NJ 07801
450	Commander Frankford Arsenal ATTN: Library, H1300, Bl. 51-2
001	Philadelphia, PA 19137
451	Commander Frankford Arsenal ATTN: W1000-65-1 (Mr. Helfrich)
001	Philadelphia, PA 19137
452	Commander Frankford Arsenal ATTN: SMUFA-W-1000 (Mr. Kerensky)
001	Philadelphia, PA 19137
455	Commander White Sands Missile Range ATTN: STEWS-ID-S Hq
001	White Sands Missile Range, NM 88002
459	Commander Edgewood Arsenal ATTN: SMUEA-TSTI-TL
001	Edgewood Arsenal, MD 21010
462	Commander U.S. Army Materials and Mech Rsch Center ATTN: AMXMR-ATL, Tech Library Branch
001	Watertown, MA 02172

No. Copies	Addressee
463	President U.S. Army Artillery Board
001	Fort Sill, OK 73503
465	Commander Aberdeen Proving Ground ATTN: STEAP-TL
001	Aberdeen Proving Ground, MD 21005
466	Commander Aberdeen Proving Ground ATTN: STEAP-MT-TF, Bldg 436
001	Aberdeen Proving Ground, MD 21005
467	Director, Ballistic Rsch Labs U.S. Army Aberdeen Rsch & Dev Cen ATTN: AMXRD-BTL (Mr. F. J. Allen)
001	Aberdeen Proving Ground, MD 21005
468	Commander U.S. Army Ballistic Rsch Labs ATTN: AMXRD-BSP (Dr. D. Reuyl)
001	Aberdeen Proving Ground, MD 21005
471	Commander U.S. Army Land Warfare Lab ATTN: CRDLWL-4A
001	Aberdeen Proving Ground, MD 21005
472	Commander U.S. Army Limited Warfare Lab ATTN: CRDLWL-7C
001	Aberdeen Proving Ground, MD 21005
473	Commander U.S. Army Land Warfare Lab ATTN: Mr. David Samuels
001	Aberdeen Proving Ground, MD 21005
476	Commander U.S. Army Electronic Proving Ground ATTN: STEEP-MT
002	Fort Huachuca, AZ 85613
478	Chief, USAECOM Field Engr Office U.S. Army Electronic Proving Ground ATTN: STEEP-LN-F (Mr. H. A. Ide)
001	Fort Huachuca, AZ 85613
480	Commander USASA Test and Evaluation Cen
001	Fort Huachuca, AZ 85613
483	U.S. Army Research Office-Durham ATTN: CRDARD-IP Box CM, Duke Station
001	Durham, NC 27706
484	U.S. Army Research Office-Durham ATTN: Dr. Robert J. Lontz Box CM, Duke Station
001	Durham, NC 27706
488	USA Security Agcy Combat Dev Actv ATTN: IACDA-EW Arlington Hall Station, Bldg 420
001	Arlington, VA 22212
492	Commandant U.S. Army Air Defense School ATTN: C&S Dept, MSL Sci Div
001	Fort Bliss, TX 79916
498	Commander U.S. Army Dugway Proving Ground Library ATTN: STEDP-TL, Technical Library
001	Dugway, UT 84022
499	Commander U.S. Army Cold Regions R&E Lab ATTN: CRREL-RP (Dr. Yin Chao Yen)
001	Hanover, NH 03755
500	Commander Yuma Proving Ground ATTN: STEYP-AD (Tech Library)
001	Yuma, AZ 85364
503	Director U.S. Army Advanced Matl Concepts Agcy ATTN: AMXAM
001	Washington, DC 20315
504	Commander U.S. Army Materiel Command ATTN: AMCRD-R (H. Cohen) 5001 Eisenhower Avenue
001	Alexandria, VA 22304
516	Commandant U.S. Army Field Artillery School ATTN: Target Acquisition Dept
002	Fort Sill, OK 73503
517	Commander U.S. Army Missile Command ATTN: AMSMI-RFG (Mr. N. Bell)
001	Redstone Arsenal, AL 35809

No. Copies	Addressee
518	Commander Harry Diamond Laboratories ATTN: AMXDO-RCB (Mr. J. Nemarich)
001	Washington, DC 20438
	Commander U.S. Army MERDC ATTN: SMEFB-JJ (Tech Reports)
002	Fort Belvoir, VA 22060
519	Commander U.S. Army Systems Analysis Agency ATTN: AMSRD-AMB (Mr. A. Reid)
001	Aberdeen Proving Ground, MD 21005
521	Commander, Frankford Arsenal Joint Laser Safety Team ATTN: SMUFA-W1000
001	Philadelphia, PA 19137
526	Commander Project MASSTER
001	Fort Hood, TX 76544
	U.S. Army Electronics Command
604	U.S. Army Liaison Office MIT, Bldg 26, Rm 131 77 Massachusetts Avenue
001	Cambridge, MA 02139
605	U.S. Army Liaison Office MIT-Lincoln Laboratory, Room A-210 P.O. Box 73
001	Lexington, MA 02173
614	Chief Missile Electronic Warfare Tech Area EW Lab, USA Electronics Command
001	White Sands Missile Range, NM 88002
616	Commander, U.S. Army Electronics Command ATTN: AMSEL-PP/P-IED, Mr. C. Mogavero 225 South 18th Street
001	Philadelphia, PA 19103
617	Chief, Intelligence Materiel Dev Office Electronic Warfare Lab., USAECOM
001	Fort Holabird, MD 21219

No. Copies	Addressee
680	Commander U.S. Army Electronics Command Fort Monmouth, NJ 07703
000	
1	AMSEL-WL-D
1	AMSEL-NL-D
1	AMSEL-TL-D
1	AMSEL-VL-D
1	AMSEL-BL-D
1	AMSEL-CB
1	AMSEL-SI-CB
1	AMSEL-MA-MP
2	AMSEL-MS-TI
1	AMSEL-GG-TD
1	CSCS-FM
1	AMSEL-RD
1	USACDC-LNO
	Director Night Vision Laboratory Fort Belvoir, VA 22060
000	
1	AMSEL-NV-D
1	AMSEL-NV-VI
1	AMSEL-NV-PA/RA
	Commander U.S. Army Strategic Communications Command ATTN: SCC-FM-D
001	Fort Huachuca, AZ 85613
	Other Recipients
701	Sylvania Electronic Systems—Western Div ATTN: Technical Reports Library P.O. Box 205
001	Mountain View, CA 94040
702	Institute of Science and Technology The University of Michigan P.O. Box 618 (IRIA Library)
001	Ann Arbor, MI 48107
703	NASA Scientific & Tech Info Fac ATTN: Acquisitions Br (S-AK/DL) P.O. Box 33
002	College Park, MD 20740
706	Advisory Group on Electron Devices ATTN: Secy, Sp Gr on Optical Masers 201 Varick St
002	New York, NY 10014
712	Electronic Properties Info Center Hughes Aircraft Company Centinela and Teale Streets
001	Culver City, CA 90230
718	Remote Area Conflict Info Center Battelle Memorial Institute 505 King Avenue
001	Columbus, OH 43201

D — 59,787 — AG — Ft Belvoir